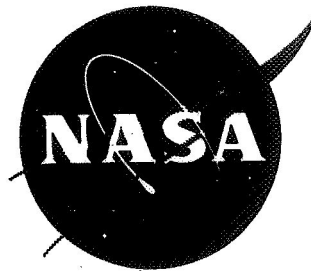


N 71-16381 K

NASA-CR-72795



**DEVELOPMENT OF ADVANCED FABRICATION TECHNIQUES
FOR REGENERATIVELY COOLED THRUST CHAMBERS
BY THE GAS-PRESSURE-BONDING PROCESS**

by

A. N. Ashurst, M. Goldstein, M. J. Ryan

prepared for

NATIONAL AERONAUTICS AND SPACE ADMINISTRATION

Contract NAS3-10305

October 6, 1970

**CASE FILE
COPY**

**BATTELLE MEMORIAL INSTITUTE
COLUMBUS LABORATORIES**

FINAL REPORT

on

DEVELOPMENT OF ADVANCED FABRICATION TECHNIQUES FOR
REGENERATIVELY COOLED THRUST CHAMBERS BY THE
GAS-PRESSURE-BONDING PROCESS

by

A. N. Ashurst, M. Goldstein, M. J. Ryan

prepared for

NATIONAL AERONAUTICS AND SPACE ADMINISTRATION

Contract NAS3-10305

October 6, 1970

NASA-Lewis Research Center
Cleveland, Ohio
John M. Kazaroff, Project Manager
Chemical Rockets Division

FOREWORD

The research described herein was conducted by Battelle Memorial Institute, Materials Design and Fabrication Division, from June 29, 1967, to April 30, 1970, and performed under NASA Contract NAS3-10305. The work was done under the management of the NASA Project Manager, John M. Kazaroff, Chemical Rockets Division, NASA-Lewis Research Center.

The authors acknowledge contributions of several individuals to the research work described in the report. Plasma-spraying experiments were performed by Mr. R. L. Heestand. Mr. C. A. MacMillan, now with Miami Industries, Piqua, Ohio, was the principal investigator on the program from its inception until June, 1969. Mr. R. J. Burian performed thermal analyses to determine heat conductivity into spool pieces during gas-pressure bonding. Mr. D. L. Cheever conducted welding experiments to insure gastight seals of the Tinamel shells and the spool pieces prior to gas-pressure bonding.

ABSTRACT

A research program was performed to develop a new fabrication technique for regeneratively cooled rocket-motor thrust chambers. The technique consisted of assembling a liner, ribs, removable tooling (to form the fluid channels and manifolds), and a spool body, and subsequently bonding them together by hot-isostatic pressing in a gas autoclave. Tooling was removed by selective acid leaching, leaving the thrust chamber as an integral part with complex internal passages. A technique for applying an adherent oxide thermal barrier coating to the surface of the liner was also developed during this program.

SUMMARY

The typical regeneratively cooled rocket thrust chamber is fabricated by brazing together a bundle of tapered and contoured tubes and brazing them to manifolds at each end. This process is expensive and tedious, and usually requires rework to achieve a satisfactory part. The objective of this program was to develop a process for solid-state bonding a thrust chamber, and to demonstrate the process by fabricating two developmental chambers.

The approach devised consisted of first bonding a liner [Hastelloy X or chromium pack diffused (chromallized) TD nickel] and a "tooling sleeve" of Tinamel to a cylindrical mandrel in a hot-gas autoclave. Longitudinal slots were then machined through the Tinamel and slightly into the liner. Stainless steel ribs were inserted in the slots, and a stainless steel spool piece was fitted over the mandrel/rib subassembly. The spool piece contained press-fitted mild-steel rings and radial spokes in each end to form the manifolds. The thrust-chamber assembly was completed by welding stainless steel closures to the ends of the mandrel and spool piece, and was subsequently exposed to the gas-pressure-bonding cycle. Two thrust chambers were fabricated, one having a Hastelloy X liner and one having a chromallized TD-nickel liner. The thrust chambers were then completed by leaching out the mild steel and Tinamel tooling in a hot (180 F) 50 volume percent nitric acid solution, thus forming the internal manifolds and cooling passages.

The TD-nickel liner was quite thin and unbonded to the ribs in one area. This was probably caused by a discontinuity in the Chromallized surface of the nickel. The Hastelloy X liner appeared well bonded to the ribs, but showed some small leaks. These were probably caused by sensitization of the Hastelloy X coupled with the long leaching time required for tooling removal. It is strongly felt that these problems can be readily solved and that the basic fabrication concept utilizing hot-isostatic bonding is feasible.

An additional task involved the development of an improved method of coating Hastelloy X and chromallized TD nickel with protective oxides. A "transfer concept" was devised in which a parting layer of alumina was first applied to the tooling plate, followed by ungraded zirconia coatings or coatings graded with Ni-20 Cr. The chromallized TD nickel or Hastelloy X was then placed on the coatings, and the assembly densified and bonded by gas-pressure bonding. Upon cooling, the alumina parting layer preferentially cracked, leaving the zirconia coatings bonded to the Hastelloy X or TD nickel. Metallographic examination showed the coatings to be dense, uniform in thickness, and well bonded to the substrates. In bend tests, the coatings did not spall or peel despite severe oxide cracking at the bend. On Hastelloy X, the graded coatings survived thermal shock best. Surprisingly, the ungraded coatings on chromallized TD nickel survived thermal shock as well as any of the graded coatings.

TABLE OF CONTENTS

	<u>Page</u>
INTRODUCTION	1
Background	1
Scope of Work	1
Special Facilities Used in Program	5
The Gas-Pressure-Bonding Process	5
Purpose of Program	5
Definition of Task Work	7
 TASK I STUDIES - FABRICATION OF FLAT-PANEL SPECIMENS AND DEVELOPMENT OF COATING TECHNIQUES	
SUBTASK I-1. DEVELOPMENT OF BONDING PARAMETERS AND FABRICATION OF SPECIMENS	8
Materials	8
Development of Bonding Parameters	8
Preliminary Leaching Studies	11
Protective Coatings and Barrier Layers	12
Fabrication of Subscale Panel Specimens	14
Group I	14
Group II	17
Fabrication of Full-Size Flat-Panel Specimens	27
Group I	27
Group II	27
 SUBTASK I-2. SPECIMEN EVALUATION AND TESTING	34
Nondestructive Testing	34
Double-Lap-Shear-Test Specimens	35
 SUBTASK I-3. DEVELOPMENT OF CERAMIC COATINGS	42
Oxide-Coating Approach	42
Group I. Coating of Small-Scale Specimens	42
Group II	42
Group III	42
Coating of Subsize Flat-Panel Specimens	43
Group I	43
Group II	45
Coating of Full-Size Flat-Panel Specimens	45
Group I	45
Group II	46
Additional Coating-Development Work	46
 TASK II. FABRICATION AND TESTING OF CYLINDRICAL SPOOL PIECES	
Basic Approach	47

TABLE OF CONTENTS
(Continued)

	<u>Page</u>
SUBTASK II-1. PREPARATION OF CYLINDRICAL-SPOOL-PIECE COMPONENTS FOR GAS-PRESSURE BONDING	48
Welding Study	48
Preparation of Components for Assembly	49
SUBTASK II-2. ASSEMBLY AND FABRICATION OF CYLINDRICAL SPOOL PIECES	50
Assembly of Specimen 1 (Hastelloy X Liner)	50
Assembly of Specimen 2 (TD Nickel Liner)	50
Welding and Sealing	54
First Gas-Pressure-Bonding Cycle	55
Postbonding Operations	55
Preparation of Specimens for Second Gas-Pressure-Bonding Cycle	55
Assembly of Specimen 1	57
Assembly of Specimen 2	57
Second Gas-Pressure-Bonding Cycle	57
Postbonding Operations	60
SUMMARY OF RESULTS	61
Task I	61
Task II	64
CONCLUSIONS	64
RECOMMENDATIONS	65
APPENDICES	
A. MATERIALS CERTIFICATIONS FOR MATERIALS USED IN TASK I	A-1
B. DENSIFICATION AND BONDING OF PROTECTIVE OXIDE COATINGS ONTO HASTELLOY X AND TD NICKEL	B-1
C. CERTIFICATION SHEETS FOR MATERIALS USED IN TASK II	C-1
D. PROCEDURAL STEPS INVOLVED IN THE MODIFIED PREPARATION AND ASSEMBLY PROCESSES FOR CYLINDRICAL-SPOOL-PIECE COMPONENTS	D-1

LIST OF FIGURES

	<u>Page</u>
Figure 1. Flat-Panel-Specimen Approach	2
Figure 2. Cylindrical-Spool-Piece Assembly	3
Figure 3. Thrust-Chamber Assembly	4
Figure 4. Cold-Wall Hot-Isostatic-Compaction Autoclave	6
Figure 5. TD Nickel Bonded to Stainless Steel Using a Tungsten Intermediate Layer	12
Figure 6. Hastelloy X Bonded to Carbon Steel with a Molybdenum Intermediate Layer	13
Figure 7. Flat-Panel-Specimen Assembly	15
Figure 8. Subscale Flat-Panel Specimen I-1.	17
Figure 9. A Section of Specimen I-1 Cooling Channels and 304 Stainless Steel Magnified About 20 X	18
Figure 10. Nature and Relative Position of Defects at Rib-Liner Interface in Specimen II-1	20
Figure 11. Microphoto of Section in Specimen II-2	22
Figure 12. Specimen II-3	24
Figure 13. Specimen II-4	26
Figure 14. Schematic Representation of Cross-Sectional View of Full-Size Flat-Panel Specimens	29
Figure 15. Full-Size Flat-Panel Specimen.	30
Figure 16. Partially Assembled Flat-Panel Specimen of the Second Group . . .	30
Figure 17. Flat-Panel Specimen FP-1 After Hydrostatic Proof Testing at 2000 Psi	36
Figure 18. Shear Specimen Design for Hastelloy X and TD Nickel - 304 Stainless Steel Liner to Rib Bonds	37
Figure 19. Shear Specimen Design for Nb-1Zr - 304 Stainless Steel Liner to Rib Bond	38
Figure 20. Shear Specimen Design for 304 Stainless Steel Rib-Shell Bond . . .	39

LIST OF FIGURES
(Continued)

	<u>Page</u>
Figure 21. Shear Specimen Design for 347 Stainless Steel Self-Bond	40
Figure 22. Double-Lap-Shear-Test Specimen.	41
Figure 23. ZrO ₂ Graded Coating Bonded to Chromallized TD Nickel	43
Figure 24. ZrO ₂ Coating Bonded to Chromallized TD Nickel	44
Figure 25. ZrO ₂ Coating Bonded to Hastelloy X	45
Figure 26. Weld in Tinamel Plate after Exposure to Simulated Autoclave Cycle.	49
Figure 27. Spool-Piece Components Partially Assembled.	51
Figure 28. Assembly of Tinamel Sleeve Over Clamped Components	52
Figure 29. Spool-Piece Specimen 2 Assembled and Ready for Welding	53
Figure 30. Slotted Tinamel Tooling Sleeve on Spool Piece	56
Figure 31. Specimen 2 Assembled and Wire Wound to Maintain Rib Positions During Assembly into the Stainless Steel Shell Forging.	58
Figure 32. Model of Spool Specimens Used for Thermal Analysis	59
Figure 33. Predicted Change in Temperature of Components in Spool Specimens During Gas-Pressure Bonding	60

LIST OF TABLES

	<u>Page</u>
Table 1. Tensile Data on Materials for Task I	9
Table 2. Hardness Data on Materials for Task I	9
Table 3. Summary of Preliminary Specimens	10
Table 4. Chemical and Electrochemical Etching Solutions and Conditions for Cleaning the Specimen Components	10
Table 5. Procedures for Plating TD Nickel Liners with Chromium	12
Table 6. Summary of First Group of 2 by 4-inch Subscale Specimens	14
Table 7. Summary of Second Group of 2 by 4-inch Subscale Specimens	19
Table 8. Microhardness Data - Specimen II-2	23
Table 9. Microhardness Data - Specimen II-3	25
Table 10. Microhardness Data - Specimen II-4	28
Table 11. Identification of Second Group of Flat-Panel Specimens	31
Table 12. Ultrasonic Test Equipment and Parameters	34
Table 13. Shear-Test Results	41
Table 14. Sequence of Plasma-Sprayed Coatings for Second Group of Full-Size Flat-Panel Specimens	46
Table 15. Description of Coating Systems Fabricated in Additional Coating-Development Work	47
Table 16. Summary of Materials Required in Task II Studies	48
Table 17. Cleaning Procedures for Liner Materials	50

FINAL REPORT

on

DEVELOPMENT OF ADVANCED FABRICATION TECHNIQUES FOR REGENERATIVELY COOLED THRUST CHAMBERS BY THE GAS-PRESSURE-BONDING PROCESS

by

A. N. Ashurst, M. Goldstein, M. J. Ryan

INTRODUCTION

Background

A regeneratively cooled rocket thrust chamber typically consists of a bundle of tapered, contoured tubes joined together and manifolded at each end for the passage of coolant, usually the engine's fuel. Present fabrication techniques for these chambers are tedious and expensive, and involve time-consuming operations such as die forming of the tubes, assembly of the tube bundle, and furnace brazing. The brazing operation in itself is difficult to perform and often requires hand repair of the brazed assembly. Moreover, alteration of fixed engine design to accommodate different propellants, nozzle contours, or area ratios is difficult and costly. Further, present designs make it difficult to incorporate schemes to control the thermal flux to the chamber walls. Difficulties have been experienced in joining dissimilar metals, and in bonding ceramics for thermal barriers to structural metals. Either of these problems, if solved, could extend the present chamber heat flux and pressure limits.

Scope of Work

This program was initiated to develop and evaluate techniques for the construction, by the gas-pressure-bonding process, of regeneratively cooled rocket thrust chambers for large rocket engines. Solid-state bonding parameters were investigated and then optimized, and flat-panel specimens simulating the chamber coolant passage design were bonded and evaluated. Experiments included in these Task I investigations involved the development of barrier layers and the application of oxide coatings. Additional work was later incorporated into the program, concerning the deposition, bonding, densification, and evaluation of oxide coatings on the liner materials. These studies produced very promising results and are described in Appendix B.

The flat-panel-specimen approach used in Task I is illustrated in Figure 1. To further develop the fabrication methods and demonstrate the fabricability of a simulated chamber, cylindrical spool pieces were constructed in Task II. A typical assembly is shown in Figure 2. The third phase of the program was to involve the construction and fabrication of segments of a thrust chamber as illustrated in Figure 3, but owing to revisions in contract objectives, Task III was omitted from the program.

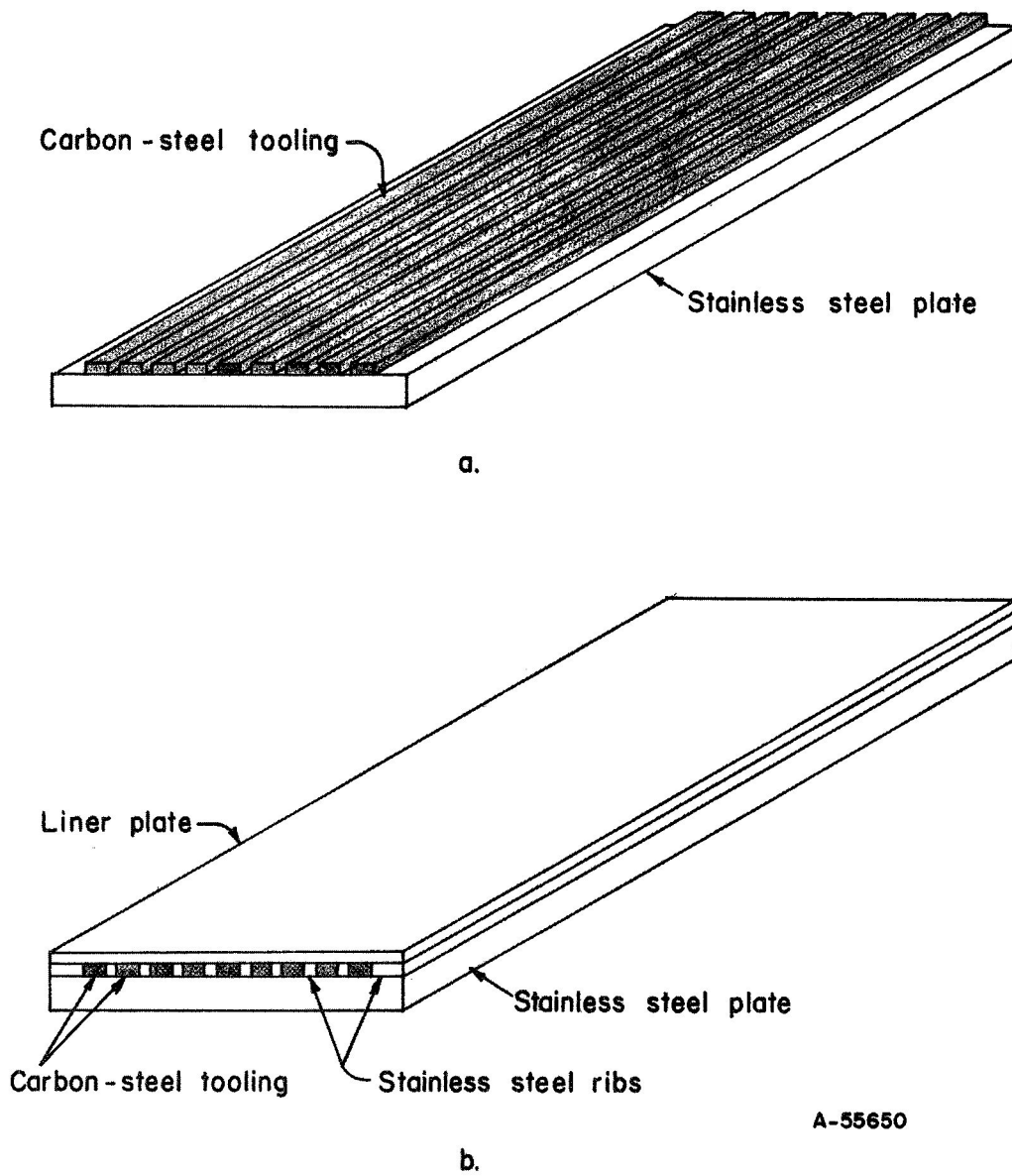


FIGURE 1. FLAT-PANEL-SPECIMEN APPROACH

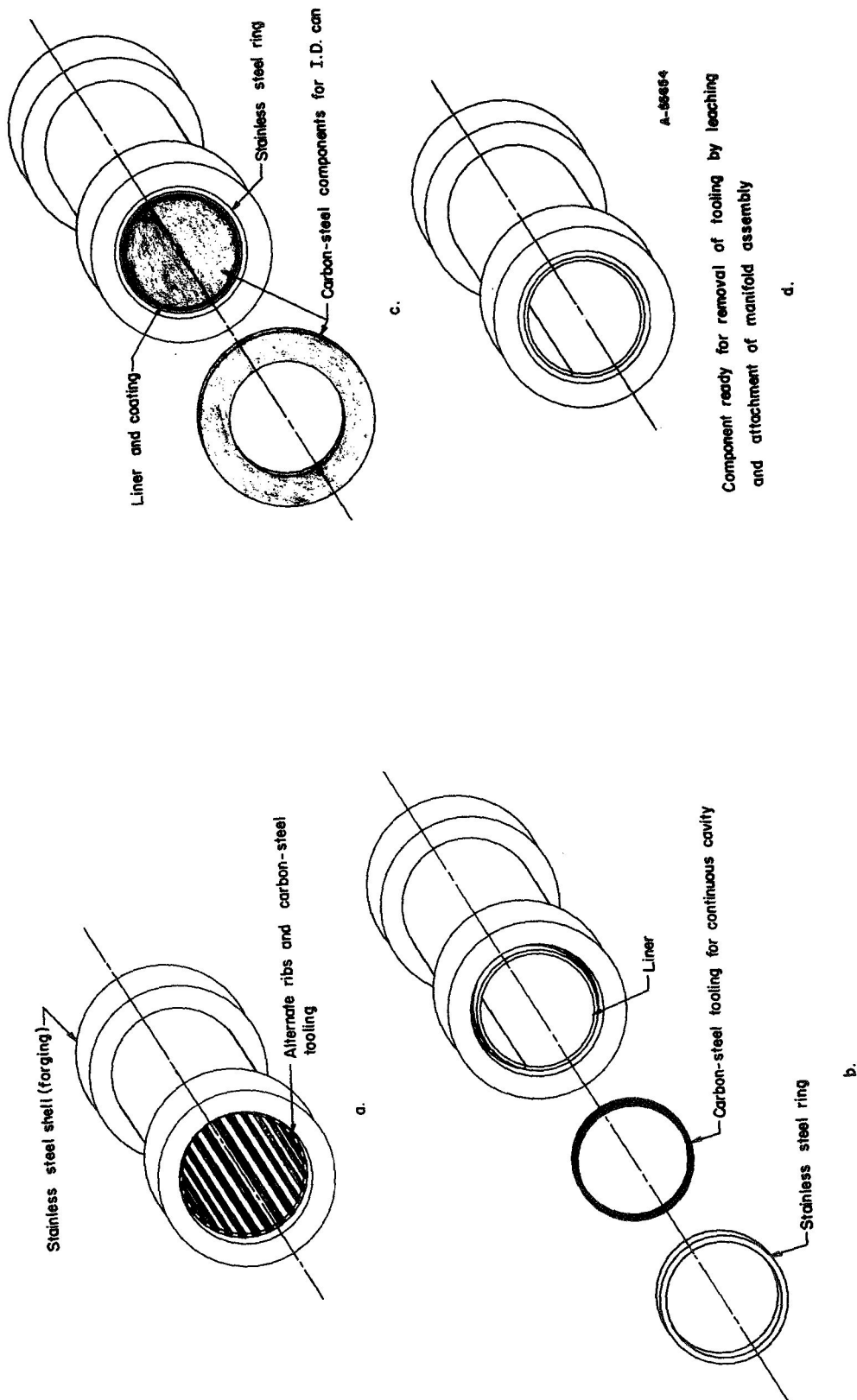


FIGURE 2. CYLINDRICAL-SPOOL-PIECE ASSEMBLY

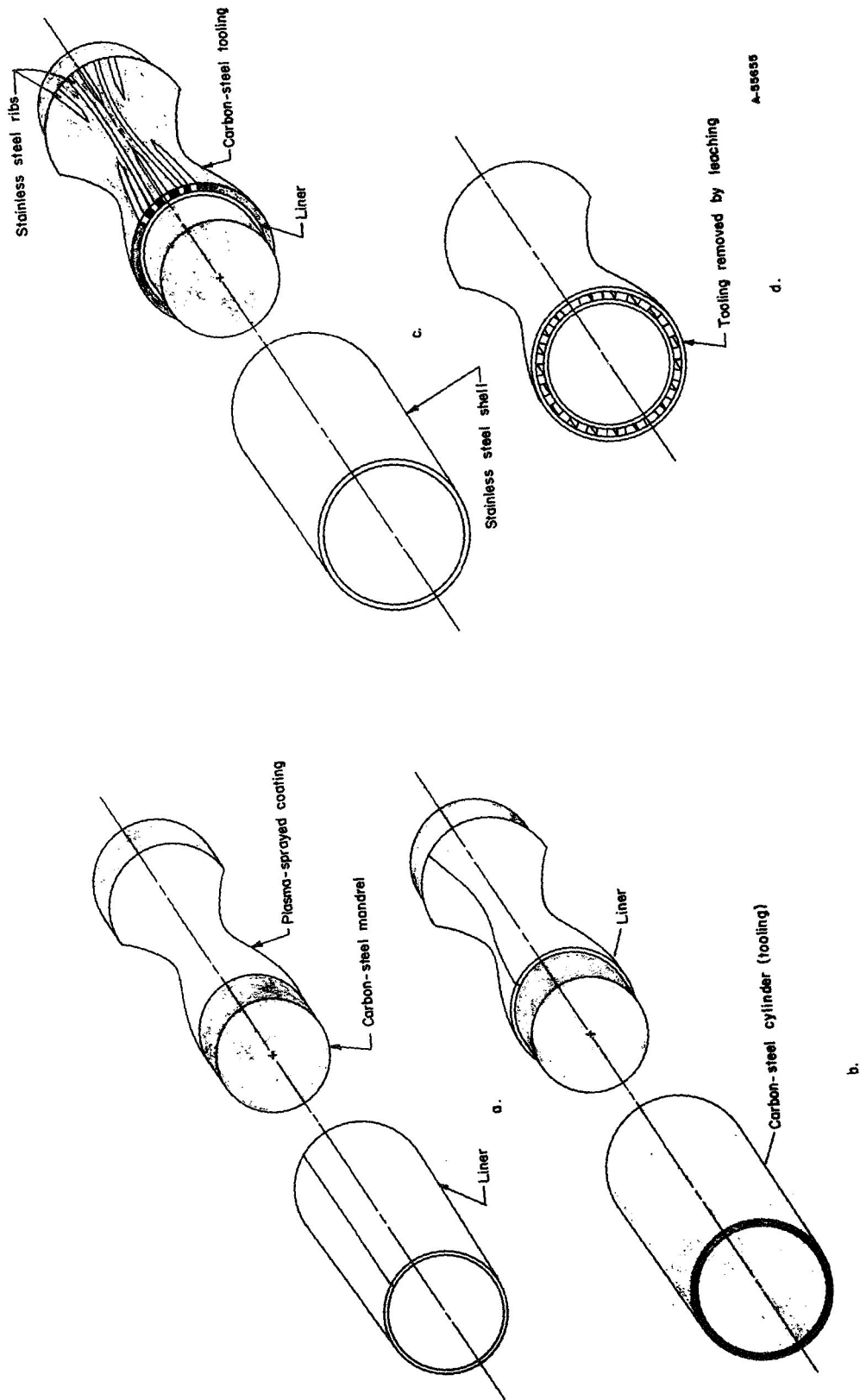


FIGURE 3. THRUST-CHAMBER ASSEMBLY

Special Facilities Used in Program

The gas-pressure-bonding units employed in this program permitted the use of the relatively low bonding temperatures to achieve suitable solid-state bonds between components, minimize tooling-compatibility problems, and avoid tooling and component distortion during bonding by virtue of the uniform, isostatic, high pressures applied to the mating surfaces. One unit, used for subscale, oxide coating, and flat-panel specimens, has a capability of 30,000 psi and 3,000 F. Lower conditions were used, however, to simulate the bonding parameters planned for the large-scale components. The largest autoclave unit was utilized to bond the cylindrical spool pieces and has a maximum capability of 15,000 psi and 2,200 F. A special heater was built to accommodate 18-inch diameter parts several feet long, corresponding to the spool piece design. This allowed two spool pieces to be bonded in one bonding operation.

A 1500-watt ultrasonic spot welder was used to join overlapping barrier foils and liner materials in the cylindrical spool pieces. Welding was accomplished at ambient temperatures.

The Gas-Pressure-Bonding Process

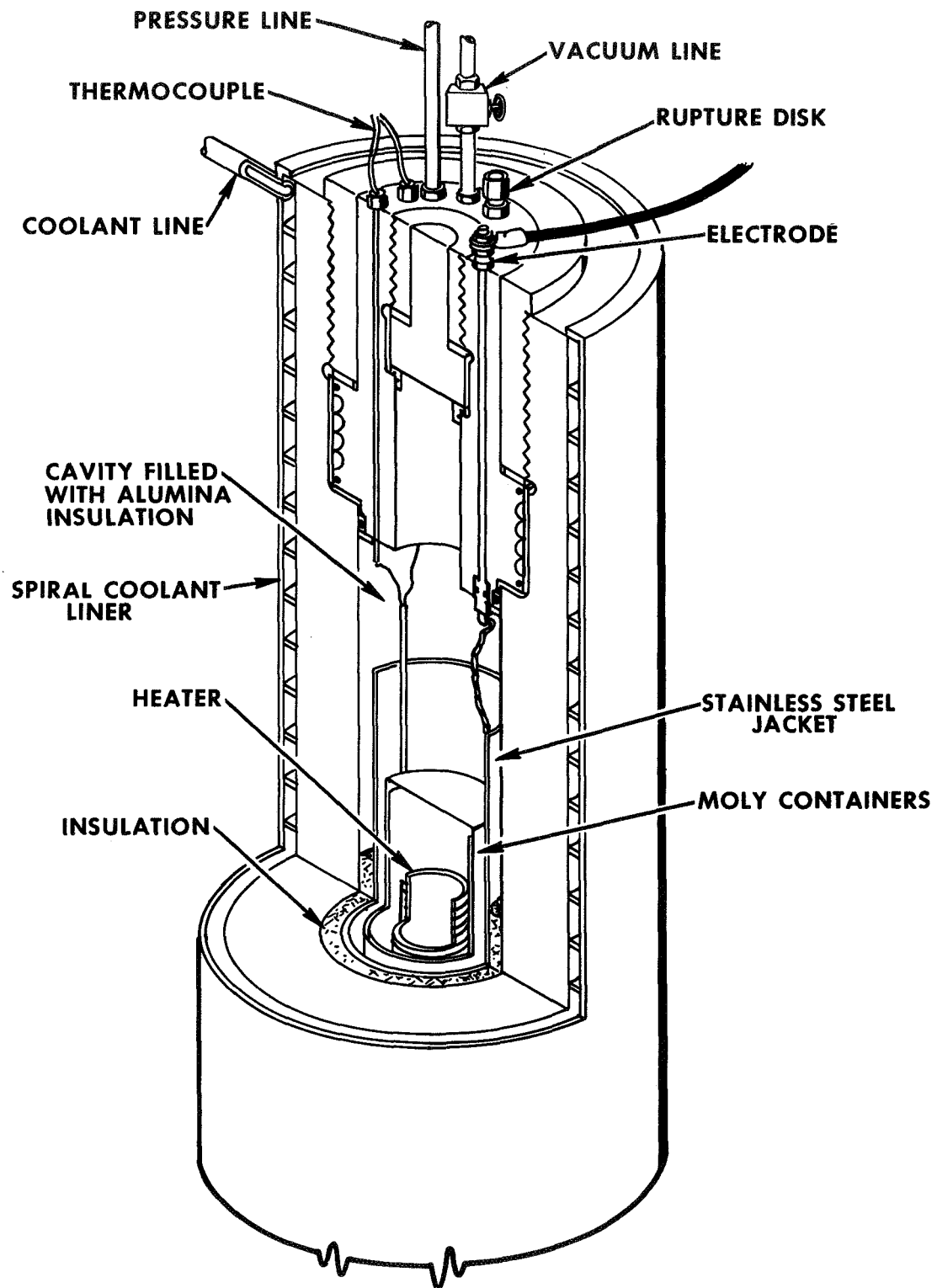
Gas-pressure bonding is an idealized solid-state bonding process performed in a high-pressure autoclave in which the bonding force is applied with inert gas at elevated temperatures. The isostatic nature of this process allows large-diameter components of various sizes and shapes to be bonded into a single unit without recourse to large dies and heavy punches and equipment.

A large cold-wall autoclave containing a resistance heater attains the high gas pressures and temperatures required for bonding. Insulating material is placed between the wire-wound furnace and the inside wall and heads of the autoclave to prevent overheating of the vessel walls. A sectional view of the large-diameter autoclave used in the program is shown in Figure 4.

To prepare assemblies for processing, the components to be bonded are cleaned and assembled into containers which are then welded, evacuated, and sealed. The sealed containers are then placed in the heater inside the autoclave, and the temperature and pressure required for bonding are applied. The high gas pressure is transmitted by plastic flow of the containers to the components, which locally deform at contact points to achieve metallurgical bonding. For most applications, the bonding container is removed by machining or selective leaching. The small specimens, oxide-coating test specimens, and flat-panel-specimens in Task I were in this category. In Task II, however, the container was actually part of the cylindrical spool piece and was retained after gas-pressure bonding.

Purpose of Program

The purpose of this program is to develop and evaluate the hot-isostatic pressure-bonding technique for the construction of regeneratively cooled rocket chambers for large rocket engines. Specific goals sought were to:



23784

FIGURE 4. COLD WALL HOT-ISOSTATIC COMPACTION AUTOCLAVE

- (1) Reduce costs by eliminating the expensive forming, assembling, brazing, and rework required by the present designs
- (2) Increase engine reliability by eliminating the through-the-wall joints that are potential leak paths
- (3) Provide design flexibility that will improve the cooling geometry and fabrication flexibility to minimize large costs associated with specific tooling accruing from a design change.

Definition of Task Work

The program was originally divided into three tasks:

Task I. Flat-Panel Specimens and Coating Techniques

Task II. Cylindrical Spool Pieces

Task III. Thrust-Chamber Segments.

The thrust-chamber segments were to be made up of a complex curvature and variable cooling passages found in a typical thrust chamber and fabricated by techniques developed in the previous two tasks. Task III was subsequently eliminated from the project work by revisions in the contract goals.

Task I studies involved three subtasks. Subtask 1 involved development of bonding parameters and the fabrication of small-scale specimens (bonding coupons, 2 by 4-inch panel segments, 4 by 8-inch flat-panel specimens, and double-lap-shear-test specimens). Subtask 2 was concerned with specimen testing and evaluation, including examination of suitable NDT techniques to determine bond integrity and completion of tooling-removal processes, and also leak checking and hydrostatic proof testing. Subtask 3 concentrated on the development of oxide coatings for the liner materials and included experimental fabrication of oxide-coated coupons and 4 by 8-inch flat panels with oxide-coated liners.

Task II studies incorporated optimum results from Task I toward the fabrication of two cylindrical spool pieces and consisted of three subtasks. Subtask 1 covered the design, preparation, and fabrication of component parts of the spool pieces. Some trade-offs in materials selection, spool-piece size and cooling-channel design, bond parameters, and liner coating application were made according to the results generated on flat-panel specimens in Task I studies, but some were also made necessary because of unforeseen difficulties that developed during the next subtask. The work in Subtask 2 involved the assembly, welding, sealing, and gas-pressure bonding of two cylindrical spool pieces, and also included the fabrication of a specially built heater for the autoclave. Additional efforts to salvage the spool pieces were necessary because of difficulties in developing sound bonds between the liner and other components in the spool pieces during the first of two scheduled gas-pressure-bonding cycles. Also included in Subtask 2 were the machining and tooling-removal processes necessary to complete the fabrication of the cylindrical spool pieces.

Subtask 3 covered the testing of the completed spool pieces by leak checking and hydrostatic proof testing prior to shipping the pieces to NASA-Lewis Research Center for actual hot testing.

TASK I STUDIES - FABRICATION OF FLAT-PANEL SPECIMENS
AND DEVELOPMENT OF COATING TECHNIQUES

SUBTASK I-1. DEVELOPMENT OF BONDING PARAMETERS
AND FABRICATION OF SPECIMENS

Materials

Materials for the fabrication of specimens in Task I were obtained from the following sources:

TD Nickel	Du Pont, Baltimore, Maryland
Hastelloy X	Union Carbide, Kokomo, Indiana
Stainless Steel	Williams and Company, Columbus, Ohio
Niobium-1 Zirconium	USAEC Surplus Property

Test reports for TD nickel, Hastelloy, and stainless steel are included in Appendix A. Tensile data are summarized in Table 1 and hardness data in Table 2.

Development of Bonding Parameters

Subscale specimens were fabricated to establish suitable bonding parameters. These specimens were of a flat coupon design and were sealed in carbon and stainless steel containers. Specimens for these optimization studies are summarized in Table 3. The cleaning techniques for the various materials are summarized in Table 4.

The first group of preliminary specimens were bonded at 2200 F and 10,000 psi for 3 hours. The first bond required in the fabrication of the flat-panel specimens was carbon steel to stainless steel. Metallurgical bonding was achieved, and the tooling became an integral part of the shell.

The bonds of the Hastelloy liner to stainless steel and to carbon-steel were sound and there was no evidence of a diffusion reaction in either component. Such bonds should provide excellent heat-transfer characteristics.

A metallurgical joint was achieved between the stainless steel rib material and TD nickel without harmful diffusion effects. Metallurgical bonding between TD nickel and stainless steel without agglomerating the ThO₂ was significant; such agglomeration is one of the major drawbacks to fusion welding this material. Some interdiffusion between TD nickel and the carbon-steel tooling after bonding was evident. This was of no consequence, however, for the TD nickel had to be coated to protect it during subsequent leaching operations.

An intermetallic compound formed at the interface of the steel - Nb-1Zr systems. Several intermetallic compounds are known to exist in the Fe-Nb system, including

TABLE 1. TENSILE DATA ON MATERIALS FOR TASK I

Material	Modulus of Elasticity, 10^6 psi	0.2% Yield Strength, 10^3 psi	Ultimate Tensile Strength, 10^3 psi	Reduction in Area, %	Elongation in 2 In., %
Hastelloy X	29.1	61.1	117.2	38.5	46
	28.9	61.8	118.0	48.7	54
	<u>29.7</u>	<u>61.3</u>	<u>118.4</u>	<u>47.3</u>	<u>48</u>
(Avg)	29.2	61.4	117.8	44.8	49
TD nickel	17.1	49.1	66.9	45.3	14
	20.1	49.1	65.5	41.0	13
	<u>19.8</u>	<u>49.0</u>	<u>65.4</u>	<u>45.0</u>	<u>15</u>
(Avg)	19.0	49.1	65.9	43.8	14
Nb-1Zr	10.1	65.8	78.6	45.7	1 ^(a)
	11.0	66.5	79.3	48.5	6
	<u>12.2</u>	<u>65.4</u>	<u>78.4</u>	<u>45.8</u>	<u>7</u>
(Avg)	11.1	65.9	78.7	46.7	7
Stainless steel shell	30.5	41.2	92.5	65.6	85
	24.8	43.7	92.5	62.8	84
	<u>23.7</u>	<u>43.1</u>	<u>93.0</u>	<u>69.9</u>	<u>84</u>
(Avg)	26.3	42.7	92.7	66.1	84
Stainless steel rib	43.4	29.5	89.7	82.4	79
	23.5	30.4	89.7	82.9	79
	<u>34.5</u>	<u>29.1</u>	<u>90.0</u>	<u>84.5</u>	<u>76</u>
(Avg)	33.5	29.7	89.8	83.3	78
Carbon-steel tooling	30.7	35.5	44.5	66.0	57
	32.7	36.5	44.3	63.3	54
	<u>31.9</u>	<u>33.6</u>	<u>44.4</u>	<u>67.7</u>	<u>57</u>
(Avg)	31.8	35.2	44.4	64.7	56

(a) Fractured outside of bench marks; not counted in average.

TABLE 2. HARDNESS DATA ON MATERIALS FOR TASK I

Material	Orientation With Respect to Rolling Direction	Hardness, Knoop
304 stainless (shell)	Parallel	159
	Perpendicular	156
304 stainless (rib)	Parallel	185
	Perpendicular	175
Carbon-steel tooling	Parallel	108
	Perpendicular	107
Hastelloy X	Parallel	292
	Perpendicular	292
TD nickel	Parallel	207
	Perpendicular	227
Nb-1Zr	Parallel	169
	Perpendicular	184

TABLE 3. SUMMARY OF PRELIMINARY SPECIMENS

<u>First Group of Coupon Specimens</u>				
<u>Specimen</u>	<u>System(a)</u>			
1	S.S./ .003 in. Mo/C.S./ .003 in. Mo/S.S.			
1	S.S./C.S./S.S.			
2	S.S./T.D. Ni/S.S.			
3	S.S./ .0005 in. W/TD Ni/ .0005 in. W/S.S.			
4	S.S./Hastelloy-X/C.S.			
5	S.S./Nb-1Zr/C.S.			
 <u>Second Group of Coupon Specimens</u>				
<u>Specimen</u>	<u>Substrate</u>	<u>Barrier System</u>	<u>Liner</u>	<u>Coating</u>
6	N/A ^(b)	N/A	Chromium-plated TD Nickel	Graded ZrO ₂
7	Stainless steel	Ni-30Cr/W	Nb/1Zr	Graded Al ₂ O ₃
8	Stainless steel	V/Ti	Nb/1Zr	N/A
9	N/A	N/A	Nickel-plated Hastelloy X	Graded ZrO ₂
10	Carbon steel	Mo	Hastelloy X	N/A

(a) S.S. = stainless steel, C.S. = carbon steel.

(b) N/A = not applicable.

TABLE 4. CHEMICAL AND ELECTROCHEMICAL ETCHING SOLUTIONS AND CONDITIONS FOR CLEANING THE SPECIMEN COMPONENTS

<u>Component</u>	<u>Etchant or Electropolishing Media</u>	<u>Etching Conditions</u>
TD nickel	40 H ₂ SO ₄ -60 H ₂ O	200 ASF current density ^(a) , <80 F
Hastelloy X	40 H ₂ SO ₄ -60 H ₂ O	400 ASF current density ^(a) , <80 F
Nb-1Zr	30 HF-30 HNO ₃ -40 H ₂ O	Ambient temperature
304, 347 stainless steel	10 HNO ₃ -10 HF-80 H ₂ O	130 F
1018 carbon steel	60 HCl-40 H ₂ O	Ambient temperature
Tungsten	45 HF-20 HNO ₃ -35 H ₂ O	Ambient temperature
Ni-30Cr	1/3 HF-1/3 HNO ₃ -1/3 H ₂ O	Boiling
Molybdenum	35 HC ₂ H ₃ O ₂ -35 H ₃ PO ₄ -16 HNO ₃ -2 H ₂ SO ₄ -12 H ₂ O	Ambient temperature
Titanium	33 HNO ₃ -2 HF-65 H ₂ O	130 F
Vanadium	MEK degrease	Ambient temperature
Selective cleaning of 304 stainless steel rib slots	63 H ₃ PO ₄ -15 H ₂ SO ₄ -22 H ₂ O	100 ASF current density ^(a) , 120 F

(a) Indicates electrolytic.

Nb_xFe_y at about 11 atomic percent Fe, Nb_3Fe_2 , $\text{Nb}_{19}\text{Fe}_{21}$ σ phase, and NbFe_2 ϵ phase. It is believed that the Laves phase, NbFe_2 , was encountered in this instance. This phase has a very broad homogeneity range extending from 58 to 78 atomic percent iron. This hexagonal ϵ phase is quite stable, as are most Laves phases, and very brittle. Such an interface would lack strength and would probably not survive thermal cycling.

To simulate the multiple bonding operations that were anticipated for Tasks II and III, the bonded specimens described above were subjected to a 6-hour heat treatment at 2200 F. The carbon steel/stainless steel bonds were essentially unaffected, although a slight diffusion zone was evident in the carbon steel. The Hastelloy-to-stainless steel bonds showed no change as a result of this thermal treatment. Likewise, no significant changes were evident in the Hastelloy-to-carbon steel bonds. The stainless steel/TD nickel (liner) bond appeared unaffected, although some scattered porosity was evident in the bond zone. Boundary migration was evident at the as-bonded TD nickel/carbon steel interface, thus resulting in a zone of Fe-Ni alloy. The thermal cycle resulted in an increase in the thickness of this zone.

The NbFe_2 zone increased slightly in thickness in the Nb-1Zr to stainless steel bond, as did the diffusion zone between the intermetallic compound and the stainless steel. The interdiffusion between the Nb-1Zr and carbon steel apparently triggered a pearlite reaction in the steel. Niobium was distributed in both ferrite and carbide phases in steel, although usually more so in the latter. The pearlite stabilization, then, is a consequence of niobium diffusion into the steel.

Preliminary Leaching Studies

The carbon-steel tooling within the component assemblies (flat panels, spool pieces, and thrust chambers) must be removed by acid leaching after all the components have been bonded. Some aspects of leaching (such as leach rate, temperature, etc.), as well as the effects of the hot acid on stainless steel ribs and shells and on the liner materials, were investigated to pinpoint and solve potential problems before scale-up.

The preferred leaching reagent for carbon steel was nitric acid. Both Hastelloy and Nb-1Zr were resistant to dilute HNO_3 ; however, TD nickel was readily attacked. The TD nickel did resist dilute H_2SO_4 , but this solution reacts only slowly with carbon steel.

The 304 stainless steel suffered some intergranular attack in the dilute HNO_3 . In a later experiment, this problem was circumvented by the use of a stabilized grade of stainless steel (Type 347). The H_2SO_4 had to be kept cold or the stainless steel was rapidly attacked. Upon leaching the tooling away from the Hastelloy, isolated areas of tooling scales resistant to the acid leach were found at the interface with the liner. Apparently, a sufficient quantity of chromium diffused into the carbon steel to render it resistant to HNO_3 . The same problem was observed at the stainless steel/carbon steel interfaces, but to a lesser degree.

Protective Coatings and Barrier Layers

Since HNO_3 was to be used to leach the tooling away from the TD nickel, this liner material had to be protected from attack. Tungsten foil (0.0005 inch) was evaluated as a possible protective layer. Figure 5 shows a stainless steel/tungsten/TD nickel bond. The bond appears sound. In the case of the carbon steel, the tungsten separated from the TD nickel. Also, there was a considerable amount of diffusion in the carbon steel. After a 6-hour heat treatment at 2200 F, the stainless steel/TD nickel bonds were unchanged. However, the tungsten rebonded to the TD nickel. A second protective coating investigated was electroplated chromium. The plating procedure is summarized in Table 5. This appeared to work quite well; the tooling could be leached readily from the TD nickel yet the liner material appeared to be protected from attack. Also, the electroplating approach was simpler from a fabrication and assembly standpoint.

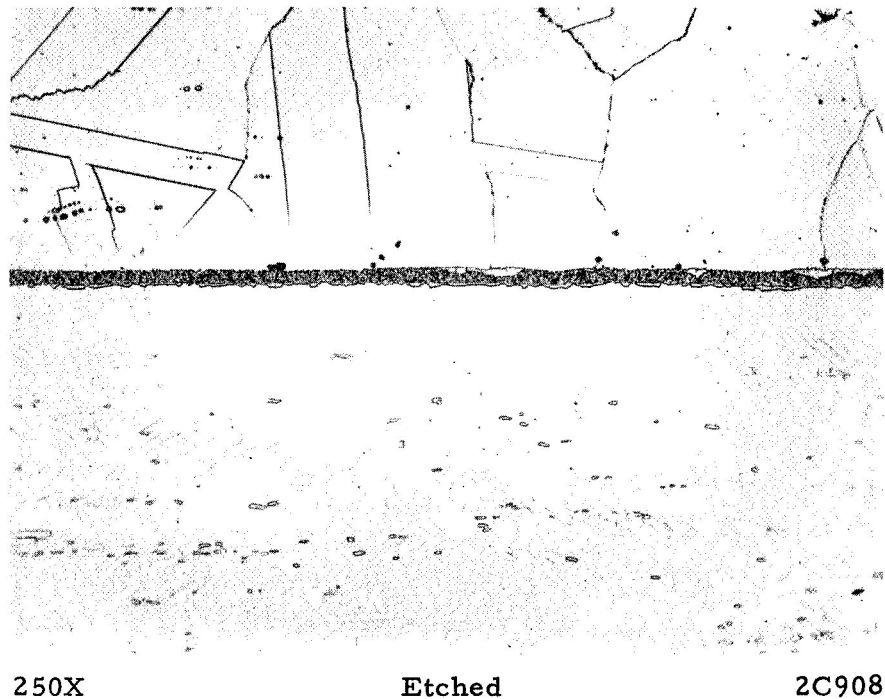


FIGURE 5. TD NICKEL BONDED TO STAINLESS STEEL USING
A TUNGSTEN INTERMEDIATE LAYER

TABLE 5. PROCEDURES FOR PLATING TD NICKEL LINERS WITH CHROMIUM

- | |
|---|
| (1) Degrease liner plate with organic solvent |
| (2) Cathodic activation - 5 volume percent H_2SO_4 , 100 ASF, 3 min |
| (3) Reverse nickel strike - 100 ASF, 1 min |
| (4) Normal nickel strike - 100 ASF, 5 min |
| (5) Rinse in water |
| (6) Electroplate in chromic acid bath - 115 F, 500 ASF |

However, it was later found that the liner was severely attacked at defect sites in the plating. These defects were difficult to correct and an alternative method was employed for protecting the TD nickel liners. This consisted of chromallizing the TD nickel liners to a depth of .005 inch with a minimum of 20 weight percent chromium.

Sections of the TD nickel liners were chromallized by Chromalloy. Electron-microprobe analysis of the sections revealed that the chromium content of the surface to a .005-inch depth was 23.5 weight percent. To test the effectiveness of the chromallizing treatment, sections of treated and untreated TD nickel sheet were immersed in a solution of 70 volume percent HNO_3 heated to 150 F. As expected, the untreated material was severely attacked but the chromallized plate was unaffected by the acid. The chromallizing treatment produces a smooth, defect-free, protective coating on the TD nickel that keeps the substrate from attack for indefinite periods. This treatment was given to all TD nickel liner materials used in subsequent tests, starting with the second group of flat-panel specimens.

To prevent nickel diffusion from Hastelloy into the tooling, a molybdenum foil was inserted at the interface; a typical bond is shown in Figure 6. The molybdenum effectively blocked interdiffusion, and could be readily removed in HNO_3 . No attempt was made to evaluate the bond strength or bond quality at this point since the sole purpose of the molybdenum foil was to prevent interdiffusion between the Hastelloy X and the carbon steel. Owing to design revisions later in the program (during Task II studies), it became necessary to achieve a good metallurgical bond between the molybdenum and the liner and tooling components. This requirement was not recognized, nor were the difficulties arising from inadequate bond strength of the molybdenum-liner couples foreseen until after the cylindrical spool pieces had gone through the bonding cycle. This problem is discussed in detail under Task II studies.

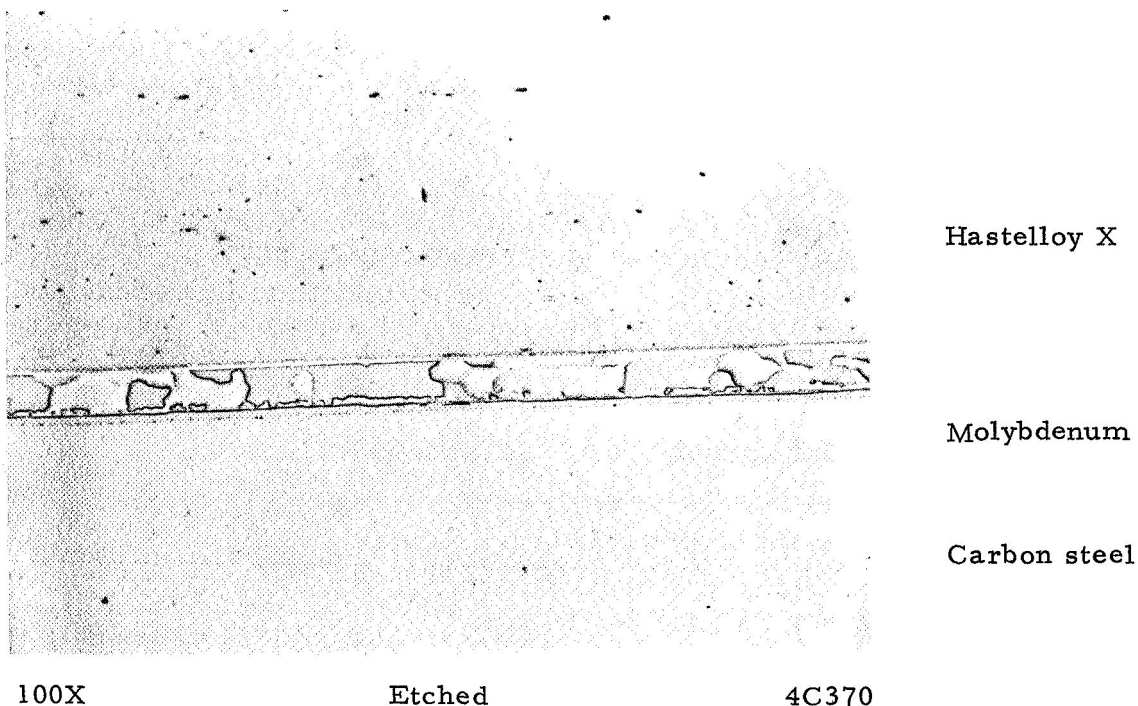


FIGURE 6. HASTELLOY X BONDED TO CARBON STEEL WITH A MOLYBDENUM INTERMEDIATE LAYER

Several barrier systems for preventing the occurrence of an intermetallic compound in the Nb-1Zr were considered, but no single material could be found that was compatible with both steel and Nb-1Zr and that also would bond to both at 2200 F. Therefore, several multicomponent systems were investigated. The first of these consisted of Nb-1Zr/tungsten/Ni-30Cr/steel. The second system contained Nb-1Zr/titanium/vanadium/steel. The former system appeared to be quite satisfactory in all preliminary tests. In the latter system, good bonding was achieved between the four components of the system; however, massive cracking was encountered in the titanium layer; therefore, the tungsten/Ni-30Cr system was selected for scale-up.

Fabrication of Subscale Panel Specimens

The approach for the fabrication of subsize and full-size flat-panel specimens consisted of bonding a sheet of carbon steel to the simulated stainless steel shell. This carbon-steel tooling was then grooved to receive premachined stainless steel ribs. The ribs were then inserted and the liner positioned over the ribs. The panels were then gas-pressure bonded to join the ribs to both the liner and shell.

The assembly and fabrication of the flat-panel specimens is depicted graphically in Figure 7. A carbon-steel plate (tooling) is bonded to the stainless steel shell in the first operation(a). The tooling is then slotted to receive the prefabricated ribs(b). The ribs are inserted(c), and the liner (plasma sprayed, if required) is positioned(d). The entire assembly is then encapsulated for bonding(e). After bonding, the carbon-steel envelope and tooling are removed by selective acid leaching(f).

Two groups of 2 by 4-inch flat-panel specimens were prepared for bonding. Following evaluation of Group I specimens, the necessary changes were incorporated in the second group (Group II).

Group I

The Group I specimens are described in Table 6. The carbon-steel tooling and stainless steel shells were machined and ground to size. These components were prepared for bonding by the previously described cleaning techniques. The two blocks were circumferentially welded together in an argon chamber by the TIG process and hermetic sealing was accomplished by electron-beam welding under a vacuum of approximately 10^{-4} torr. These specimens were bonded at autoclave parameters of 2100 F and 10,000 psi for 3 hours.

TABLE 6. SUMMARY OF FIRST GROUP OF 2 BY 4-INCH SUBSCALE SPECIMENS

Specimen	Liner	Rib Size, inch	Liner Coating	Remarks
I-1	Hastelloy X	.040	None	
I-2	TD nickel	.060	None	Defective
I-3	Hastelloy X	.040	ZrO ₂	
I-4	TD nickel	.060	ZrO ₂	
I-5	Nb-1Zr	.060	Al ₂ O ₃	Barrier system

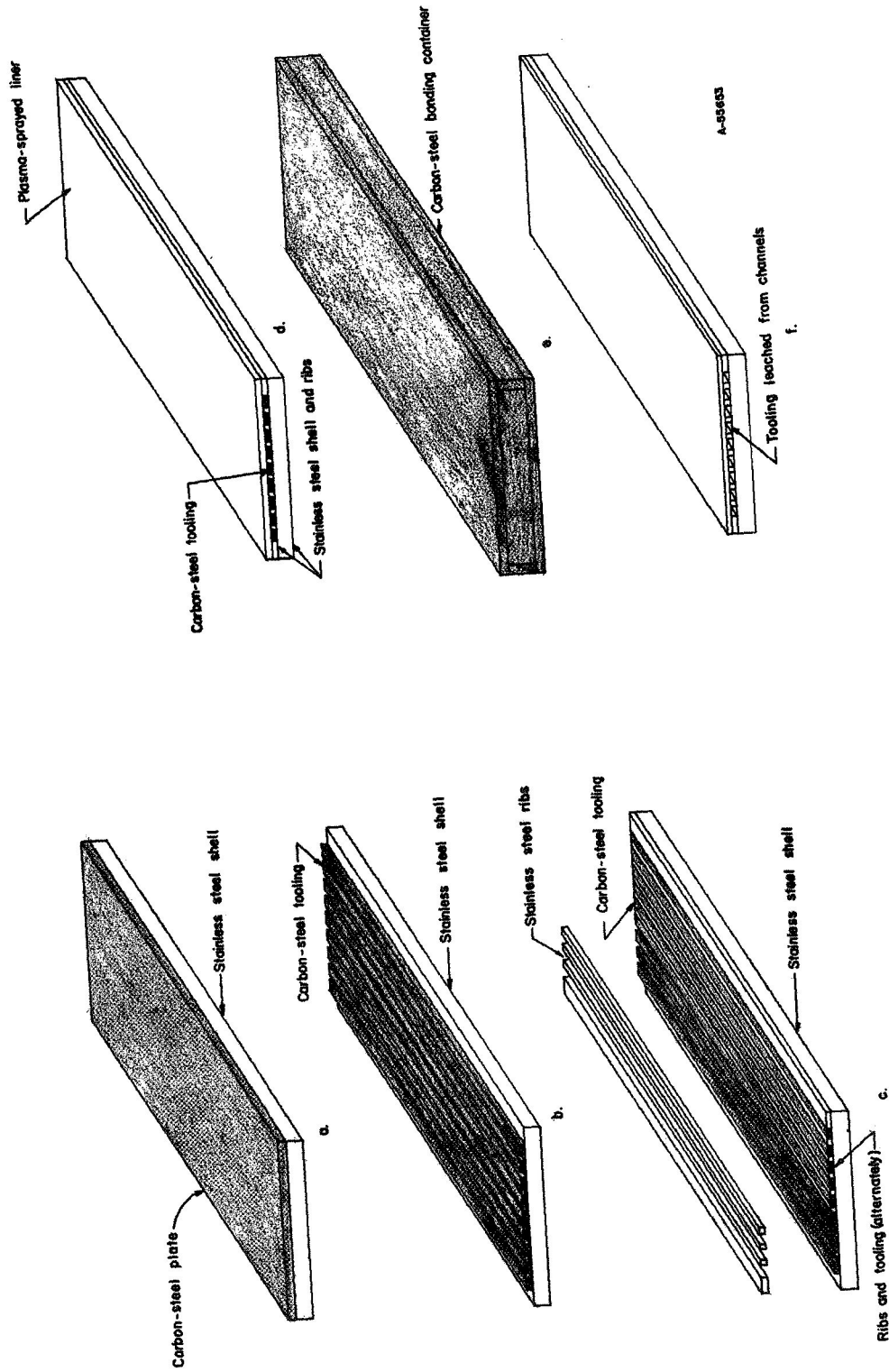


FIGURE 7. FLAT-PANEL-SPECIMEN ASSEMBLY

The bonded shell-tooling assembly showed a slight curvature as a result of the unbalanced condition, i.e., carbon steel on only one side of a stainless steel plate.

The peripheral weld of the bonded shell-tooling assembly was removed, and the rib grooves were machined in accordance with NASA Drawing CB620401. The rib elements were machined from 0.140-inch-thick 304 stainless steel plate. The liner plates were sheared to required dimensions. For these initial tests, oxide coatings were plasma sprayed on carbon steel and Armco iron plates. These coatings had a uniform thickness of .030 inch. The bonding containers were of a flanged design and were fabricated from carbon steel.

All specimen components were cleaned by the techniques developed in the subscale studies. The specimens were assembled and placed in the bonding container. The specimens were then outgassed at 1000 F for 1 hour under a vacuum of approximately 10^{-5} torr, after which the furnace was backfilled with argon. The specimens were then sealed in a plastic bag filled with argon and transferred to an electron-beam welder for hermetic sealing. The sealed specimens were helium leak checked at 200 psi.

Autoclave parameters of 2200 F and 10,000 psi for 3 hours were utilized for bonding. For the initial portion of the autoclave cycle, the specimens were heated to 1200 F before pressurizing above 30 psi. This preheat operation was performed to both stress relieve the container welds and impart plasticity to the container before extensive deformation occurred. After bonding, the specimens were cooled under pressure.

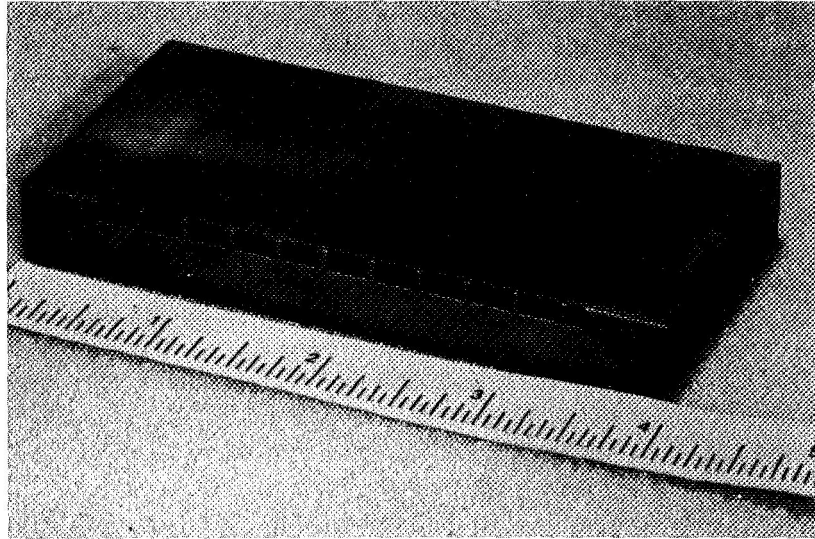
The specimens with Hastelloy and Nb-1Zr liners were leached with a 50 percent aqueous solution of HNO_3 , whereas those with TD nickel liners were leached with a 20 percent aqueous solution of H_2SO_4 . Specimen I-1 with the container and tooling removed is shown in Figure 8.

The bonding containers were removed from Specimens I-2 and I-4 (TD nickel liners) with a 20 percent H_2SO_4 solution. This required approximately 48 hours. When the solution was heated to speed up the reaction, the 304 stainless steel rib and shell components were rapidly attacked. The temperature at which the 304 stainless steel is noticeably attacked is approximately 120 F. Following these tests it was concluded that it would be necessary to protect the TD nickel liners with a coating so that the nitric acid solution could be utilized.

Specimens I-1 and I-3 were leached with the 50 percent HNO_3 solution. The temperature of this solution during the leaching operation was 150 F. The outer bonding containers and internal tooling were removed from the specimens in approximately 32 hours. Some persistent tooling spots remained on the Hastelloy X liner and at the tooling-shell interface. A molybdenum-foil barrier was placed between the tooling and Hastelloy X liners in subsequent specimens. This prevented the diffusion of corrosion-resistant elements from the Hastelloy X into the carbon steel. Specimen I-5 leaked during bonding, and bonds were only partially formed.

Specimen I-1 was examined metallographically. A cross-sectional view of a leached passage in this specimen is shown in Figure 9.

Removal of the tooling with the hot nitric acid solution resulted in slight intergranular attack to the 304 stainless steel components and occurred as a result of slow cooling from the bonding conditions, which caused the precipitation of chromium carbide. Depletion of chromium in the grain-boundary zones caused these zones to become anodic



40636

FIGURE 8. SUBSCALE FLAT-PANEL SPECIMEN I-1

Hastelloy X liner was bonded to the 304 stainless steel ribs and ends by gas-pressure bonding at 2200 F and 10,000 psi for 3 hours. The carbon-steel container and internal tooling were removed by acid leaching.

to both the surrounding matrix and precipitate. In HNO_3 solution, these zones were selectively attacked. Because of this, the use of 304 stainless steel was terminated at the end of Task I studies and stabilized 347 grade used in substitution.

The ZrO_2 coatings on the liners of Specimens I-3 and I-4 were cracked and did not bond to the liners. This cracking was attributed to the liner-oxide-container thermal-expansion mismatch. Attempts were made to minimize these effects in subsequent tests by the utilization of graded ceramic coatings.

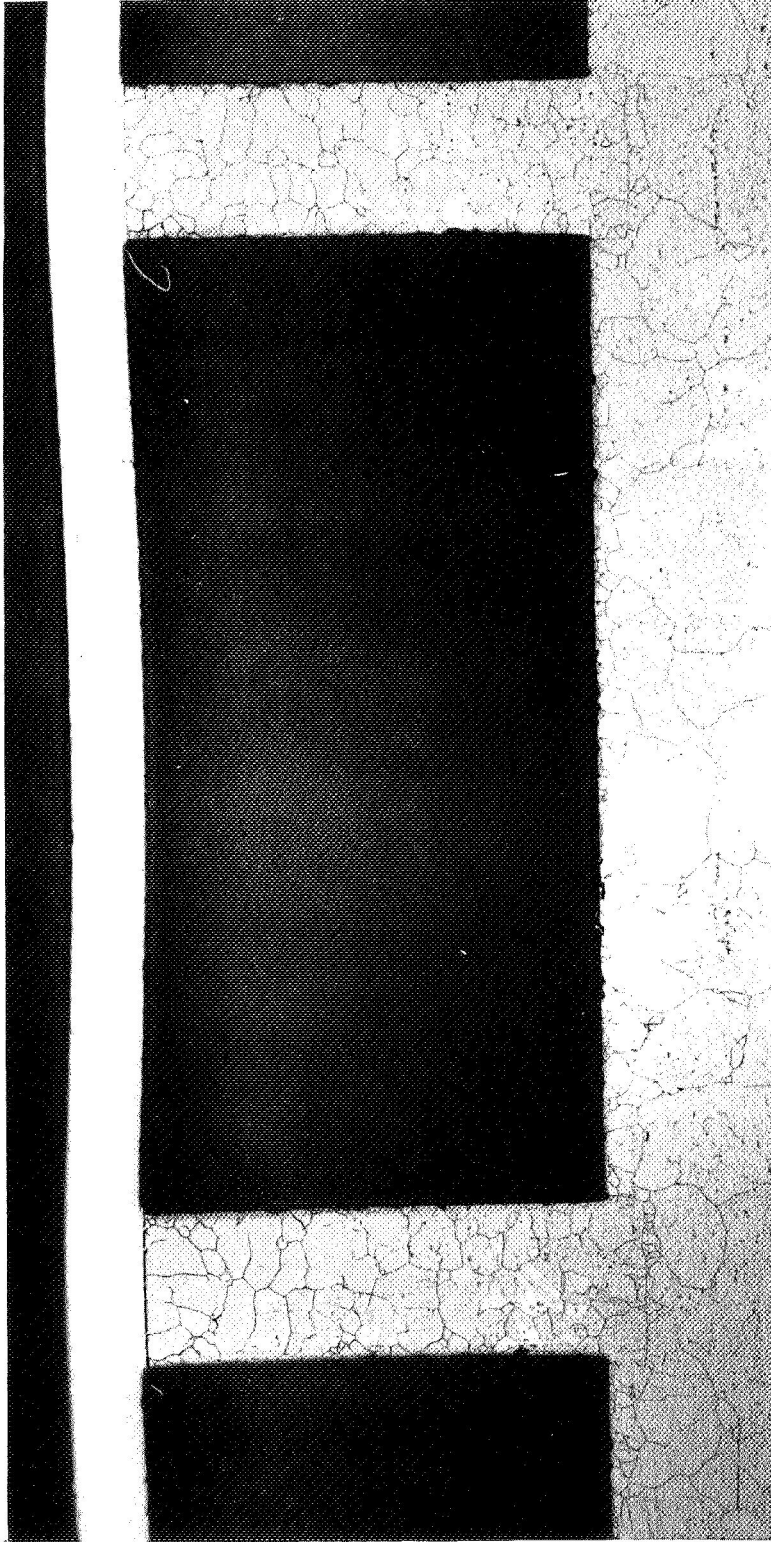
Group II

Following the evaluation of the Group I specimens and subsequent tests with subscale coupons, the Group II subsize panel specimens were fabricated. These specimens are described in Table 7.

Hastelloy-X

304 S/S Ribs

304 S/S Plate



6C678

FIGURE 9. A SECTION OF SPECIMEN I-1 COOLING CHANNELS AND 304 STAINLESS STEEL
MAGNIFIED ABOUT 20 X

The ribs are recessed into the stainless steel plate. No detectable upsetting of ribs occurred; some waviness of the liner is evident but is very slight (less than 10 mils).

20X

TABLE 7. SUMMARY OF SECOND GROUP OF 2 BY 4-INCH SUBSCALE SPECIMENS

Specimen	Liner	Rib Size, inch	Liner Coating	Remarks
II-1	Hastelloy X	.040	None	Defect specimen
II-2	TD nickel ^(a)	.060	None	
II-3	Hastelloy X	.040	Ni-graded ZrO ₂ coating	
II-4	TD nickel ^(a)	.060	Ni-graded ZrO ₂ coating	
II-5	Nb-1Zr	.060	Nb-graded Al ₂ O ₃ coating	Barrier system

(a) Chromium plated.

The following changes were incorporated in this group of specimens:

- (1) All TD nickel liner plates were electroplated with .003 inch of chromium.
- (2) Molybdenum foil .003-inch thick was inserted between the liner and tooling of all specimens except Specimen II-4.
- (3) The shell at the base of the grooves for the ribs was selectively electropolished without attacking the carbon-steel tooling (see Table 4).
- (4) The oxide coatings for these specimens were graded. The Al₂O₃ was graded with niobium powder and the ZrO₂ with nickel powder. The graded coatings were applied to Armco iron and carbon-steel plates by plasma spraying. The sequence of application was
 - (a) Plasma spray .009 inch of pure oxide on the plate
 - (b) Plasma spray .009 inch of 60 volume percent oxide-40 volume percent metal on the pure oxide coating
 - (c) Plasma spray .009 inch of 40 volume percent oxide-60 volume percent metal on the previous coating.

Defects were incorporated at the rib-liner interface in Specimen II-1 during fabrication. The nature and locations of the defects are shown in Figure 10. The molybdenum and steel components would be removed during acid leaching and the MgO coating would cause a discontinuity in the rib-liner bond. This specimen was fabricated for the evaluation of the various nondestructive testing techniques. The defect-specimen components were prepared, assembled, outgassed, and sealed by the previously described techniques.

Autoclave parameters of 2200 F and 15,000 psi for 3 hours were utilized for bonding. Prior to pressurizing above 300 psi, the specimens were heated to 1200 F. After bonding, the specimens were cooled under pressure.

Following removal of the container and carbon-steel tooling, Specimen II-1 was subjected to various nondestructive tests to determine whether the intentional defects could be located. The results of these tests are discussed in the section on nondestructive testing.

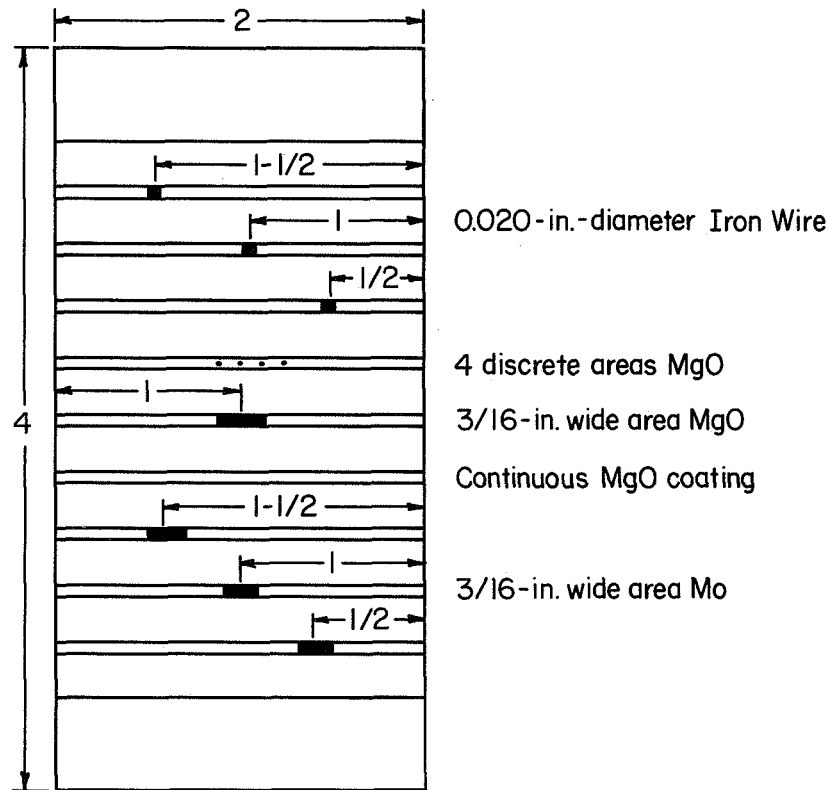


FIGURE 10. NATURE AND RELATIVE POSITION OF DEFECTS AT RIB-LINER INTERFACE IN SPECIMEN II-1

Specimens II-2, -3, and -4 were sectioned for metallographic analysis. The specimens were examined for bond integrity, interdiffusion between components, dimensional integrity, and bonding and quality of the coating. In addition, microhardness traverses were made through representative bonds. Specimen II-5 failed during bonding, and detailed evaluations were not performed. The test results for each specimen are summarized below.

Specimen II-2. (304 stainless steel shell and ribs, chromium-plated TD nickel liner, molybdenum-foil barrier between tooling and liner – no ceramic coating).

A metallographic section of this specimen is shown in Figure 11. Upon etching it was found that interdiffusion had occurred at the rib/Cr-plated liner interface. No reaction occurred between the molybdenum foil and chromium-plated TD nickel; however, carbon from the steel tooling diffused into the molybdenum. This left a .0075-inch zone of carbon depletion in the tooling. These diffusional effects have no influence on the leaching operation. No appreciable distortion occurred in any of the shell-rib-liner components.

Microhardness data for the interface traverses are summarized in Table 8. These tests revealed that the thermal processing caused a reduction in the hardness values of most materials. The chromium plating exhibited high values of hardness (458 to 805 KHN) as compared with the other materials. The carbon-depleted matrix in the steel tooling adjacent to the molybdenum-foil barrier had a hardness value of 273 KHN. This increase may be due to the formation of molybdenum carbide in this area.

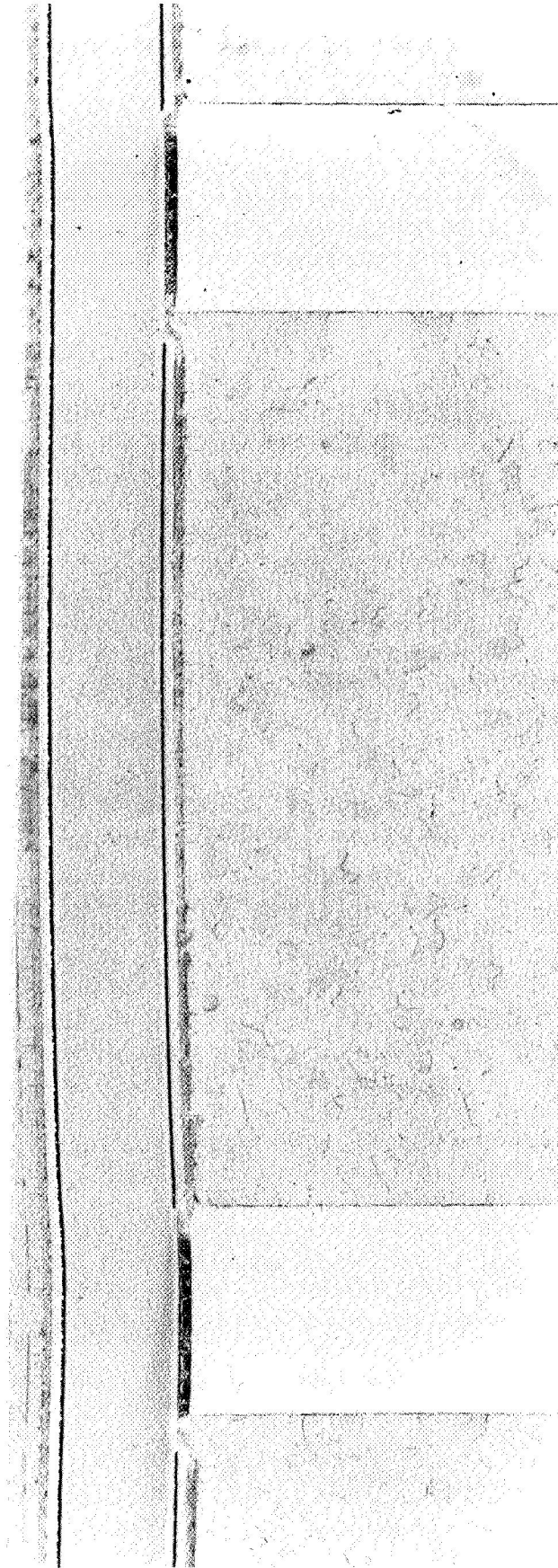
Specimen II-3. (304 stainless steel shell and ribs, Hastelloy X liner, molybdenum-foil barrier between tooling and liner, and graded ZrO_2 ceramic coating).

A metallographic section of this specimen is shown in Figure 12. The bonds in this specimen appeared to be excellent; however, some evidence of oxide contamination was found in the 304 stainless steel rib/shell bonds. The molybdenum-foil barrier did not appear to react or interdiffuse with the Hastelloy liner. The initial layers of the ceramic coating (60 volume percent Ni-40 volume percent ZrO_2 to 40 volume percent Ni-60 volume percent ZrO_2) were completely densified. The crack-free cermet portion of the graded coating is well bonded to the Hastelloy liner. The final layer of ZrO_2 exhibits cracking. This is barely visible at the top of Figure 12. These cracks are attributed to the thermal-expansion mismatch between the liner, coating, and container elements. No appreciable distortion occurred in any of the components.

Microhardness data for the interface traverses are summarized in Table 9. These tests revealed that the thermal processing had caused a slight general decrease in the hardness values of the various materials. As in the case of Specimen II-2, the carbon-depleted zone demonstrated a hardness value greater than that of either the carbon steel or molybdenum.

Specimen II-4. (304 stainless steel shell and ribs, chromium-plated TD nickel liner, and graded ZrO_2 coating).

Figure 13 is a photomacrograph of a typical channel section of Specimen II-4. The bonds in this specimen appear to be excellent, but as in the case of Specimen II-3, some



20X

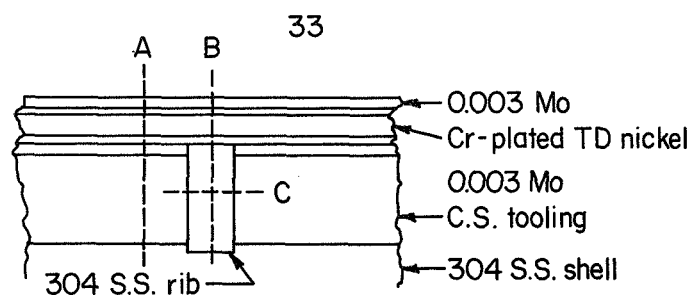
Etched

7C420

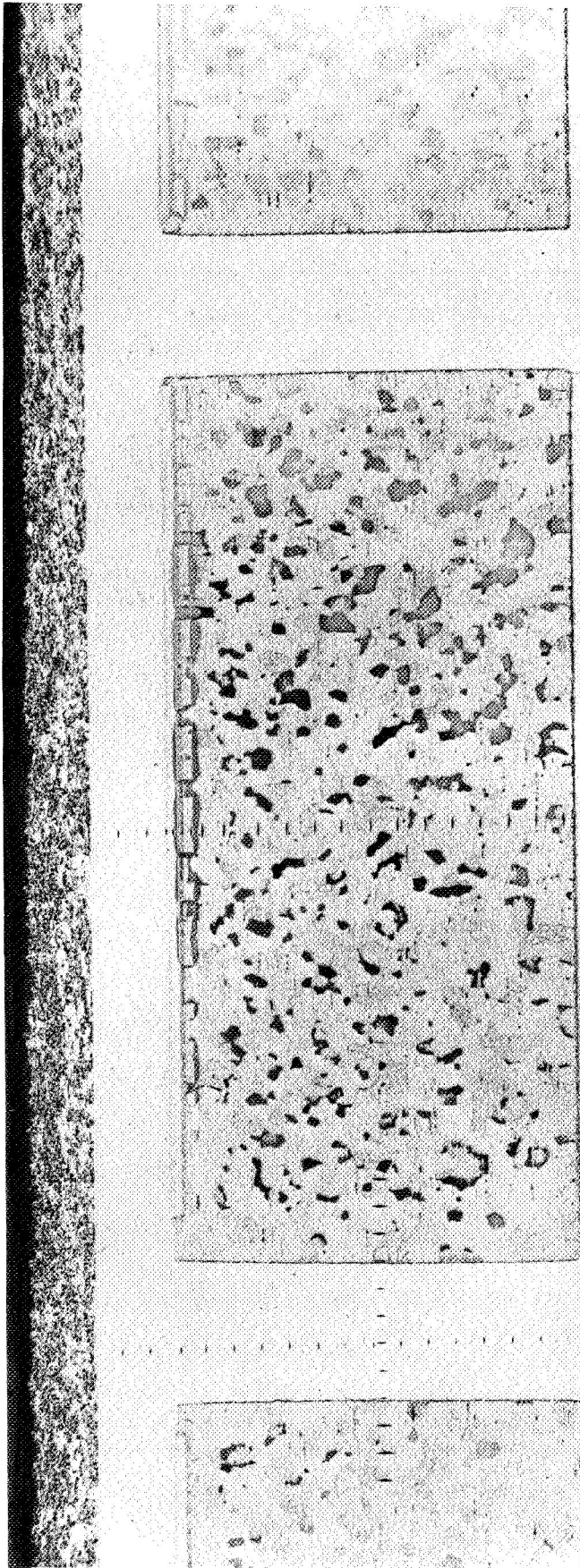
FIGURE 11. MICROPHOTO OF SECTION IN SPECIMEN II-2

Good bonding between the various components was achieved. Diffusion zones are evident at rib and liner interfaces and between the molybdenum foil, liner, and tooling interfaces. Separations at the molybdenum-liner interface are due to thermal expansion.

TABLE 8. MICROHARDNESS DATA - SPECIMEN II-2



Traverse A			Traverse B			Traverse C	
	Distance, cm	KHN		Distance, cm	KHN	Location	KHN
Mo	0.0032	207	Mo	0.0032	207	C.S.	80.8
Cr	0.0082	508	Cr	0.0082	458		88.3
TD Ni	0.013	240	TD Ni	0.0125	237		89.6
	0.033	197		0.033	202	S.S.	142
	0.053	197		0.053	187		185
	0.073	193		0.073	191		156
	0.084	303	Cr	0.089	805		154
Cr	0.088	547		0.095	862		164
Mo	0.091	204	S.S.	0.100	168		170
C.S.	0.098	273		0.120	138		172
	0.106	181		0.140	163	C.S.	91.0
	0.120	91.0		0.160	165		103
	0.140	82.0		0.180	193		85.6
	0.160	95.2		0.200	163		
	0.180	89.6		0.220	172		
	0.200	80.3		0.240	158		
	0.220	81.4		0.260	165		
	0.240	84.4		0.280	160		
	0.260	90.6		0.300	170		
	0.280	78.1		0.320	163		
	0.300	88.9		0.340	149		
	0.320	82.0		0.360	177		
	0.340	95.1		0.380	183		
	0.360	98.1	Rib-shell	0.400	158		
S.S.	0.380	168		0.420	145		
	0.400	181		0.440	168		
	0.420	166		0.460	175		



20X

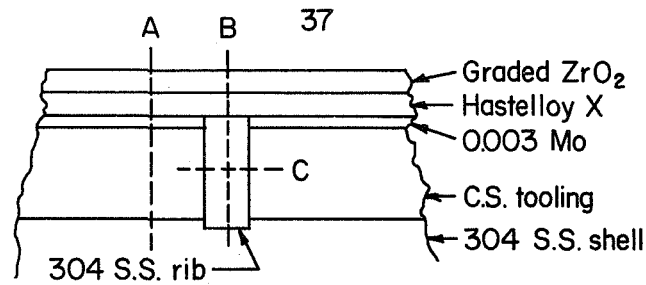
Etched

7C416

FIGURE 12. SPECIMEN II-3

Microhardness indents traverse across various components. Good bonds were achieved between all interfaces. Interdiffusion is evident between the molybdenum foil and tooling pieces but not between the foil and liner. The graded ZrO_2 layer next to the Hastelloy X liner is dense, well-bonded to the liner, and crack free. The pure ZrO_2 above the graded layer is cracked.

TABLE 9. MICROHARDNESS DATA - SPECIMEN II-3



Traverse A			Traverse B			Traverse C	
	Distance, cm	KHN		Distance, cm	KHN	Location	KHN
Hast. X	0.020	202	Hast. X	0.020	209	C.S.	67.4
	0.040	197		0.040	211		70.0
	0.054	206		0.060	163		72.6
Mo	0.059	223		0.080	165	S.S.	197
C.S.	0.066	241		0.100	163		181
	0.072	140		0.120	186		142
	0.080	70.0		0.140	165		166
	0.095	73.2		0.160	168		179
	0.120	73.6		0.180	186		105
	0.140	79.8	S.S.	0.200	185	C.S.	77.6
	0.160	84.1		0.220	162		70.6
	0.180	75.0		0.240	176		73.6
	0.200	72.6		0.260	193		
	0.220	76.6		0.280	149		
	0.240	83.4		0.300	161		
	0.260	79.8		0.320	163		
	0.280	73.0		0.340	173		
	0.300	75.0		0.360	187		
	0.320	77.6		0.380	195		
	0.340	79.8		0.400	175		
S.S.	0.360	161	Rib-shell	0.420	167		
	0.380	127		0.440	159		
	0.400	143					



20X

7C419

FIGURE 13. SPECIMEN II-4

The chromium plating on the liner prevented interdiffusion at the liner-tooling interface. Elsewhere good bonds were achieved. The graded ZrO_2 is well densified, and well bonded to the liner.

evidence of oxide contamination was found in the 304 stainless steel rib/shell bonds. No apparent interdiffusion occurred between the chromium plating and carbon-steel tooling. The layers of the ceramic coating (60 volume percent Ni-40 volume percent ZrO_2 to 40 volume percent Ni-60 volume percent ZrO_2) completely densified. The cermet portion of the graded coating, which bonded to the chromium-plated TD nickel liner, is crack-free, but the final layer of ZrO_2 exhibits some cracking. The thermal-expansion mismatch between the liner-coating-container elements probably caused cracking of the brittle ceramic. No appreciable distortion occurred in any of the panel components.

Microhardness data for the interface traverses are summarized in Table 10. As noted previously, thermal processing resulted in a slight loss in hardness.

Specimen II-5. This specimen was unsatisfactory owing to a container failure during bonding.

Fabrication of Full-Size Flat-Panel Specimens

Group I

The first set of full-size panels had the same configuration as the Group II subscale specimens and are schematically illustrated in Figure 14. The oxide coating procedures and results are described in Subtask I-3. These coatings were prepared as before and gas-pressure bonded at 2200 F and 15,000 psi for 3 hr.

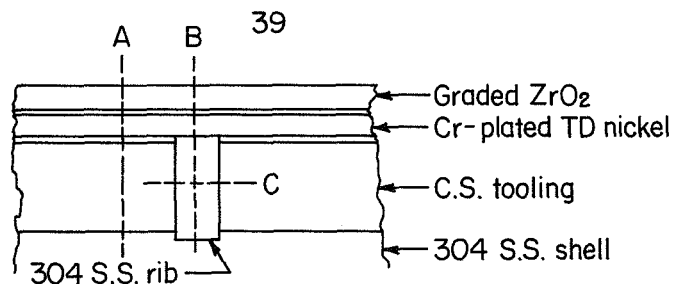
The bonding containers were removed from the specimens by leaching with hot 50 percent nitric acid solution. This phase of the leaching operation required approximately 3 hours. The tooling was removed from the channels either by leaching the specimens in a vertical position or by forced flow of the leachant into the channels. This phase of the leaching operation could be completed in less than 48 hours. The molybdenum-foil barriers were effective in preventing scales of acid-resistant tooling on the inner surface of the liners, although some scales remained at the shell wall. Several areas where the chromium plating was defective were found in Specimens F2 and F4, and the liner was attacked in these areas. The chromium plating did perform satisfactorily where the plating was continuous. A completed 4 by 8-inch flat-panel specimen is shown in Figure 15.

Group II

The second set of 4 by 8-inch flat-panel specimens included three with Hastelloy X liners and three with TD nickel liners. These specimens incorporated end closures (shown partially assembled in Figure 16) which were integrally bonded to facilitate hydrostatic proof testing but otherwise followed the same design as in NASA Drawing CB620401. To preclude nitric acid attack of the TD nickel liners, the liners were chromallized so that the surface had a chromium content of at least 20 weight percent to a depth of .005 inch. Three of the specimens contained liners coated with graded layers of ZrO_2 . The specimens are described in Table 11.

The flat-panel specimens were encapsulated in Armco iron containers, welded by the Heliarc process and sealed by electron-beam welding. The specimens were leak

TABLE 10. MICROHARDNESS DATA - SPECIMEN II-4



	Traverse A			Traverse B		Traverse C	
	Distance, cm	KHN		Distance, cm	KHN	Location	KHN
TD Ni	0.030	202	TD Ni	0.020	202	C.S.	100.5
	0.040	202		0.040	195		94.5
	0.060	199		0.060	202		90.3
	0.080	253	Cr	0.080	522	S.S.	158
Cr	0.084	398	S.S.	0.100	181		197
C.S.	0.089	80.8		0.120	185		165
	0.100	71.8		0.140	197		170
	0.120	74.0		0.160	197		175
	0.140	77.6		0.180	166		185
	0.160	75.6		0.200	165		170
	0.180	80.4		0.220	171	C.S.	105.5
	0.200	80.4		0.240	165		98.3
	0.220	77.6		0.260	156		91.1
	0.240	86.0		0.280	163		
	0.260	74.4		0.300	166		
	0.280	98.6		0.320	187		
	0.300	95.4		0.340	183		
	0.320	87.2		0.360	193		
	0.340	78.0		0.380	161		
	0.360	101		0.400	144		
S.S.	0.380	191		0.420	146		
	0.400	171	Rib-shell	0.440	144		
	0.420	187		0.460	197		
	0.440	149					

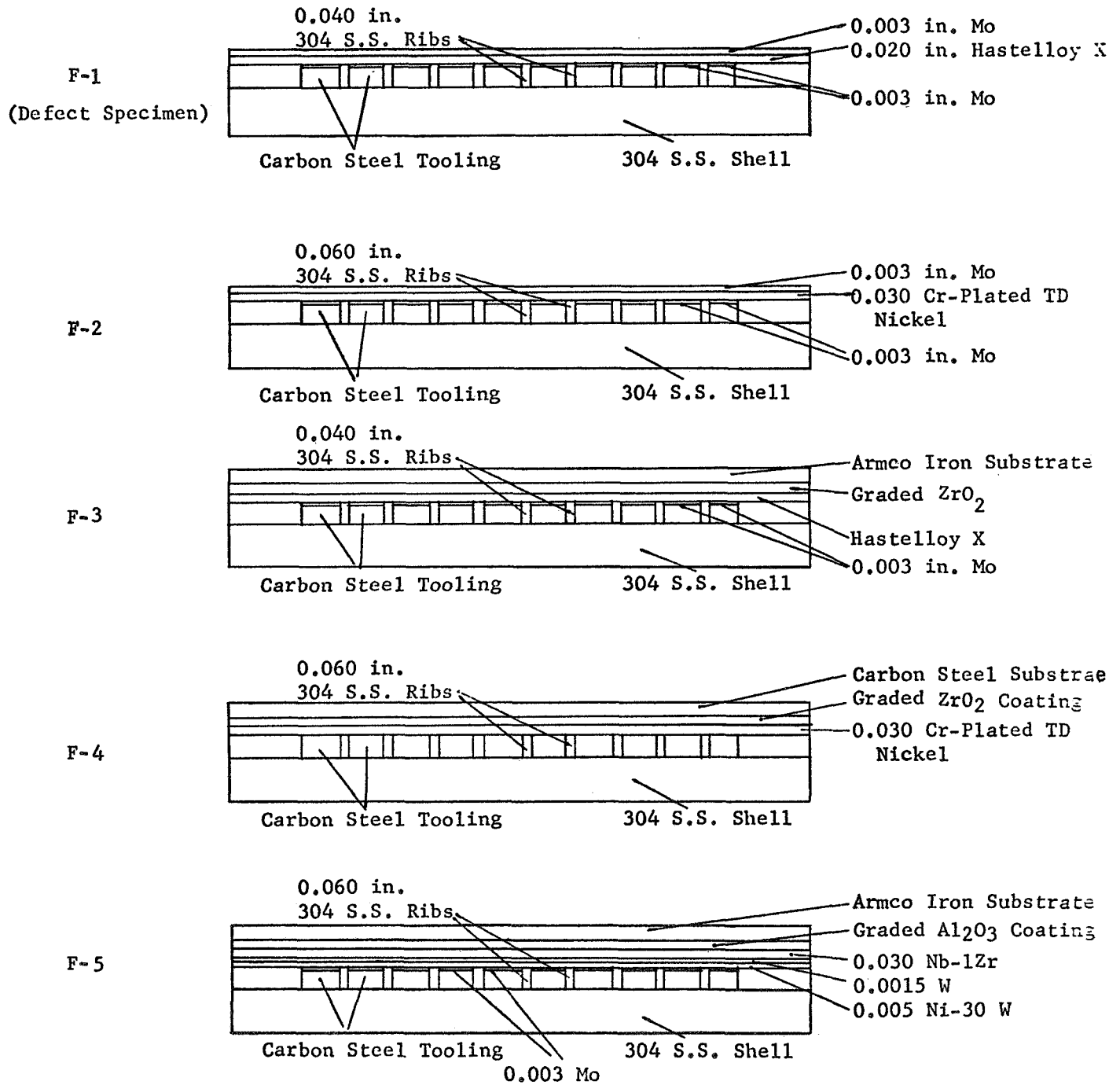
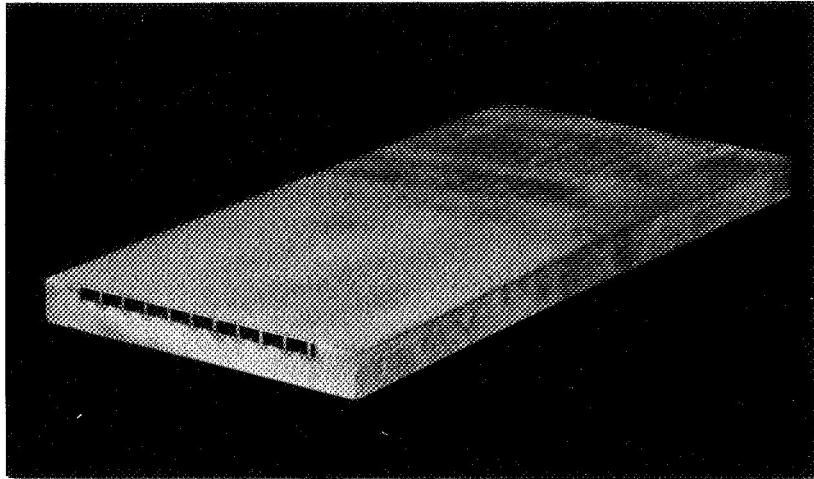
Specimen No.Construction

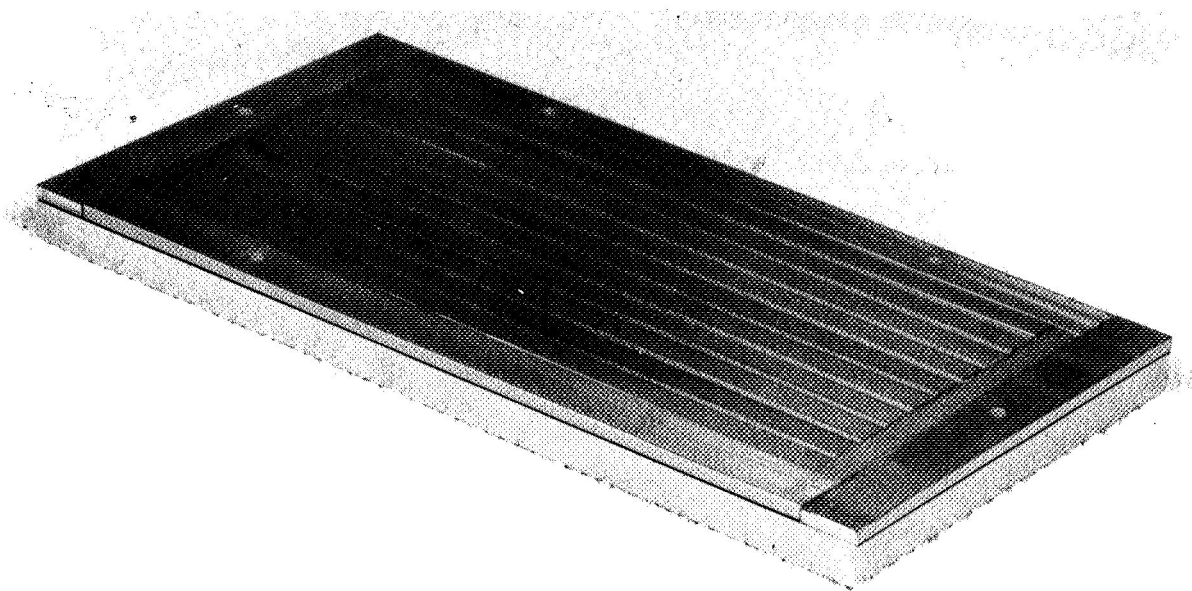
FIGURE 14. SCHEMATIC REPRESENTATION OF CROSS-SECTIONAL VIEW OF FULL-SIZE FLAT PANEL SPECIMENS



41665

FIGURE 15. FULL-SIZE FLAT-PANEL SPECIMEN OF FIRST GROUP

Specimen F3 is shown here after gas-pressure bonding at 2200 F and 15,000 psi for 3 hours. The tooling within the channels was removed with nitric acid.



45350

FIGURE 16. PARTIALLY ASSEMBLED FLAT-PANEL SPECIMEN OF THE SECOND GROUP

Stainless steel end plates assembled on each end were incorporated to facilitate burst testing.

TABLE 11. IDENTIFICATION OF SECOND GROUP OF FLAT-PANEL SPECIMENS

Specimen	Liner Material	Coating System ^(a)	Separator Layer ^(b)
FP-1	Chromallized TD nickel	Graded ZrO ₂	Be
FP-2	Chromallized TD nickel	None	None
FP-3	Chromallized TD nickel	None	None
FP-4	Hastelloy X	Graded ZrO ₂	Be
FP-5	Hastelloy X	Graded ZrO ₂	Al ₂ O ₃
FP-6	Hastelloy X	None	None

(a) The graded ZrO₂ coatings consisted of the following layers:

- 1st layer (next to liner) - 75 weight percent NiCr + 25 weight percent ZrO₂ (.006 inch thick)
- 2nd layer - 50 weight percent NiCr + 50 weight percent ZrO₂ (.006 inch thick)
- 3rd layer - 25 weight percent NiCr + 70 weight percent ZrO₂ (.006 inch thick)
- 4th layer - 100 weight percent ZrO₂ (.004 inch thick).

(b) Separator layers were plasma sprayed between the 4th layer of ZrO₂ and the Tinamel mandrel to promote preferential cracking and separation away from the protective oxide layers. (see Subtask I-3 for detailed description of coating developments).

checked by externally pressurizing the containers for 10 minutes with 200 psi of helium and immediately submerging the containers in an alcohol bath to inspect for leaks. No leaks were detected. The containers were gas-pressure bonded at 2200 F and 15,000 psi for 3 hours. After the bonding cycle, five of the six containers appeared slightly bulged. Pinhole leaks were found in the welds of the five suspect containers. The sixth container, Specimen FP-1, was gastight. The defective containers on the five specimens were machined off to inspect the panel components. In four of the five specimens, only partial bonding between components was achieved. In the fifth specimen, no bonding had occurred between the component parts. The components in these five panel specimens were disassembled, recleaned, and etched. The container design and welding procedures were modified to prevent leaks from developing during gas-pressure bonding. The specimens were recanned, welded, and sealed, and then gas-pressure bonded at 2150 F and 10,000 psi for 3 hours. The containers were leak checked after the bonding cycle and no leaks were detected. The containers were then removed by leaching in nitric acid.

Visual inspection of the five flat-panel specimens revealed the following:

- (1) The liners appeared to be well bonded to the stainless steel ribs and frame. Slight ripples in the liner surface outlined the rib location.
- (2) The edges of the TD nickel liners were slightly attacked during chemical leaching of the containers. The dissolution of nickel at the edges apparently resulted from exposing the unchromallized core of the chromium-diffusion treated TD nickel liners when the original containers, which leaked after the first bonding cycle, were cut off. Two edges of four were so cut, and after the second bonding cycle, as the containers were leached off, this exposed core of TD nickel was attacked to a depth of about 1/16 inch from the edge. The edges not cut, of course, were resistant to nitric acid and remained sound.
- (3) Slight deformation ripples were observed in the liner surface that could not be attributed to the ribs or tooling. These ripples occurred diagonally across the liner surface. It is believed that these ripples were caused by the .003-inch thick molybdenum-foil strips that became displaced from their original locations on the tooling pieces between the stainless steel ribs.
- (4) The oxide coatings on two of the three coated flat panels appeared to be well bonded to the liner, but the coating on one flat-panel liner was severely blistered. The blistered coating occurred on a panel with a Hastelloy X liner.

The displacement of molybdenum-foil strips across the ribs between the rib/liner interface had a double effect. The tooling/liner interfaces that came into contact because of the absence of the foil barrier left a scab of acid-resistant tooling at these locations because of chromium diffusion from the liner into the tooling. Also, this region where the molybdenum-foil strip intervened at the stainless steel rib/liner interface was unbonded since the molybdenum was removed during the leaching process.

To prevent further acid attack at the exposed edges of the TD nickel liners, attempts were made to seal the exposed edges. A small weld bead was put down at one TD nickel liner edge on two panels that contained no oxide. Because of the large heat-affected zone that resulted, it was felt that this method was not suitable.

Attempts were made to apply chemical-resists, paints, enamels, and resins to protect the edges of the TD nickel liners on which the unchromallized core was exposed. While a number of these produced impermeable protective coatings and looked promising, all coatings eventually broke down (became embrittled, cracked, attacked) when exposed to hot nitric acid solution for long periods (several days). Breakdown generally started at corners and edges. Polyvinylchloride (PVC) coatings provided protection for about 1 week, but then became embrittled and cracked. During this period the tooling in the flat panels was removed intermittently until about 50 percent of the tooling was removed from all panels. However, when the protective coatings broke down, nitric acid seeped in and came into contact with the unchromallized cores of the TD nickel liners. The exposed TD nickel cores were eventually attacked to a depth of about 1/4 inch.

It was evident that further attempts to remove the tooling without adequate protection at the edges of the unchromallized TD nickel liners would ruin the flat panels. Therefore, acid leaching was terminated and the development of a suitable method for protecting the unchromallized edges was undertaken.

Surplus pieces of chromallized TD nickel were used to develop a suitable protective coating. These were cut to expose the unchromallized core. The pieces were cleaned and coated with chromium by a commercial process, Udyllite's Cromylite K-50 system. The pieces were coated on the edges with about .0010 inch of chromium at 125 F. A current density of 75 amp/ft² was used initially to deposit about .0001 inch and then increased to 125 amp/ft² to build up to .0010 inch. Higher current densities deposited chromium at a faster rate but the coating was usually hard, very brittle, and cracked. The coating also had a greater tendency to build up at corners and edges at higher current densities.

After coating the TD nickel edges with chromium, the pieces were heated to 1600 F and held at this temperature for periods ranging from 1 hour to 30 hours in order to diffuse the chromium into the exposed edges of the TD nickel pieces. Since nickel with about 20 percent chromium resisted nitric acid attack, it was determined that these diffusion conditions provide 20 percent chromium at about .0015 inch in 1 hour to about .0025 inch in 15 hours. The samples were then exposed to the hot nitric acid solution to determine which diffusion conditions provided the best protection. Only one of four samples protected the TD nickel edges for short periods (less than 3 days). This was a chromium-coated sample heated at 1600 F for 8 hours. This sample protected the edges from acid attack for about 6 days; then the TD nickel core was attacked, slowly at first and then more severely with time. Since none of these techniques successfully protected the exposed TD nickel cores, further efforts to protect the two flat-panel specimens with TD nickel liners were terminated.

The three flat-panel specimens containing Hastelloy X liners were heat treated and quenched to desensitize the liners and preclude intergranular attack during tooling-removal processes. During leaching of the tooling in hot nitric acid solution, the reaction was initially vigorous but reduced in activity after about 1/2 inch of the tooling in the channels was removed. Attempts to increase the reaction by flushing and injecting the channels with fresh acid, heating the solution to 200 F, and using other acid solutions to remove passivated layers were of no avail. The tooling had become acid resistant owing to the loss of the diffusion-barrier (molybdenum foil) protection during gas-pressure bonding [see observation (3) above], which allowed the nickel and chromium in the Hastelloy X liners to diffuse into the low-carbon-steel tooling. The acid-resistant scales were thus incapable of being removed by acid-leaching techniques.

SUBTASK I-2. SPECIMEN EVALUATION AND TESTING

Nondestructive Testing

Nondestructive tests were initially conducted in subscale Specimen II-1 which contained a number of intentional defects. This panel was evaluated by thermal techniques and by ultrasonic testing.

One test evaluated was Bondcheck, a heat-affected fluid. This particular formulation is repelled by warm areas and coalesces in cooler areas. Magnaflux BC-4 liquid was sprayed on the liner surface and the part was heated from the shell side. In principle, the ribs should preferentially conduct the heat to the liner, thus establishing thermal gradients on the surface. This technique did delineate the rib locations, although the resolution was poor. Owing to the poor resolution, it was impossible to positively identify any defects. The liner acted as a heat sink. Heat is conducted laterally as well as through the liner, and temperatures tend to stabilize in the vicinity of a rib. This test would probably gain sensitivity as the thickness of the liner decreased.

Similar difficulties were experienced with liquid crystal testing. Heat-sensitive crystals, which respond to temperature changes of only 3 C with a series of color changes, are premixed with a wax carrier. The mixture was flowed onto the surface of the liner and allowed to dry. A thermal gradient was established, either by heating or cooling the panel from the side of the stainless steel shell. As with the heat-affected fluid, resolution was very poor. No defects could be positively identified. Again, the problems are apparently due to the thickness of the liner and the tendency of temperature to equalize in the area of a rib.

Initial ultrasonic testing was performed by the Columbus laboratory of Sperry Division of Automation Industries. The specimen was immersed in water, and transmission by reflection was the technique utilized. Both the rib-liner and rib-shell bonds were examined. The testing parameters involved the utilization of four different sensitivity settings. Equipment and testing parameters are summarized in Table 12.

TABLE 12. ULTRASONIC TEST EQUIPMENT AND PARAMETERS

Testing Head	3/4-inch-diameter focused lithium sulfate transducer (15 megahertz resonant frequency)
Test Instrument	UM 715 Reflectoscope
Technique	Specimen was suspended in H ₂ O media between testing head and aluminum reflector plate; 1-1/2 or 1-1/4-inch water path between testing head and specimen
Pulse Frequency	5 megahertz
Sensitivity Settings (Relative)	0.8 x 1, 1.4 x 1, 2 x 1, 10 x 1

Only the gross defects (3/16-inch-wide slots) were found by examination from the Hastelloy X liner side. However, in subsequent testing at Battelle, all of the planned defects were located using the through-transmission technique. It was necessary to locally fabricate a beam collimator from Styrofoam. In addition to these planned defects, several additional spots of questionable bond integrity were discovered.

The first set of full-sized panels were successfully hydrostatic proof tested at 500 psi. The technique involved placing a manifold system in the channels at one end of the specimen and then sealing both ends of the specimen with a low-melting alloy (wood's metal). The panels were then pressurized hydraulically to 500 psi. Following this operation the alloy was removed and panels were examined for interchannel leaks. The only defects discovered were pinholes that had leached through the TD nickel liner at defects in the chromium plating.

The panels could not be tested at 2000 psi, because of unsuccessful attempts to seal the panels by welding or brazing. A second group of flat-panel specimens was fabricated by gas-pressure bonding for the purpose of incorporating end plates to facilitate hydrostatic proof testing at 2000 psi. One flat-panel specimen from the second group was subsequently proof tested. This was Specimen FP-1, shown sectioned in Figure 17a after hydrostatic proof testing was completed. The specimen leaked at one corner because of intrusion by the displaced molybdenum foil. Figure 17b shows the effect of molybdenum displacement on the rib bond to the liner.

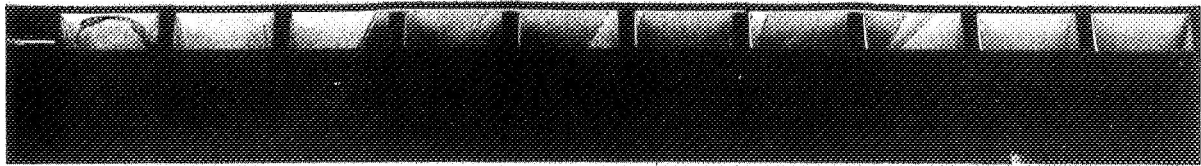
Double-Lap-Shear-Test Specimens

A total of five double-lap-shear-test specimens were fabricated and gas-pressure bonded at 2200 F and 15,000 psi for 3 hours. These specimens were fabricated to test the bond strengths of the various materials combinations encountered in the fabrication of the specimens. This required four specimens. In addition, one specimen was fabricated from 347 stainless steel.

The specimen designs for the five material combinations are shown in Figures 18 through 21. The specimens incorporated carbon-steel spacer components which were removed after bonding by leaching. These specimens were encapsulated in flanged bonding containers. The specimen components were cleaned by the previously developed techniques, and were outgassed, sealed, and bonded with the first group of full-size panels.

A postbond leak check revealed that Specimens S-2, -3, and -4 leaked during bonding. The leaks occurred because the container walls were of insufficient thickness.

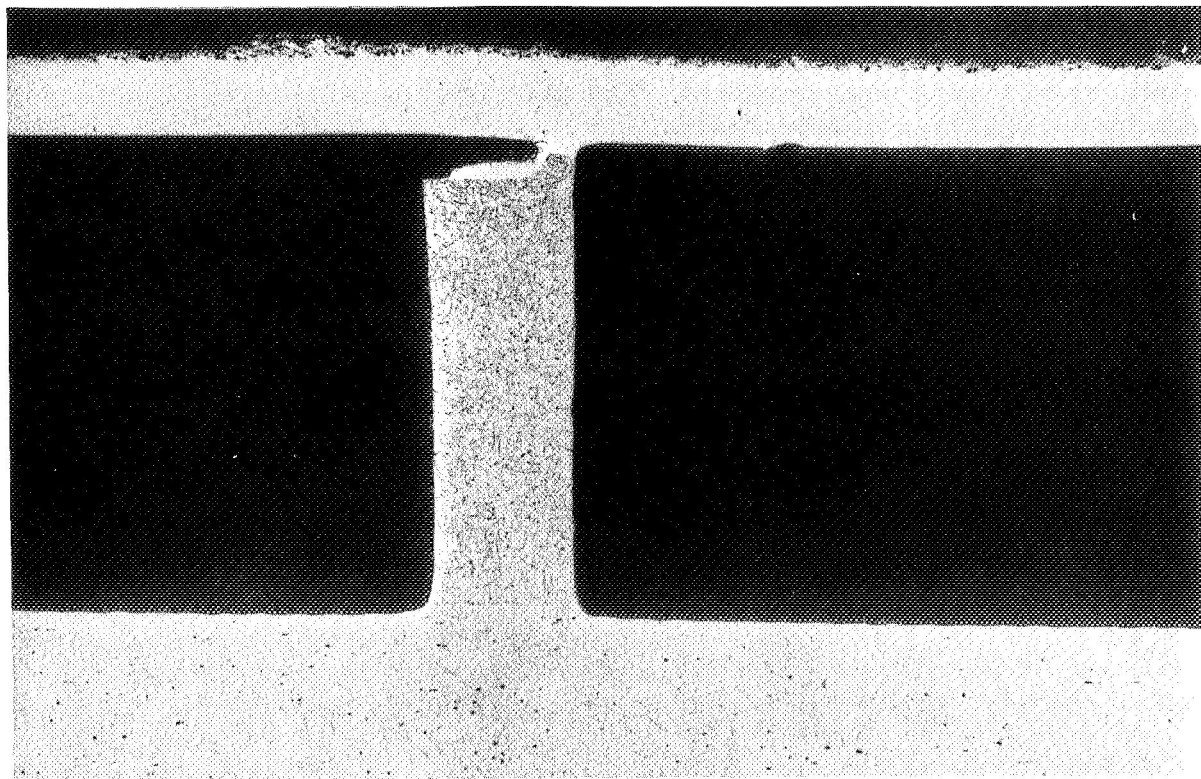
The remaining two specimens were leached with 50 percent nitric acid solution. After leaching, the 3-1/2-inch-wide specimens were cut into 1-inch-wide strips for testing. A typical specimen is shown in Figure 22. The specimens were tested at a strain rate of $.002 \text{ minute}^{-1}$. The test results (summarized in Table 13) were much lower than anticipated, and it is believed that the specimen components were contaminated by oxides prior to bonding.



2X

A

7E468



20X

B

7E467

FIGURE 17. SECTION OF FLAT-PANEL SPECIMEN FP-1 AFTER HYDRO-STATIC PROOF TESTING

Leaks occurred in corner owing to displacement of molybdenum foil. The misarrangement is detectable by the patterns on the inside surfaces of the liner. The foil was leached away at the same time the steel tooling was removed and left unbonded rib-to-liner regions.

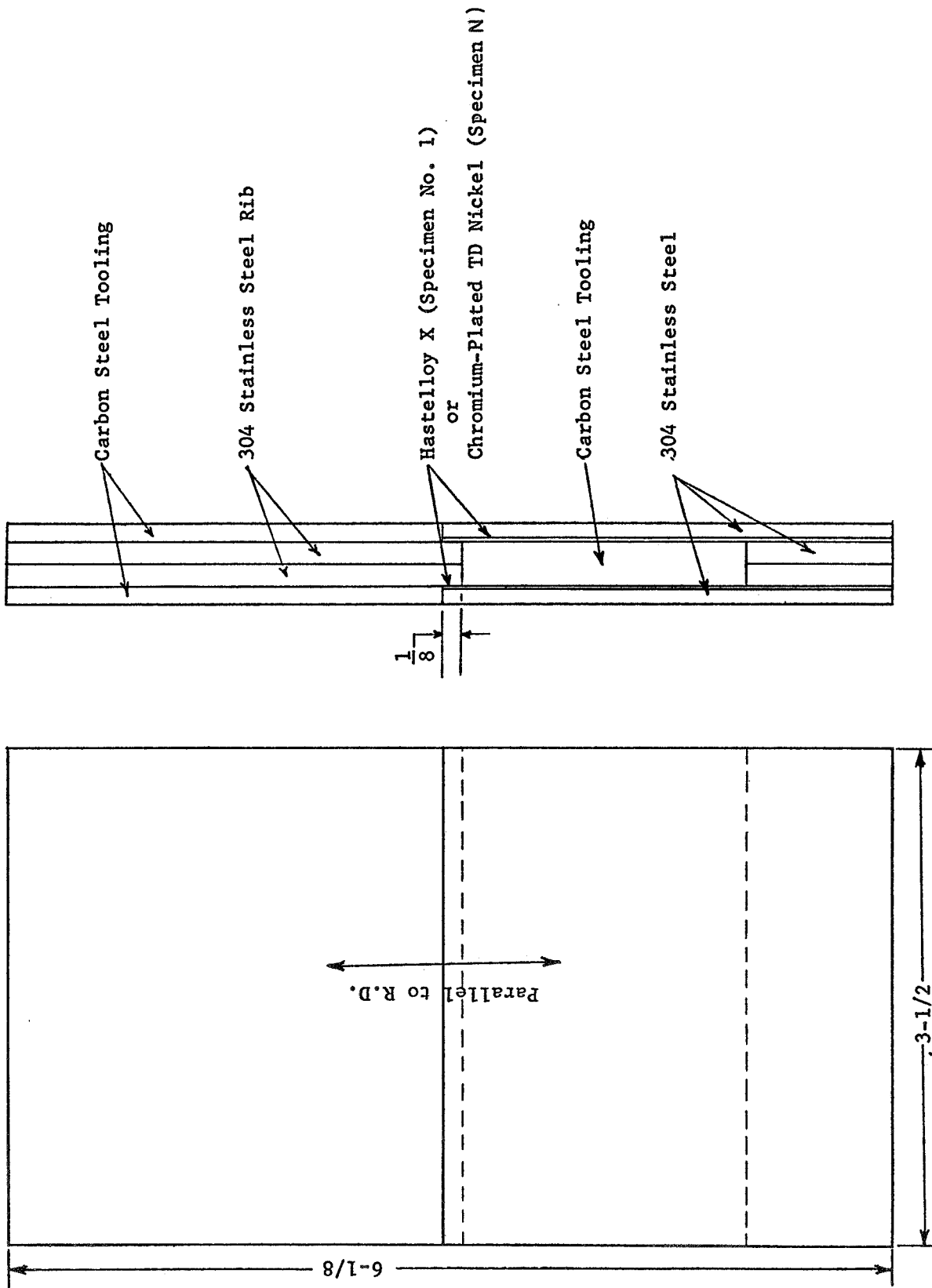


FIGURE 18. SHEAR-SPECIMEN DESIGN FOR HASTELLOY X AND TD NICKEL-304 STAINLESS STEEL LINER TO RIB BONDS (SPECIMENS 1 AND 2)

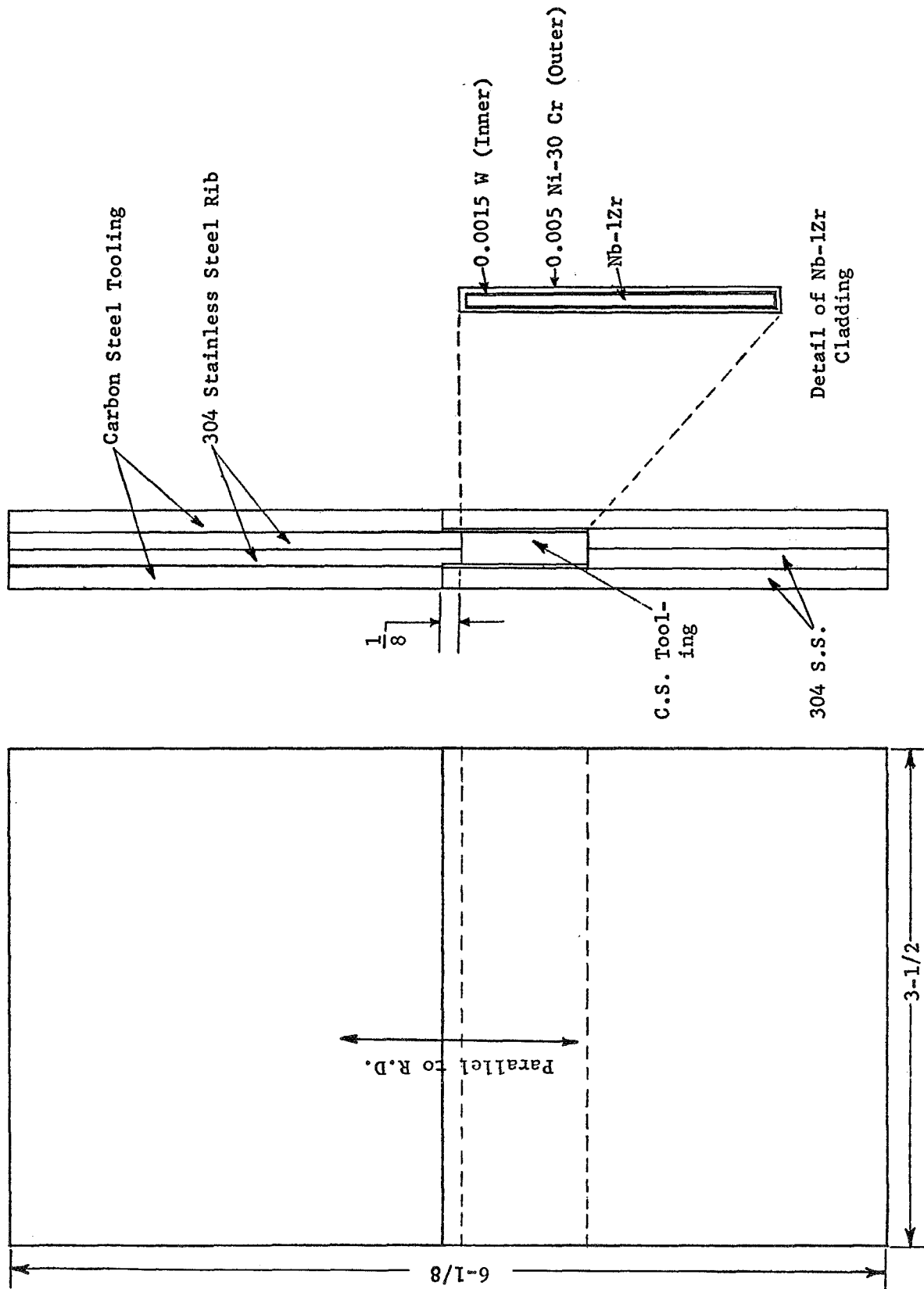


FIGURE 19. SHEAR-SPECIMEN DESIGN FOR Nb-1Zr - 304 STAINLESS STEEL LINER TO RIB BOND (SPECIMEN 3)

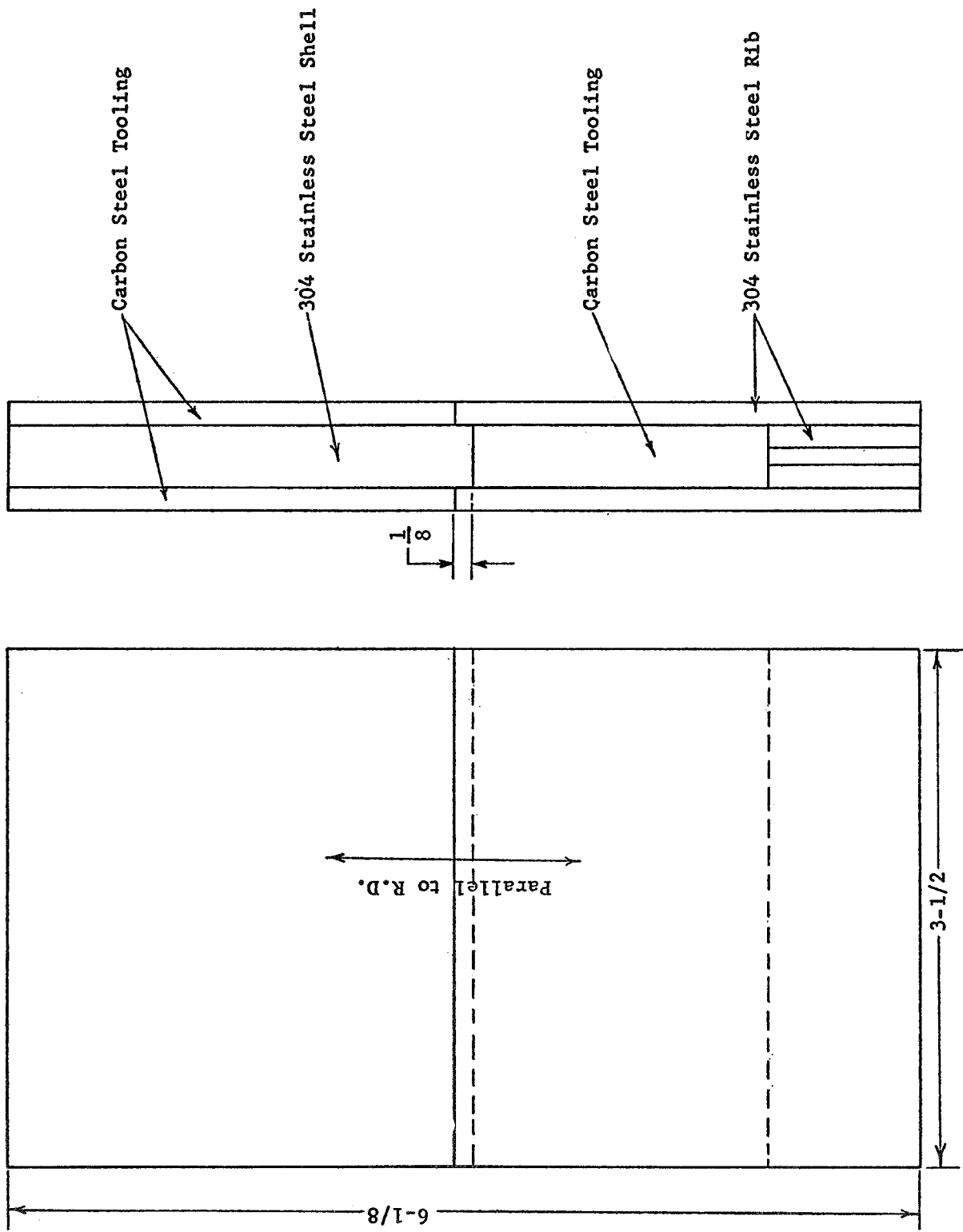


FIGURE 20. SHEAR-SPECIMEN DESIGN FOR 304 STAINLESS STEEL RIB-SHELL BOND (SPECIMEN 4)

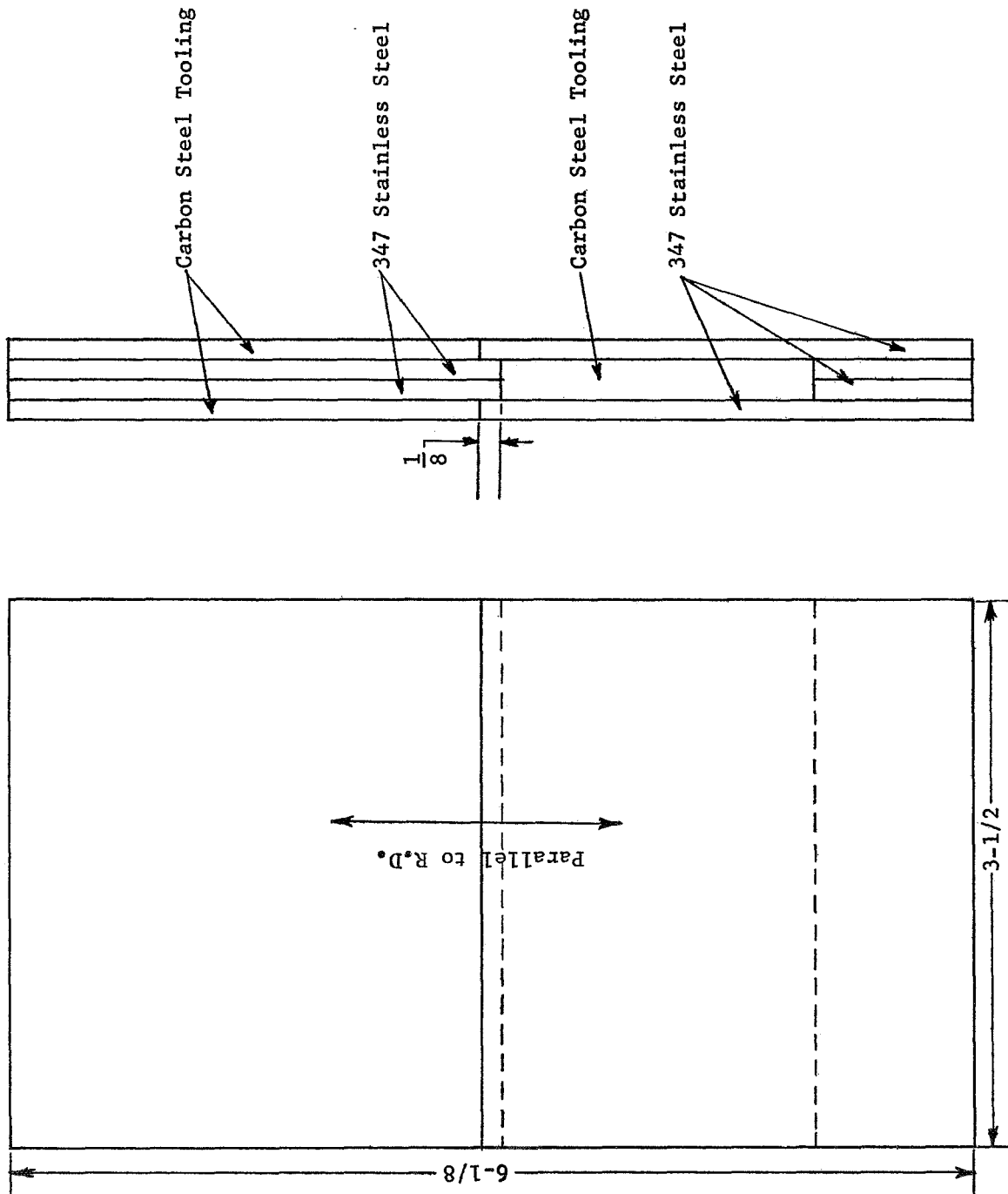
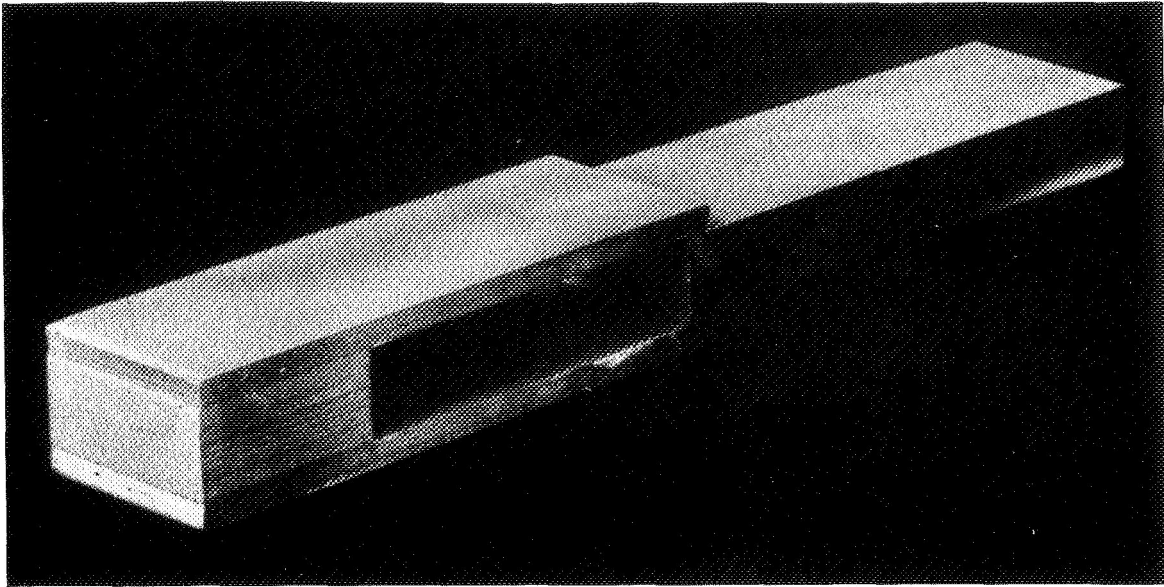


FIGURE 21. SHEAR-SPECIMEN DESIGN FOR 347 STAINLESS STEEL SELF-BOND (SPECIMEN 5)



41667

FIGURE 22. DOUBLE-LAP-SHEAR-TEST SPECIMEN

This specimen was prepared from 304 stainless steel and simulated from the rib-to-stainless steel shell bond to be expected in spool-piece fabrication.

TABLE 13. SHEAR-TEST RESULTS

Specimen	Bond	Bond Strength, ksi	Fracture
S-1	304 SS rib:Hastelloy X liner	10.2	Brittle(a)
	304 SS rib:Hastelloy X liner	2.5	Brittle
	304 SS rib:Hastelloy X liner	6.2	Brittle
		avg. 6.3	
S-5	304 SS rib:304 SS shell	25.3	Ductile
	304 SS rib:304 SS shell	28.7	Ductile
	304 SS rib:304 SS shell	27.2	Ductile
		avg. 27.1	

(a) The 304 stainless steel:Hastelloy X bonds appeared to be contaminated.

SUBTASK I-3. DEVELOPMENT OF CERAMIC COATINGS

Oxide-Coating Approach

The approach selected for application of the oxide coatings was to plasma spray either Al_2O_3 or ZrO_2 onto a metal (either carbon steel or Armco iron) mandrel which would then be positioned over the liner with the oxide in contact with the liner for bonding. The reason for the selection of such an approach rather than spraying directly on the liner was that the liner will be deformed during fabrication and assembly. Any plasma-sprayed coating would crack and spall off. Instead, the nondeformable carbon-steel mandrel was to be plasma sprayed.

Group I. Coating of Small-Scale Specimens

In the first group of subscale specimens, an attempt was made to bond Al_2O_3 to Nb-1Zr and ZrO_2 to Hastelloy and to TD nickel. These test specimens were bonded at 2200 F and 10,000 psi for 3 hours. When these specimens were sectioned in the containers and examined metallographically, it appeared that none of the coatings had adhered to their respective liner materials. Therefore, it was decided to evaluate a graded oxide coating using the same approach, i.e., spray a plate other than the liner and transfer the oxide coating to the liner.

Group II

A ZrO_2 -nickel cermet was bonded to nickel-plated Hastelloy X. Slight cracking occurred in the cermet layer, probably because of thermal-expansion mismatch. The bonding between the liner and coating was good, however. Several test coupons prepared in this manner were bend 90 degrees over a 1/4-inch radius without spalling the coating.

Figure 23 shows chromium plated TD nickel with a graded ZrO_2 coating. The integrity of the cermet portion of the coating is excellent, but the pure oxide portion contained a number of cracks. The oxide-coated Nb-1Zr was similar.

Group III

Later in the program, it was found that the oxide coatings could be bonded directly to the liner materials. This was accomplished with the aid of a friable layer, in this case an aluminum silicate felt (Fiberfrax), which was placed between the can material and coating. The specimen liners were prepared by mechanical abrasion. The oxides were placed on the liner plates by mechanical means rather than by plasma spraying, and a layer of Fiberfrax felt was inserted between the ceramic and the bonding container. During cooling from the bonding conditions, the Fiberfrax fractured and caused a separation between the oxide and container. Thus, the oxide coating had only to adjust to the thermal-expansion differences of the liner.

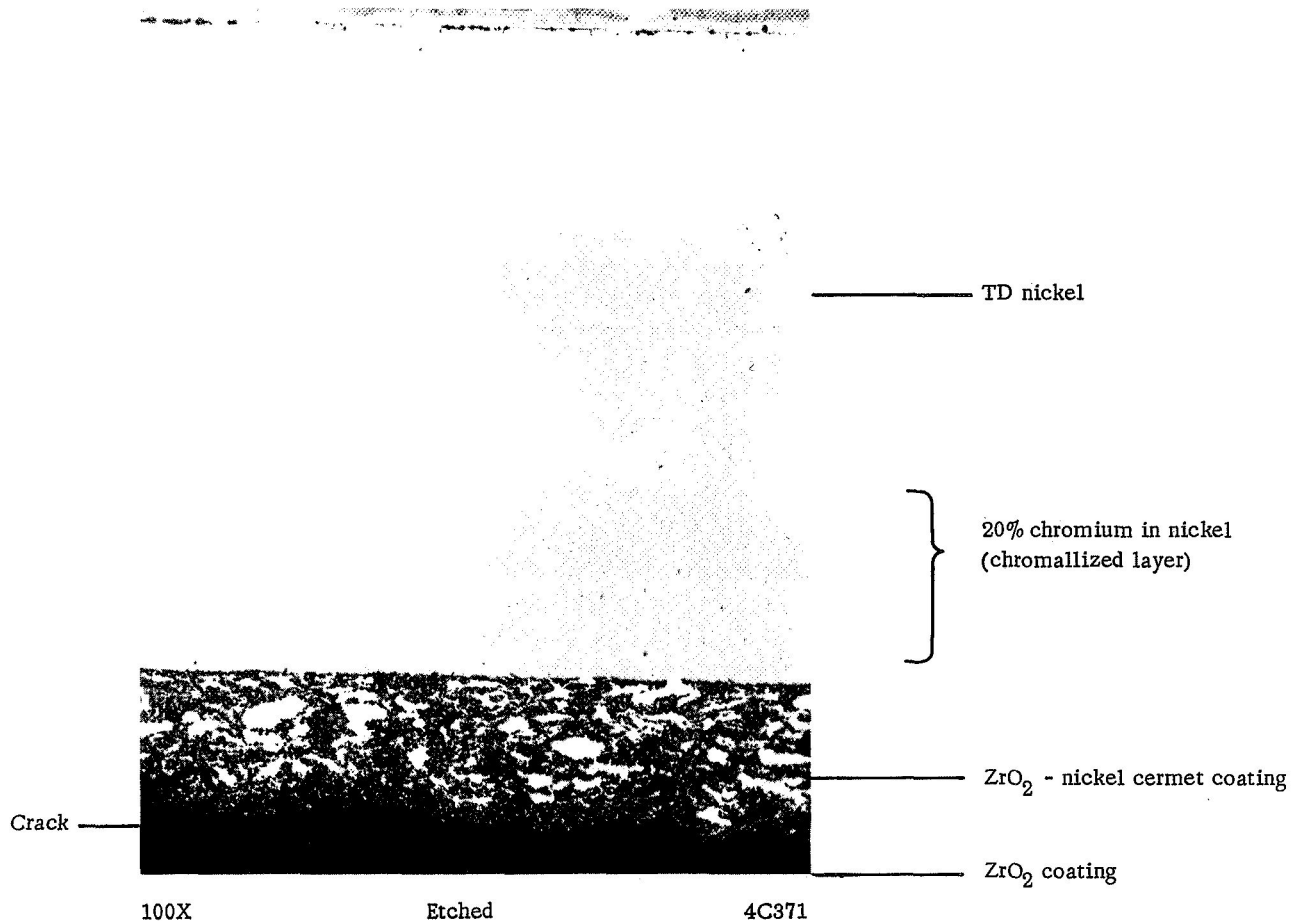


FIGURE 23. ZrO_2 GRADED COATING BONDED TO CHROMALLIZED TD NICKEL

The ZrO_2 coating separated from the cermet layer.

The ZrO_2 coatings on Hastelloy X and TD nickel liners are shown in Figures 24 and 25. The coatings appear to be bonded to the liners, and it was apparent that mechanical interlocking of the coating and liner was a factor in bonding. The coatings are somewhat porous, but this can be attributed to the initial mode of application. Plasma-sprayed coatings would have a higher bonded density. This approach was later adopted in supplementary work discussed in the section on Additional Coating Development Work.

Coating of Subsize Flat-Panel Specimens

Group I

Three specimens in the first group of five subsize flat-panel specimens had oxide coatings plasma sprayed onto the liners. As indicated previously in Table 6, Specimens I-3 and I-4 had ZrO_2 coatings and Specimen I-5 had an Al_2O_3 coating. After gas-pressure bonding at 2200 F and 10,000 psi for 3 hours, it was found that the ZrO_2 coatings had cracked and did not bond to the liners. This was attributed to

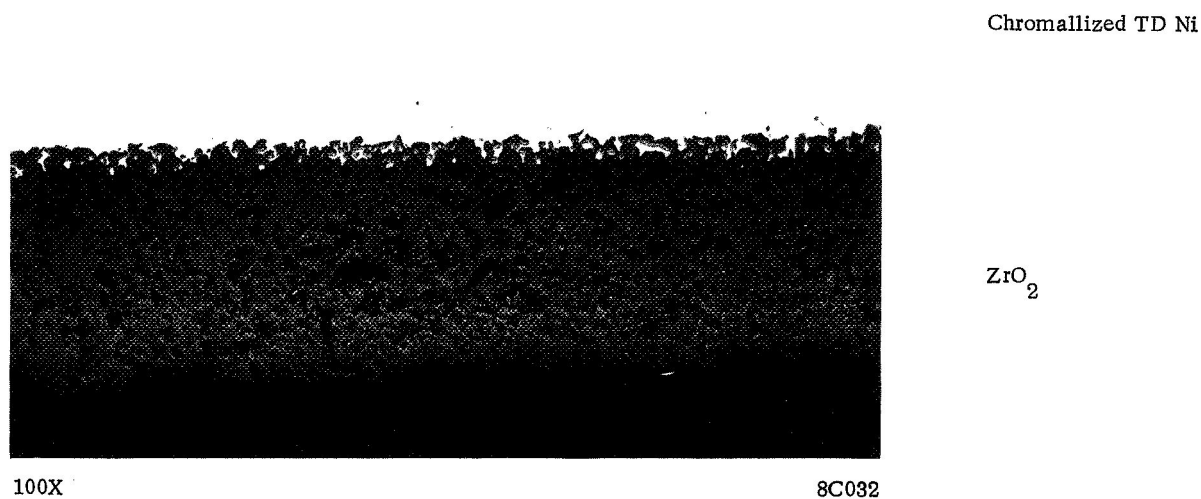


FIGURE 24. ZrO_2 COATING BONDED TO CHROMALLIZED TD NICKEL

The oxide powder was applied mechanically rather than plasma sprayed. Some porosity in the oxide is evident. The oxide penetrated the metal surface and produced strong mechanical bonds as well as chemical bonds.



FIGURE 25. ZrO_2 COATING BONDED TO HASTELLOY X

The ZrO_2 powder was applied mechanically and gas-pressure bonded at 2200 F and 15,000 psi for 3 hours. Some porosity in the oxide still exists. Mechanical interlocking of oxide and metal is evident.

thermal-expansion mismatch between the container (low-carbon steel) and the coatings. The coating on Specimen I-5 did not densify owing to a container leak during gas-pressure bonding.

Group II

Three specimens in the second group of five subscale flat-panel specimens also had oxide coatings plasma sprayed onto the liners, but these coatings were graded with nickel or niobium powder. Specimens II-3 and II-4 had nickel-graded ZrO_2 coatings and Specimen II-5 had a niobium-graded Al_2O_3 coating (see Table 7). The liner on Specimen II-3 was Hastelloy X, that on Specimen II-4 was chromallized TD nickel; and that on Specimen II-5 was Nb-1Zr. After gas-pressure bonding at 2200 F and 15,000 psi for 3 hours, the containers were leached off and the coatings examined metallographically. Specimen II-5 was not examined because of a container leak which precluded densification of the oxide coating. In the other two specimens, the graded portions of the oxide were crack-free, dense, and well bonded to the liners. The 100 percent ZrO_2 layer on top of the graded layers was cracked in both specimens. The cracking was attributed to thermal-expansion mismatch between the oxide and the graded layers.

Coating of Full-Size Flat-Panel Specimens

Group I

The first group of full-size flat-panel specimens contained five graded layers of ZrO_2 blended with nickel powder. The sequence of gradations was as follows:

- (1) Plasma sprayed .006 inch of pure oxide on a steel plate mandrel
- (2) Plasma sprayed .006 inch of 80 volume percent oxide-20 volume percent metal on oxide coating
- (3) Plasma sprayed .006 inch of 60 volume percent oxide-40 volume percent metal
- (4) Plasma sprayed .006 inch of 40 volume percent oxide-60 volume percent metal
- (5) Plasma sprayed .006 inch of 20 volume percent oxide-80 volume percent metal.

During gas-pressure bonding, the fifth layer was transposed onto the metal liner and the pure oxide layer (first layer) was expected to separate from the mandrel. Gas-pressure bonding was accomplished at 2200 F and 15,000 psi for 3 hours. After the containers were leached off, it was observed that the ZrO_2 coating layers had cracked. The cracked regions allowed nitric acid to penetrate into the graded-layer region, and the acid attacked the nickel portion of the graded layers. The oxide layers spalled off thereafter.

Group II

The Group II full-size flat-panel specimens were designed primarily to bond end plates to the open ends and permit the flat panels to be burst tested. Three of the six panels also had ceramic-coated liners (Specimens FP-1, FP-4, and FP-5). The coatings consisted of ZrO_2 graded with Ni-30Cr powder in two to three distinct layers, plus a thin parting agent, as indicated in Table 14.

TABLE 14. SEQUENCE OF PLASMA-SPRAYED COATINGS FOR
SECOND GROUP OF FULL-SIZE FLAT-PANEL SPECIMENS

Specimen	Layer	Mixture	Thickness, inch
FP-1	(1)	75 NiCr-25 ZrO_2	.006
	(2)	50 NiCr-50 ZrO_2	.006
	(3)	100 ZrO_2	.005
	(4)	100 Be(a)	.002
FP-4	(1)	75 NiCr-25 ZrO_2	.006
	(2)	50 NiCr-50 ZrO_2	.006
	(3)	100 ZrO_2	.005
	(4)	100 Be(a)	.002
FP-5	(1)	50 NiCr-50 ZrO_2	.006
	(2)	100 ZrO_2	.005
	(3)	100 Al_2O_3 (a)	.002

(a) Beryllium and Al_2O_3 were deposited as parting layers to induce cracks and easy separation between the ZrO_2 coating and the low-carbon-steel mandrel.

These flat-panel specimens was gas-pressure bonded at 2200 F and 15,000 psi for 3 hours. After completing the bonding cycle, five of the six flat-panel specimens, including two with oxide coatings, were slightly bulged, which indicated that the containers had leaked during the cycle. One specimen, FP-4, remained gastight during the bonding cycle. This specimen was decanned by leaching off the container. The oxide coating on Specimen FP-4 appeared to be dense, sound, and well bonded to the liner. Since the other containers leaked, the specimens were removed, recanned, and gas-pressure bonded at 2150 F and 10,000 psi for 3 hours. During this second cycle, all the containers remained gastight. The containers were removed by leaching in nitric acid. Inspection of the coatings on Specimens FP-1 and FP-5 revealed that the coating was sound and well bonded to the TD nickel liner on Specimen FP-1 but that the coating on the Hastelloy X liner of Specimen FP-5 was severely blistered.

Additional Coating-Development Work

A primary difficulty in developing a suitable coating for Hastelloy X and TD nickel liners was that in transferring the coatings from a plasma-sprayed mandrel onto the liners during gas-pressure bonding the coatings would crack owing to thermal expansion mismatch. To solve this problem, two alternative approaches were examined simultaneously. One involved the use of graded coatings. The other involved the use of parting layers to preferentially crack and release the coating from the mandrel surface. Twelve coating systems consisting of 2 by 2-inch flat coupons were formulated for

evaluation. These systems included six different parting-layer materials on ungraded and graded layers of ZrO_2 . The coatings were bonded to either Hastelloy X or chromalized TD nickel liner materials. A description of the twelve coating systems is given in Table 15.

As a consequence of this additional coating-development work, significant results of special interest evolved. These are described in Appendix B.

TABLE 15. DESCRIPTION OF COATING SYSTEMS FABRICATED IN
ADDITIONAL COATING-DEVELOPMENT WORK

System Designation	Liner	Coating and Barrier System
C-1	TD nickel	Graded - Be
C-2	Hastelloy X	Graded - Al_2O_3
C-3	Hastelloy X	Graded - MgO
C-4	Hastelloy X	Graded - Mo
C-5	Hastelloy X	Graded - W
C-6	Hastelloy X	Graded - Nb-1Zr
C-7	Hastelloy X	ZrO_2 - Be
C-8	Hastelloy X	ZrO_2 - Al_2O_3
C-9	TD nickel	ZrO_2 - MgO
C-10	TD nickel	ZrO_2 - Mo
C-11	Hastelloy X	ZrO_2 - W
C-12	Hastelloy X	ZrO_2 - Nb-1Zr

TASK II. FABRICATION AND TESTING OF CYLINDRICAL SPOOL PIECES

Basic Approach

Two spool-piece chambers were to be fabricated according to Drawing No. D620402 and delivered to NASA-LeRC for hot testing. A completed spool-piece chamber would look similar to the drawing in Figure 2b, but would have in addition the plenum assembly to admit the coolants. At NASA-LeRC, the chambers were to be hot tested with both hot water and liquid-hydrogen cooling. These tests are to prove the fabrication concept using actual rocket firing conditions. The chamber is bolted to a hydrogen-oxygen injector and a nozzle section, and is fired and checked intermittently to establish the chamber's response to actual conditions and to determine failure mechanisms.

The chambers fabricated during this task had 347 stainless steel outer shells and ribs (instead of the 304 type used in Task I). One chamber was fitted with an inner liner of TD nickel, and the other with a Hastelloy X liner. The liner was bonded to a carbon-steel mandrel simultaneously with an outer layer of tooling. This outer layer was to be grooved to receive the premachined stainless steel ribs. The stainless steel shell was then to be positioned over the ribbed structure and the final bond effected.

After bonding and removing the tooling with acid, the chambers were to be non-destructively tested for bond integrity and residual tooling, leak checked, and hydrostatic proof tested as called for in Drawing D620402 before sending them to NASA-LeRC for actual hot-testing.

SUBTASK II-1. PREPARATION OF CYLINDRICAL-SPOOL-PIECE COMPONENTS FOR GAS-PRESSURE BONDING

Materials used in this task are listed in Table 16; the property data are given in Appendix C. The Tinamel tooling sleeves were roll formed from 0.45-inch thick plates to fit around the mandrel-liner assembly. The mating edges of the roll-formed sleeve were seam welded. The sleeves were then machined to a thickness of 0.30 inch to provide thick weldments and ensure a good gastight seal during gas-pressure bonding.

TABLE 16. SUMMARY OF MATERIALS REQUIRED IN
TASK II STUDIES

Component	Material
Tooling	Titanium-killed iron plate (Tinamel)
Liner	Hastelloy X sheets ^(a)
Liner	TD nickel sheet ^(a)
Rib	347 stainless steel sheet (18 gage) ^(a)
Mandrel	Hot-rolled round (1018 carbon steel)
Shell	347 stainless steel rolled-ring forgings
Barrier	Molybdenum foil (.003 inch)

(a) Properties are given in Appendix C.

Welding Study

Since the sleeve was to be welded to the low-carbon-steel mandrel, and to insure that all welds would be of highest integrity, a study was initiated to determine the best technique for welding, welding parameters, and joint design. The initial studies were performed with low-carbon-steel plates. After the welding parameters and joint design were established, welds were made with enameling-iron plate. The gas-tungsten-arc-welding technique was selected. A constant voltage head was employed and shielding was provided with helium gas. Linde 65 deoxidizing filler was utilized for filler material. This is an aluminum-killed steel that lessens oxygen-induced porosity. The following weld parameters were established:

Voltage	16 volts
Amperes/Pass	200
Helium-Shielding-Gas	
Flow Rate	50 feet ³ /hour
Heat-Travel Speed	15 inches/minute
Filler-Feed Speed	40 inches/minute

The joint design for the sleeve closure was a 90-degree level with a 1/16 inch land. Eight passes were required to fill the joint. A weldment composed of Tinamel base plates with silicon-killed steel filler were subjected to a simulated autoclave cycle. The weldment was heated to 2300 F, held for 3 hours, and furnace cooled. The specimen was then sectioned for metallographic examination. No detrimental effects were observed. A typical section is shown in Figure 26. The grain size of the material in the final weld passes was smaller than the initial grain size, because of the greater content of filler material in this area.

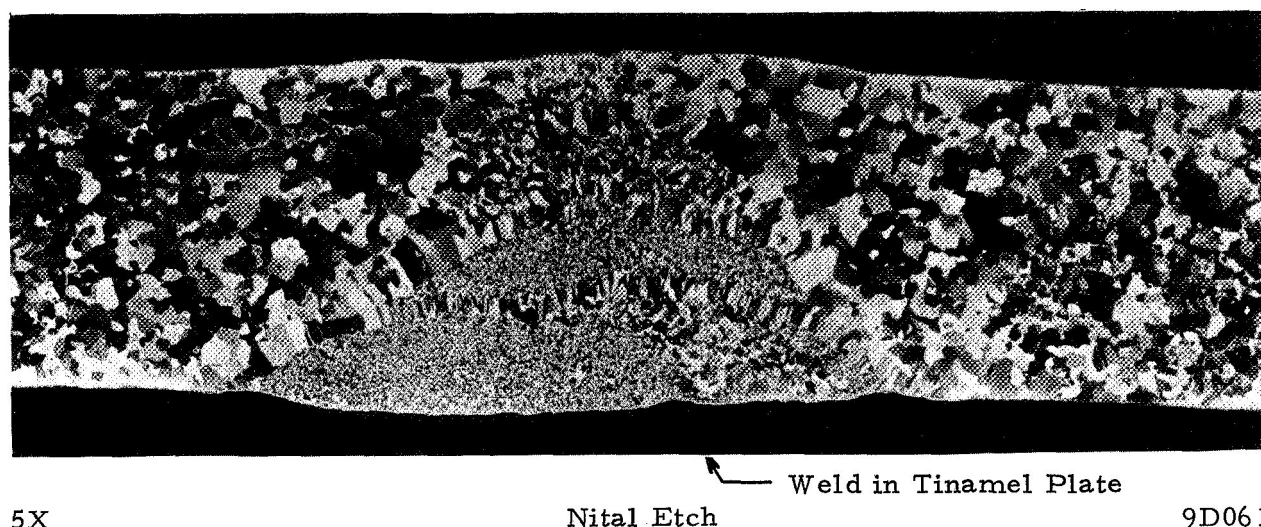


FIGURE 26. WELD IN TINAMEL TEST PLATE AFTER EXPOSURE TO SIMULATED AUTOCLAVE CYCLE AT 2300 F FOR 3 HOURS

Preparation of Components for Assembly

After these parameters were determined, hot-rolled 1018 carbon-steel rounds for the mandrels were machined, degreased, vapor blasted, and cleaned. The liners, consisting of chromallized TD nickel sheet .037 inch thick and Hastelloy X sheet .032 inch thick, were roll formed, chem-milled at the overlapping edges about 1/4 inch wide, degreased, and cleaned. The molybdenum-foil diffusion barriers .003 inch thick, were cleaned by degreasing and chemically etching the surfaces. The overlapping edges (about 1/4 inch wide) were photoetched to remove 1.5 mils. The foils were to be placed between the mandrel and the liner and between the liner and the tooling sleeve so as to prevent diffusion of carbon from the mandrel into the liners and to prevent diffusion of chromium and nickel from the liners into the steel mandrel and into the Tinamel tooling sleeve.

SUBTASK II-2. ASSEMBLY AND FABRICATION OF
CYLINDRICAL SPOOL PIECES

Assembly of Specimen 1 (Hastelloy X Liner)

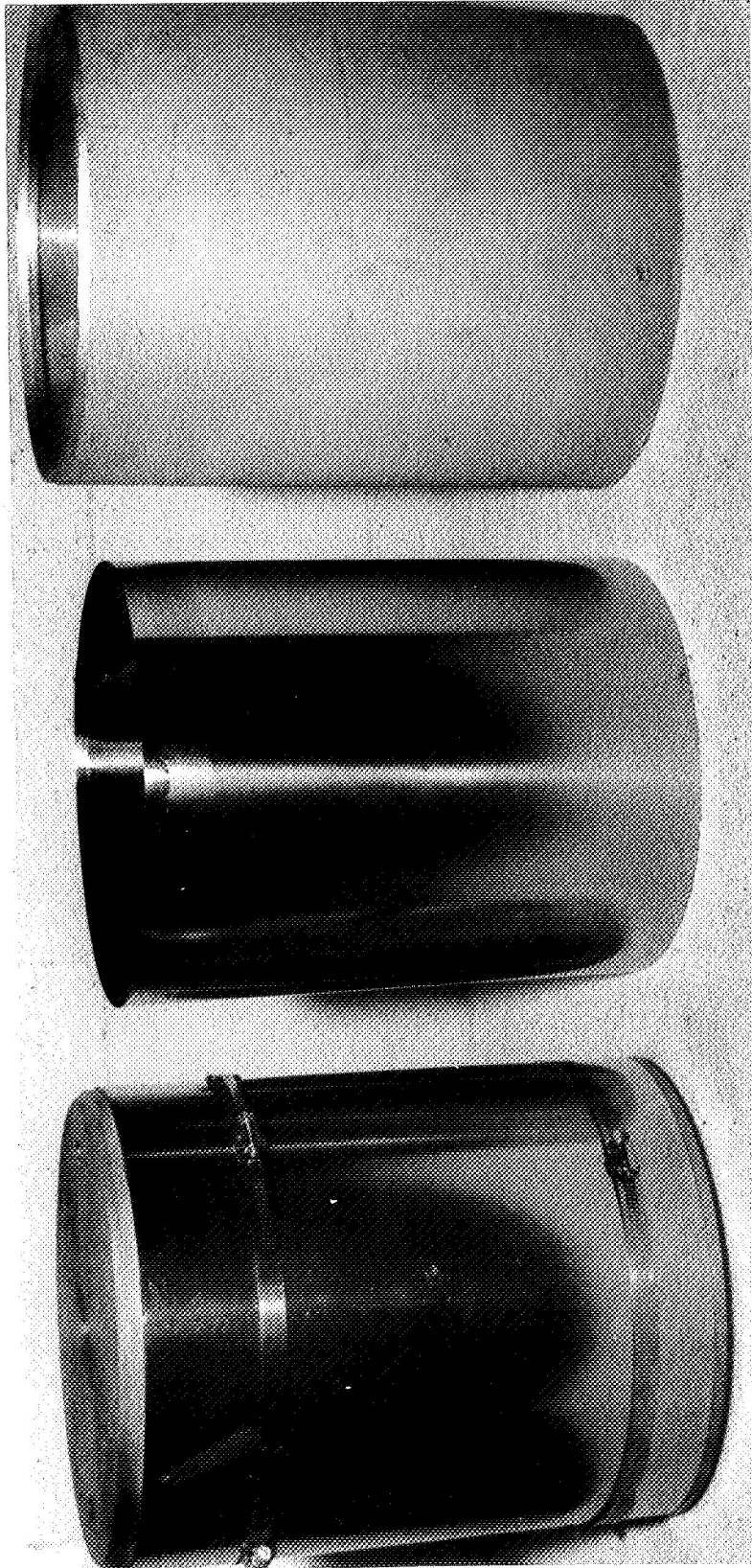
Initial attempts to assemble Specimen 1 containing the Hastelloy X liner were unsuccessful because the Tinamel sleeve was out-of-round by about 1/16 inch on the 10.83-inch diameter and had a taper on the ID amounting to .030 inch over a 13-inch length. The sleeve was press formed, which reduced the out-of-roundness tolerance to $\pm .015$ inch. The taper was then machined out from the inner surface. The steel mandrel was vapor blasted to remove oxide from the surfaces. The molybdenum foils and Hastelloy X liner were cleaned, as summarized in Table 17, and assembled onto the mandrel. The components are shown in Figure 27. The Tinamel sleeve was fitted over the assembly, as illustrated in Figures 28 and 29, and then welded to the steel mandrel by TIG welding in an argon atmosphere. A 1/4-inch stainless steel evacuation stem was positioned through the Tinamel sleeve at one end to facilitate outgassing and sealing. The specimen was inspected for leaks with a helium leak detector by evacuating through the stem while flooding the external surfaces with helium. No leaks were detected. The specimen was then outgassed at 550 F for 2 hours and sealed by forge welding the evacuation stem.

TABLE 17. CLEANING PROCEDURES FOR LINER MATERIALS

Step	Operation	Temperature, F	Time, min	Current Density, amp/ft ²
1	Degrease with MEK and alcohol	RT		
2	Scrub with detergent and rinse	RT		
3	Scrub with Shipley Scrub-Cleaner No. 11 and rinse	RT		
4	Electropolish in 20 volume percent H ₂ SO ₄ -80 volume percent H ₃ PO ₄			
	(a) Chromallized TD nickel	120	3	500
	(b) Hastelloy X	120	1-1/2	300
5	Cold rinse	RT		
6	Hot rinse	150		
7	Hot rinse with distilled water	130		
8	Alcohol rinse	RT		
9	Store in alcohol	RT		

Assembly of Specimen 2 (TD Nickel Liner)

Initial attempts to assemble the TD nickel liner and inner molybdenum foil around the steel mandrel of Specimen No. 2 were frustrated by slight warpage and increased dimensions of the liner due to the chromium diffusion treatment. This was corrected by filing the overlapping edges to the proper dimensions. To prevent initiation of micro-cracks in the hard liner surface by this corrective measure, only light strokes in one direction with the face of the file flat against the edge of the liner were permitted. Subsequent cleaning of the components and the assembly were accomplished without further difficulty.



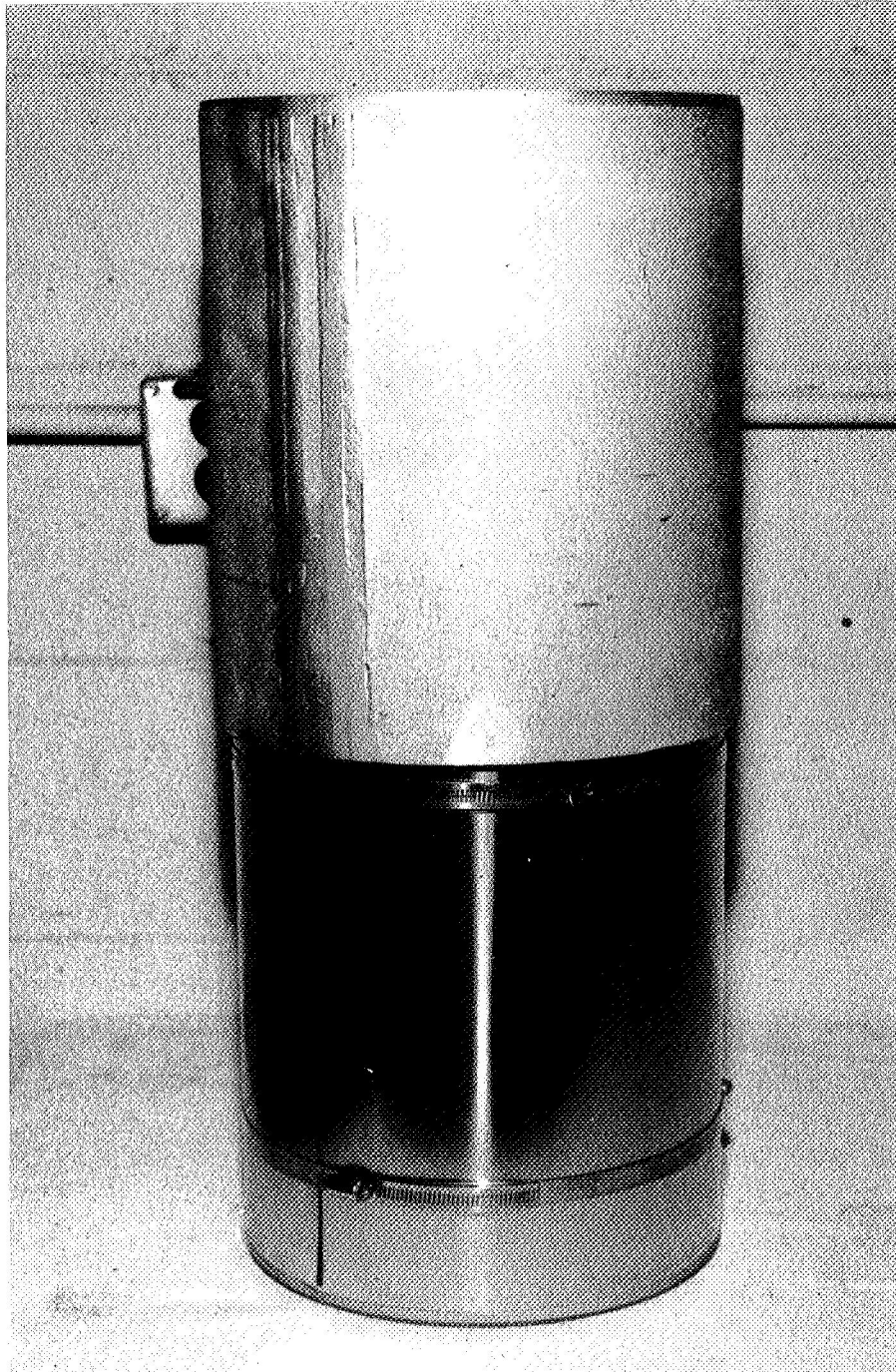
66268

Tinamel Sleeve

Outer Molybdenum Foil

Steel Mandrel Wrapped with
Inner Molybdenum Foil and
Liner

FIGURE 27. SPOOL-PIECE COMPONENTS PARTIALLY ASSEMBLED



46270

FIGURE 28. ASSEMBLY OF TINAMEL SLEEVE OVER
CLAMPED COMPONENTS



46271

FIGURE 29. SPOOL-PIECE-SPECIMEN 2 ASSEMBLED AND
READY FOR WELDING

Welding and Sealing

Welding of the Tinamel sleeve to the mandrel was conducted by TIG welding in an argon atmosphere to prevent oxidation and contamination of the inner and outer molybdenum foils. Welding was accomplished according to the parameters established by the weld study above.

The circumferential weld was made to seal the Tinamel sleeve to the mild-steel mandrel. The stress imposed on this joint was expected to be small. The joint was a single-V, 90-degree included angle 3/8 inch deep. The assemblies were placed in an oil-diffusion-pumped vacuum chamber and evacuated to at least 5 microns. Pumping time was at least 15 hours. The chamber was then backfilled with welding-grade helium (for Specimen 2) or helium plus argon (for Specimen 1) for welding. Specimen 1 was welded up completely by the manual GTA process. Specimen 2 had only the root-pass welded in the chamber. When the first weld on one end was completed, the chamber was opened. The assembly was turned over and the chamber pumped down again so that the same procedure could be followed on the joint at the other end.

Because no vent hole was provided in Specimen 1, the last weld tended to form a blowhole as the gas trapped inside the heated assembly expanded through the liquid weld metal. The blow holes were sealed by allowing the assembly to cool and then quickly welding over the blowhole.

Specimen 2 had only the root pass completed in the weld chamber. An evacuation tube was welded to the sleeve to prevent any serious blowholes from forming. The assembly was allowed to cool in the welding chamber. A Tygon hose was attached to the evacuation tube and the hose was sealed at one end. This allowed an inert gas atmosphere to be present in the assembly while the final welds were made, thus minimizing oxidation of the internal components. The circumferential welds on Specimen 2 were completed using an automatic, voltage-controlled GTA head. One end was sealed in three passes, the other end in five passes. Wire brushing with a stainless steel brush was used to clean between passes. Welding conditions were:

Welding Current	200 to 210 amperes
Welding Voltage	17.2 to 17.4 volts
Arc Travel Speed	8.5 ipm
Filler Wire	1/16-inch-diameter Linde 65 to 40 ipm
Shielding Gas	Helium at 50 cfh

All welds were inspected visually and no cracks were observed. One small pore in the root pass of the first weld in Specimen 2 was repaired manually. After the welding of Specimen 1 was completed, a 1/4-inch stainless steel evacuation stem was positioned through the Tinamel sleeve at one end to facilitate outgassing and sealing. Outgassing was necessary to remove any moisture or alcohol retained on the shell components from the cleaning process. The specimen was first checked for leaks by evacuating through the stainless steel tube into a helium mass spectrometer and purging the welds externally with a stream of helium. No leaks were detected. Specimen 2 was outgassed at 550 F. After outgassing, the specimens were sealed hot and then allowed to cool in air. This prevented backstreaming of air or other contaminants from the pump into the specimen.

First Gas-Pressure-Bonding Cycle

The two spool-piece specimens were gas-pressure bonded at 2200 F and 10,000 psi for 3 hours. The temperature was raised initially to about 1750 F before applying a pressure of more than 1500 psi; then the temperature and pressure were raised simultaneously to the bonding conditions. After the 3-hour hold period, the spool pieces were cooled under pressure, with a pressure of at least 5200 psi remaining on the specimens after they had cooled to below 200 F.

Postbonding Operations

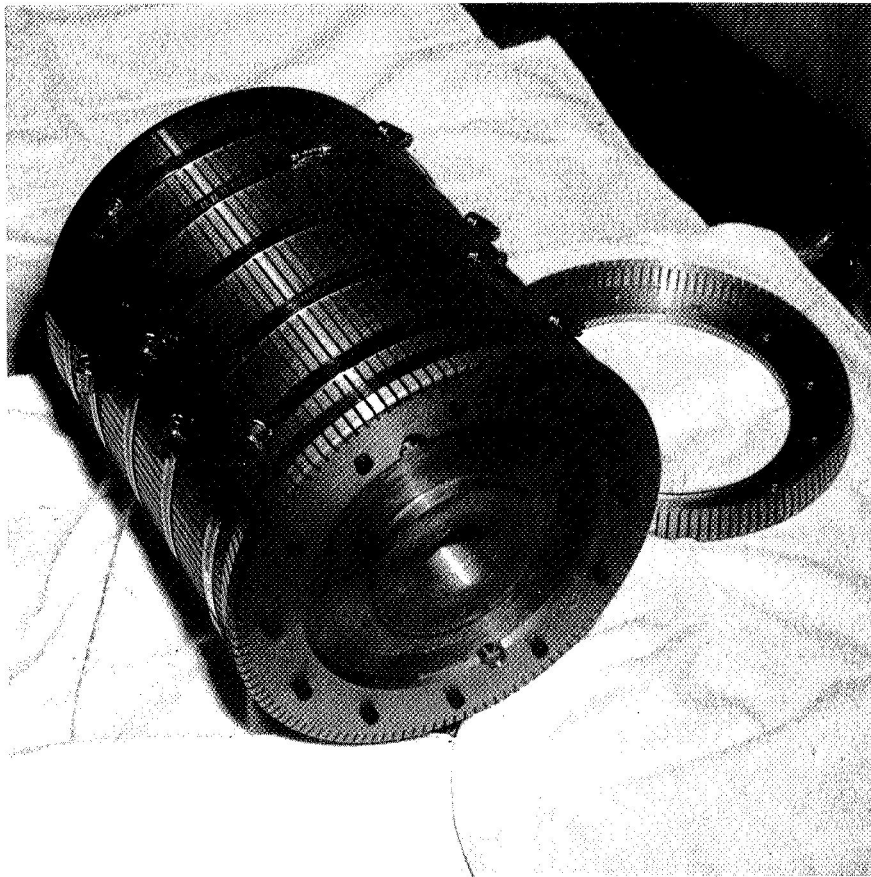
The next step was to machine the spool pieces and provide slots for the stainless steel ribbing in the Tinamel sleeve. The liners were located accurately by facing the ends of each spool piece, thereby exposing the liners. After referencing the liners, the Tinamel sleeve was machined to about .092-inch wall thickness. One hundred and twenty slots, each .100 inch deep, were to be machined into the sleeve to cut through the outer molybdenum foil (.003-inch thick and located between the Tinamel sleeve and the liners) and provide a .005-inch-deep slot in the liners for each stainless steel rib. However, upon cutting the first two slots, it was discovered that the molybdenum-foil barriers did not bond completely to the Tinamel sleeve and caused separation of the Tinamel sleeve from the liners. On the spool with the TD nickel liner (Specimen 2), the separation was complete and the sleeve was removed. On the spool with the Hastelloy X liner (Specimen 1), partial bonding of the molybdenum foil to the sleeve was achieved, and the sleeve could not be removed.

Since the molybdenum-foil barriers did not bond completely to the Tinamel sleeve, it was probable that the inner molybdenum-foil barrier did not bond completely to the steel spool mandrel. No attempt was made to remove the liners and inner foil barriers from the mandrel. Instead, efforts were initiated to salvage the spool pieces and sleeves, and to prepare the tooling, stainless steel forgings, and other components for assembly and gas-pressure bonding.

Preparation of Specimens for Second Gas-Pressure-Bonding Cycle

The steps involved in these salvaging efforts were numerous (34 steps in all to prepare the spool pieces for gas-pressure bonding) and these are given in Appendix D along with related work drawings. Figure 30 shows the slotted Tinamel spool piece after completion of Step 6 (Appendix D). One end clamp is shown pulled off from one end of the spool piece.

Measurements on the liner indicated that the spool piece was slightly out-of-round. Grooving of the Tinamel tooling sleeve was required to be deeper than planned in order to assure that the slots cut through the 3-mil molybdenum outer barrier layer and into the liner. If the outer molybdenum layer was not removed, the stainless steel ribs inserted into these slots would not bond to the liner during gas-pressure bonding. As a result of the deeper slots (grooving) made in the Tinamel, the original stainless steel ribs (made .100 inch high) were unsuitable and additional (347 type) stainless steel ribs had to be cut and made about .115 inch high. This corresponded to redoing Step 7 (Appendix D).



Spool-Piece-Specimen 2

47631

FIGURE 30. SLOTTED TINAMEL TOOLING SLEEVE ON SPOOL PIECE

One end clamp, used to hold the Tinamel ribs in place, is shown removed. Five aero clamps also help to fix and hold location of slotted Tinamel ribs.

Assembly of Specimen 1

After slotting of Specimen 1 (with the Hastelloy X liner) was completed, the stainless steel ribs were inserted between the Tinamel tooling ribs and the stainless steel forged ring shells and end closures were welded in place. Guide rails to protect the thermocouples were welded to the shell periphery. A stainless steel evacuating stem was placed in the top end closure to facilitate leak checking and sealing. The specimen was leak checked on a helium mass spectrometer and no leaks were detected. The specimen was evacuated overnight and sealed at 7×10^{-3} torr by forge welding the evacuation stem.

Assembly of Specimen 2

Specimen 2 containing the chromallized TD nickel liner was assembled first by using end clamps to hold the Tinamel ribs in place and aero clamps to hold the stainless steel ribs in place. Once the stainless steel ribs were in place, it was noted that the ribs had a tendency to twist, even with the clamps in place. Since the aero clamps eventually had to be removed during assembly into the forged shell, it was feared the ribs would shift excessively. To prevent this, the assembled spool was wound with thin-gage steel wire. The wire held the stainless steel and Tinamel ribs in place during assembly and would become an integral part of the specimen. The assembled and wound specimen is shown in Figure 31. The spool piece was then assembled into the forged shell and the end closures were welded in place. During leak checking, it was found that the weld had cracked in two places. These cracks were repaired and the specimen was again helium leak checked. No leaks were detected.

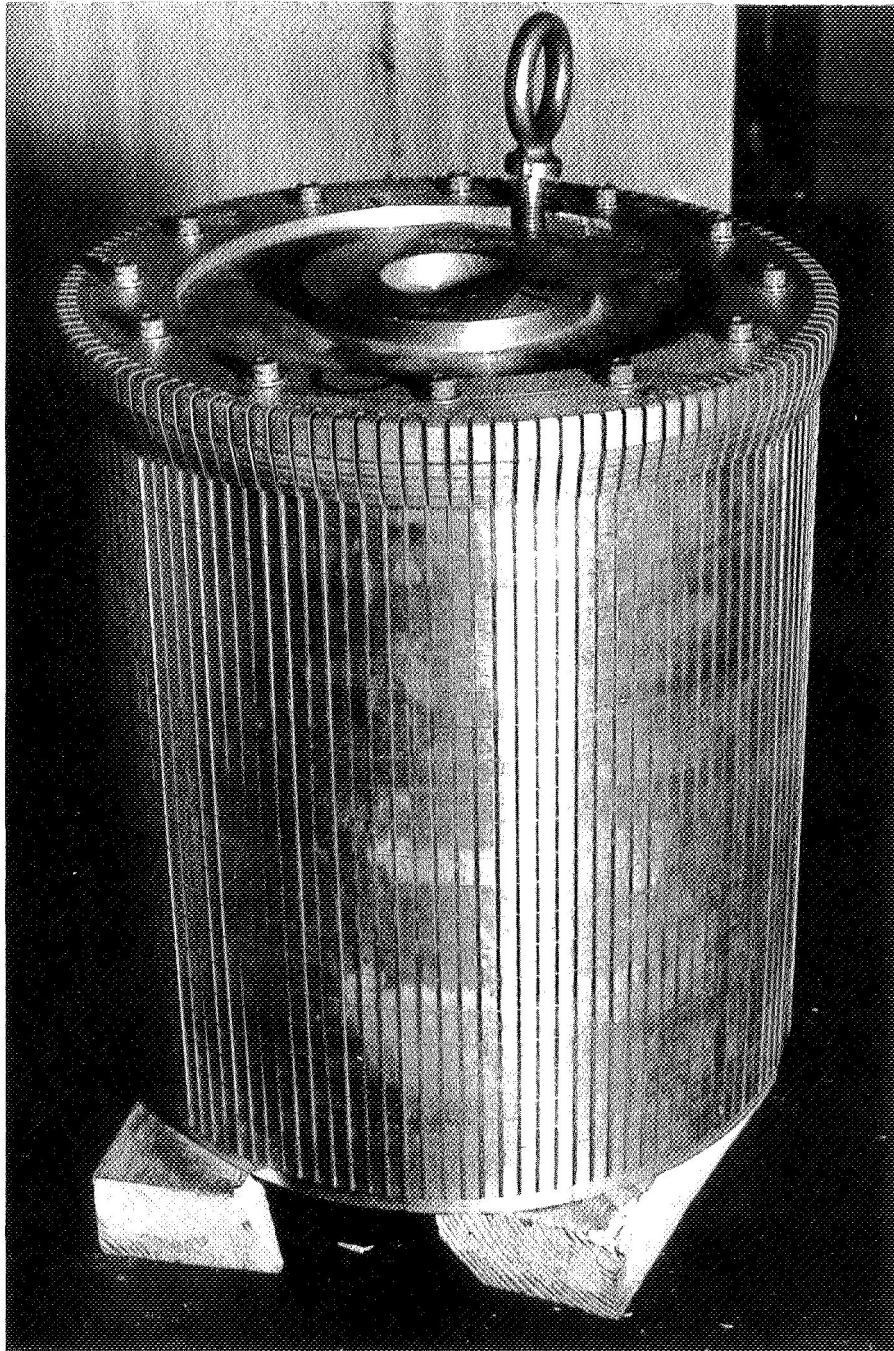
Specimen 2 was evacuated overnight and then sealed at less than 10^{-3} torr by forge welding the evacuation stem.

Second Gas-Pressure-Bonding Cycle

Both specimens were placed in the autoclave and separated by about 6 inches of bubbled alumina. Thermocouples were placed through the guide rails on each specimen to monitor temperature at the shell surface during gas-pressure bonding.

A thermal analysis was conducted to determine the amount of time required to bring all components within the specimen to an adequate temperature for diffusion bonding. The thermal-analysis model started with the shell surface at 2150 F, with 15,000 psi helium-gas pressure at the surface. Figure 32 shows a cross section of the specimens used to determine heat conduction through the components. Figure 33 shows how temperature should vary with time at different points in the specimens.

Within 2 hours the liner components inside the shell should be at 1900 F. Within 3 hours these same points are within 15 degrees of 2100 F. The components reach a steady temperature of 2140 F in about 5 hours. In the actual bonding cycle, the surface temperature was raised gradually to 2150 F so that the internal components could reach a stable temperature near 2150 F in much less time than predicted by the thermal study once the skin temperature reached 2150 F. Then, to assure that adequate diffusion between components occurred, particularly between the 347 stainless steel ribs and the liner, the specimens were subjected to a temperature of 2150 F for at least 4 hours.



47974

FIGURE 31. SPECIMEN 2 ASSEMBLED AND WIRE WOUND TO MAINTAIN RIB POSITIONS DURING ASSEMBLY INTO THE STAINLESS STEEL SHELL FORGING

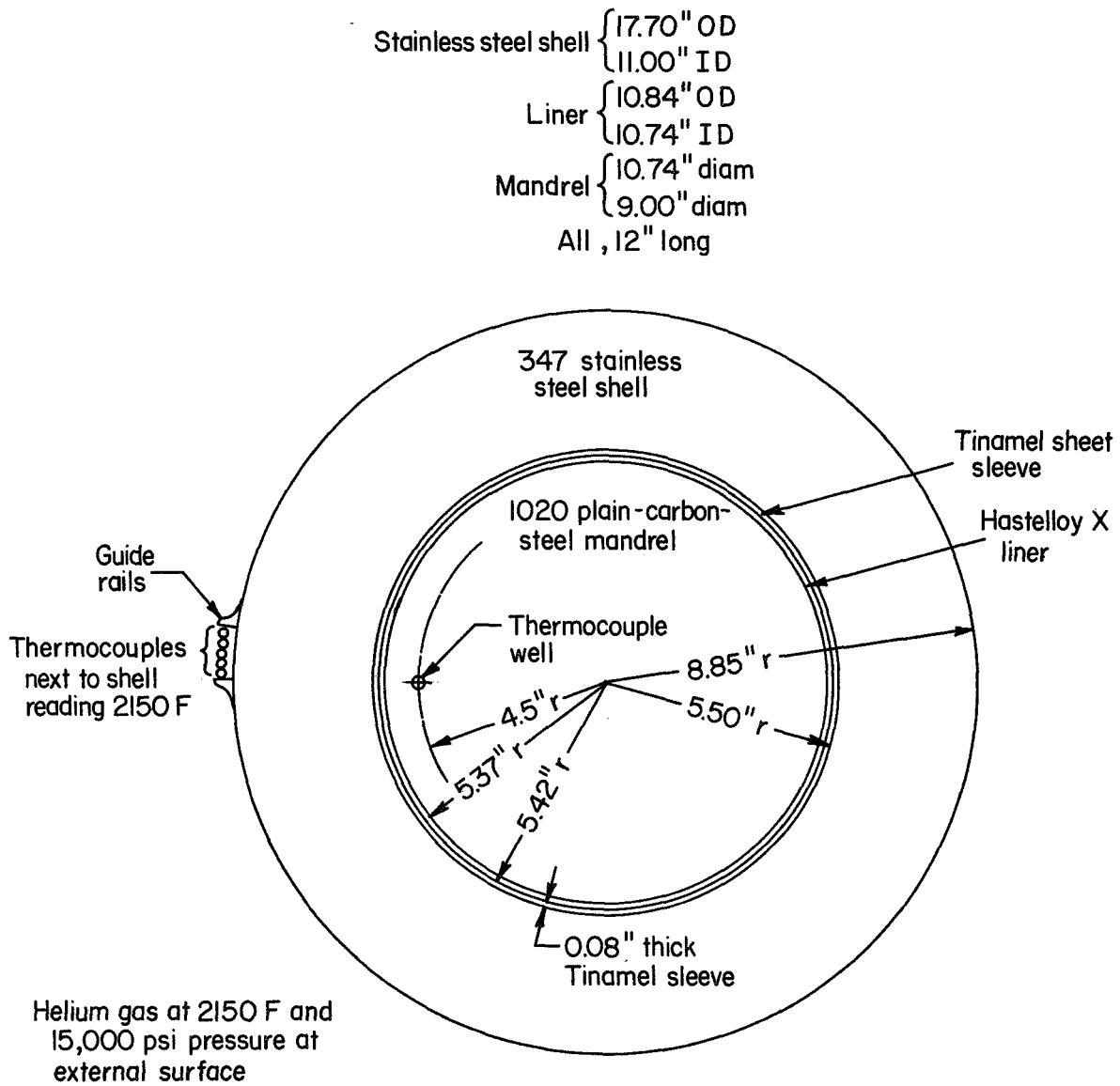


FIGURE 32. MODEL OF SPOOL SPECIMENS USED FOR THERMAL ANALYSIS

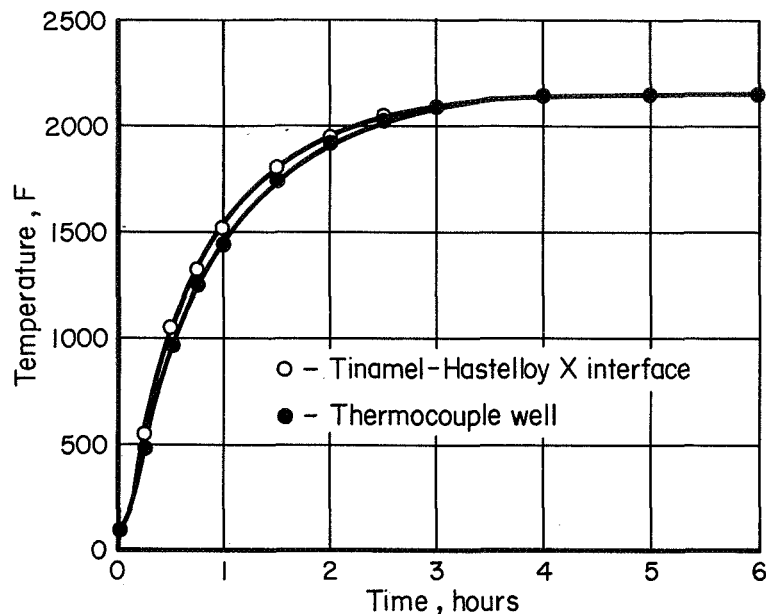


FIGURE 33. PREDICTED CHANGE IN TEMPERATURE OF COMPONENTS IN SPOOL SPECIMENS DURING GAS-PRESSURE BONDING

Interdiffusion between the stainless steel and liner components after 4 hours at 2150 F was calculated to be about 3 to 5 mils on either side of the interface, assuming, of course, that the components are in intimate contact from the beginning of the diffusion run. The complete collapse and subsequent creep of the stainless steel forging ring onto the rib components was expected by the time the temperature and gas pressure had reached their maximum values; however, an additional 2 hours was allowed for diffusion bonding. Thus the specimens were held at these conditions (2150 F and 15,000 psi) for 6 hours. The specimens were cooled in the autoclave overnight, with the gas pressure held to at least 11,000 psi. The rib components thus experienced an estimated 2 additional hours of temperature and pressure sufficient to achieve strong metallurgical bonds.

Postbonding Operations

The two cylindrical spool pieces were examined for leaks. Attempts were made to leak check through the evacuation stems, but when these were cut through, it was found that they had completely collapsed and bonded, sealing off the holes that were to be used for leak check. This indicated that a gastight condition was retained during gas-pressure bonding, and that the components (ribs, liner, shell, etc.) probably achieved good-quality bonds.

The two pieces were then machined in preparation for removing the tooling by acid leaching. The major portion of the steel mandrel was bored out, and 1-inch-diameter holes were drilled radially into each end of the part to penetrate the stainless steel outer shell and expose the tooling rings forming the manifolds. These holes also would be used later for the weld plenum tube fittings.

Tooling was removed by leaching in 50 weight percent HNO_3 . Initial removal of the remaining portion of the center mandrel and the major portion of the manifold tooling rings was accomplished by simple immersion. The reaction itself provided sufficient agitation of the acid solution to avoid stagnant areas. Removal of the Tinamel tooling in the small longitudinal channels required mechanical agitation of the acid solution to avoid gas blockage and stagnation in the channels.

SUMMARY OF RESULTS

Task I

Bonding experiments conducted at 2200 F and 10,000 psi for 3 hours resulted in good quality bonds between the following material couples:

304 stainless steel to 304 stainless steel
 304 stainless steel to Hastelloy X
 304 stainless steel to TD nickel
 304 stainless steel to tungsten
 304 stainless steel to 1018 steel
 304 stainless steel to Ni-20Cr
 304 stainless steel to vanadium

1018 steel to Hastelloy X
 1018 steel to TD nickel
 1018 steel to molybdenum

Titanium to vanadium
 Titanium to Nb-1Zr

Tungsten to Ni-30Cr

At the same conditions, the following couples achieved either marginal or weak bonds:

Tungsten to TD nickel
 Molybdenum to Hastelloy X
 Molybdenum to Ni-20Cr
 Nb-1Zr to Ni-30Cr
 Nb-1Zr to 1018 steel
 Nb-1Zr to 304 stainless steel.

Because of the weak bonds achieved by the molybdenum to Hastelloy X and molybdenum to Ni-20Cr couples, the bonding of spool components during the first bonding cycle of Task II was unsuccessful and required a difficult and complicated series of procedures to salvage the spool-piece specimens. It appears highly probable that the use of molybdenum tooling ribs (in the channels only) would have solved many of the difficulties that were encountered in the program.

Good-quality bonds on all other couples assured that all the separate thrust-chamber components would become an integral part and remain soundly bonded up to the melting point of the base metal.

During bonding tests on ribbed flat panels, no excessive dimensional changes or distortions were detectable. Hardness tests on the bonded components showed only slight decreases in hardness across bond interfaces and within the base materials. The exception was the Nb-1Zr couples with 1018 steel or 304 stainless steel. Hardness increased in these couples owing to intermetallic-phase formation.

Bond strengths measured by double-lap-shear tests on 304 stainless to Hastelloy X specimens were not considered representative because of the apparent oxide contamination of the components prior to gas-pressure bonding. However, both the bond strengths and the ductility as measured by double-lap-shear tests on 304 stainless to 304 stainless specimens were adequate.

Leaching studies were conducted on a variety of plain-carbon steels, and HNO_3 acid solutions proved to give the most satisfactory results. In addition, it is known that molybdenum, if used as tooling, would also be easily removed with HNO_3 solution. The use of molybdenum tooling rather than plain-carbon steel tooling would, despite its higher cost, reduce the processing costs. First, it would reduce leaching times by preventing passivation difficulties encountered with the steel tooling; second, it would eliminate corrosion-resistant scales that occur in steel owing to interdiffusion of nickel or chromium with iron; and, finally, it would simplify the process by precluding the need for molybdenum-foil barriers. The leaching tests also showed that nitric acid was compatible with Nb-1Zr and with Hastelloy X, provided Hastelloy X was not cooled slowly from the bonding temperature of 2200 F. If this be the case, Hastelloy X would require a postbond heat treatment to preclude intergranular attack by nitric acid. A similar effect was found with 304 stainless steel, but here a substitute stabilized grade (347 stainless steel) was feasible and was subsequently used in Task II studies. Nitric acid severely attacked TD nickel and these liners had to be protected from acid attack by chromium coating. Chromium electroplating proved to be ineffective because of attack at cracks or point defects in the coatings. A proprietary chromium-pack-diffusion technique (chromallizing) which diffused about 20 weight percent chromium into the TD nickel to a depth of .005 inch protected the TD nickel from nitric acid attack.

In order to obtain complete densification of the ceramic powder, as well as achieve satisfactory bonding of the coating to the liner materials, the bonding pressure was increased in 15,000 psi. (This pressure increase was also regarded as necessary in Task II to achieve suitable deformation of the large mass of stainless steel ring forgings to bring interfaces into intimate contact for subsequent bonding; thus the increase in bonding pressure actually served a double purpose.)

Protective oxide coatings on Hastelloy X and chromallized TD nickel substrates were applied by plasma spraying along with a preferential parting layer, densified and bonded by gas-pressure bonding, and evaluated primarily by metallographic analyses following scratch tests, bend tests, and thermal-shock tests. Ungraded zirconia coatings and coatings graded with Ni-20Cr alloy powder were prepared and compared, and six different parting layers were examined. Two larger (4 by 8 inch) Hastelloy X plates were coated with the ungraded oxide, and an alumina parting layer was used on these samples.

All of the small (2 by 2 inch) samples were gas-pressure bonded at 2200 F and 15,000 psi for 3 hours. The larger plate samples were gas-pressure bonded at 2150 F and 15,000 psi for 6 hours.

Metallographic examinations on the small samples showed that the coatings were sound, dense, and of uniform thickness, and they appeared to be well bonded to the substrates. In cases where the coating sample was cut through before leaching off the bonding container, the protective oxide coating was severely cracked locally and the parting layers tended to stick to the container instead of cracking preferentially. When the coating samples were first decanned by leaching and then sectioned, the protective coatings did not crack but were retained intact on the substrate, and the parting layers were either removed or in some cases even retained on top of the protective oxide coating.

Metallographic examination of the oxide coating on the larger samples showed that the oxide had relatively uniform thickness over the surface, was thicker (.0065 inch) than the oxide layers on the smaller samples (which was .003 inch), was dense, was well bonded, and had achieved significant penetration into the metal substrate surface.

The MgO and beryllium parting layers were the only parting layers that had any effects on the microstructure, and these were minor. The Mo-ZrO₂ parting layer produced cracking in the protective oxide coatings. The Nb-1Zr parting layer may have contributed to a gross reaction in one specimen, and this reaction tended to obscure useful results on this specimen.

The ceramic-to-metal bonds were, in general, fairly strong mechanical bonds for ungraded coatings. The notable exceptions to this were the ceramic-to-metal bonds on chromallized TD nickel substrates. These bonds were chemical-diffusion bonds which produced exceptionally tight bonds at the ceramic-metal interfaces. Graded coatings all produced satisfactory bonding between the Ni-20Cr alloy powder filler and the metal substrate.

Graded coatings, in general, survived thermal-shock tests from 2000 F better than ungraded coatings. The ungraded coatings on chromallized TD nickel substrates survived thermal-shock tests much better than any of the other ungraded coating systems and as well as any of the graded coating systems.

The initial oxide-coating samples were disappointing because of cracking of the oxide while cooling from the bonding temperature. However, the use of friable layers of Fiberfrax (and, later in the program, sprayed metal and ceramic separator layers) caused preferential cracking through these layers away from the protective oxide coatings, thereby producing a sound and well-bonded oxide layer on the liner materials.

Nondestructive tests, by heat-sensitive fluids, liquid crystals, and ultrasonics, were attempted on ribbed flat-panel specimens. Although the heat-sensitive fluids and liquid crystals looked promising for thin-gage material, they were insensitive to defects under the thicker liner materials. Ultrasonic inspection proved to have the best potential for picking up both large and relatively small bond defects in the ribbed structures.

Destructive testing of the first group of flat-panel specimens were successful in that the 500-psi proof test was accomplished. However, proof testing at 2000 psi was not possible because of inadequate end seals. Attempts made with a second group of flat panels to incorporate integrally bonded end closures were unsuccessful primarily because of displacement of molybdenum-foil barriers. These foils were jostled into positions across the stainless steel ribs and into the sides near the edges. In all cases, after the molybdenum had been leached out with the steel tooling, leaks were found near the edges where the foils had been, and proof testing could not be concluded on the

flat-panel specimens. Again, the use of molybdenum tooling ribs rather than plain-carbon steel ribs (which required the use of barrier foils to prevent acid-resistant scabs) would have eliminated the source of these leaks.

Task II

Two spool-piece specimens simulating the configuration, materials, and process parameters expected for the thrust-chamber segments to be fabricated in Task III* were prepared, assembled, and gas-pressure bonded in two bonding cycles. The first cycle was made at 2200 F and 10,000 psi for 3 hours; the second cycle was completed at 2150 F and 15,000 psi for 6 hours. Inadequate bonding between the liner and molybdenum-foil barriers in the first bonding cycle caused unplanned for, additional steps in the procedures in order to salvage the materials and previous work completed on the spool-piece components. Despite numerous complications during the salvaging process, the two spool-piece components were assembled and bonded in the second bonding cycle. Visual examination of the parts indicated that both had achieved satisfactory deformation for bonding. Removal of the steel tooling from the spool pieces required a time longer than anticipated because of periodic passivation of the steel, blockage of the leaching solution due to entrapped gas bubbles produced in the acid reaction, and stagnation of spent acid in the tooling channels. Passivation was overcome by heating the acid solution and the spool piece to 200 F. Bubble entrapment and stagnant reacted solution were removed by improvising a mechanical agitator and periodically tipping or turning the spool pieces.

Examination of the chamber with the TD nickel liner disclosed that a portion of the liner was not bonded to the ribs, and thus would fail under pressure. The unbonded area, approximately 5 square inches, was roughly triangular. The liner was also quite thin in this area, which suggests the possibility that pinholes in the chromallized surface allowed some attack by the hot nitric acid used for tooling removal.

The chamber with the Hastelloy X liner had a marginal bond to the spool body at one end of the liner. This was repaired by welding. The thrust chamber was then leak checked with helium, and was found to have some leaks directly through the liner. These leaks were caused by tiny pinholes or by what appeared to be small porous areas, which most likely resulted from sensitization of the Hastelloy X during the bonding cycle coupled with the extensive leaching time (4 weeks) required for tooling removal.

CONCLUSIONS

- (1) Fabrication of advanced-design regeneratively cooled thrust chambers by gas-pressure bonding is feasible provided molybdenum tooling is used to form the coolant channels, or faster methods of leaching out mild-steel tooling are devised. The use of TD nickel liners will require quality assurance of the integrity of the chromallized surfaces. With Hastelloy X liners, it will be necessary to use a cooling rate fast enough to avoid sensitization, coupled with shorter acid leaching times.

*Owing to revisions in contract objectives, Task III was omitted from the program.

- (2) Dense and impermeable protective oxide coatings can be strongly bonded to metal surfaces by a combination of plasma spraying and gas-pressure bonding. The resultant coatings are scratch resistant, remain bonded to the metal despite severe deformation of the metal substrate, and show high thermal-shock resistance, particularly if the coatings are bonded to Ni-20Cr liners.
- (3) Parting layers that crack preferentially aid in transferring the coating from a mandrel to the liner surface that requires protection. This transfer concept simplifies the coating of internal surfaces and makes the process attractive for protecting thrust-chamber liners, internal engine parts, nozzle surfaces, afterburner walls, and piping subjected to hot, corrosive fluids and gases.

RECOMMENDATIONS

Fabrication of thrust chambers with intricate internal passages by gas-pressure-bonding techniques has been proven feasible. To further improve this technique for production use, faster removal of the tooling material would be desirable, particularly where long passages of relatively small cross sections are involved. Cooling rates after the bonding process should also be increased to avoid sensitization of Hastelloy X parts. An investigative program on alternative tooling materials and removal methods is recommended, with particular emphasis placed on suitability for long passages having sharp bends and curves. The program ideally should include fabrication of a full-scale or subscale nozzle-shaped part.

APPENDIX A

MATERIALS CERTIFICATIONS FOR MATERIALS USED IN TASK I

METAL PRODUCTS

Page 1 of 2

H. T. Condition Stress Relieved **Form** Sheet

*Refer to packing ticket or invoice for exact quantities.

Date _____



E. I. DU PONT DE NEMOURS & COMPANY
INCORPORATED

PIGMENTS DEPARTMENT

CURTIS BAY, BALTIMORE, MD.

METAL PRODUCTS

TEST REPORT

Customer BATTELLE MEMORIAL INSTITUTE, COLUMBUS, OHIO

Customer Order No. V-205

Plant Order No. KM-1011

Specification DPN(G)-01A and DPN(P)-201B

Page 2 of 2

Alloy Nickel-2% Thoria

H. T. Condition Stress Relieved Form Sheet

TRANSVERSE Mechanical Properties

Heat or Lot No.	Tensile, ksi	Yield Strength, ksi	Elongation, % in 1"	Stress Rupture Life Hrs. @ 5.5 KSI	Stress Rupture Elongation % in 1"
1773 Room	65.2	50.8	17.2		
2000°F	14.2	12.5	3.2	Exceeds 20	2.7
Heat or Lot No.	Other Properties				
1773	105° Bend Radius 1T				

Remarks

I certify that this is a true and correct
copy of the results shown on our laboratory records.

By *[Signature]* 6/23/61
Technical Section Date
Metal Products
Du Pont Metals Center

SHIPPED TO
 BUYER
 BATTLE MEMORIAL INSTITUTE
 ATTN: INV AUDIT & Rowles, Buyer
 505 KING ST
 COLUMBUS OHIO 43201



SHIP TO
 BATTLE MEMORIAL INSTITUTE
 505 KING ST
 COLUMBUS OHIO 43201

V-741		QUANTITY ORDERED		QUANTITY SHIPPED		REMARKS:								
1PC		1 pc.		1 pc.		<input checked="" type="checkbox"/> 1. THIS MATERIAL HAS PASSED THE PEND TEST AND IS CAPABLE OF MEETING THE STRESS RUPTURE REQUIREMENTS PER SPECIFICATION. <input type="checkbox"/> 2. THIS MATERIAL IS CAPABLE OF MEETING THE STRESS RUPTURE REQUIREMENTS PER SPECIFICATION. <input type="checkbox"/> 3. THIS MATERIAL IS CERTIFIED TO THE CHEMISTRY ONLY. THE ABOVE PROPERTIES ARE REPORTED FOR INFORMATION. <input type="checkbox"/> 4. TEST SPECIMEN OBTAINED FROM A FORGE TEST INGOT THAT IS PROPERLY HEAT TREATED.								
.019/.022X24X4LG CRS ANL AND PICKLE HASTELLOY ALLOY X														
AMS-5536E														
HEAT NO.	PIECES	Cr	W	Fe	C	Si	Co	Ni	Mn	Cb+Ta	V	Mo	P	S
1 260-6-4772		22.14	.47	18.09	.08	.39	1.85	Bal.	.27			8.76	.016	.00
2														
3														
4														
5														
6														
Al	Ti	B	Cu	Zr	Ta	Mg	O ₂	H ₂	N ₂					
1														
2														
3														
4														
5														
6														
TENSILE TEST AT ROOM TEMPERATURE										TENSILE TEST AT _____ °F				
ULTIMATE PSI	.2% YIELD PSI	.02% YIELD PSI	% ELONG IN 2"	% R. A.	ULTIMATE PSI	.2% YIELD PSI	.02% YIELD PSI	% ELONG IN 2"	% R. A.					
1 115,700	58,950		40.0		1									
2					2									
3					3									
STRESS RUPTURE										THIS IS TO CERTIFY THAT THE ORIGINAL OF THIS REPORT HAS BEEN PROPERLY SIGNED AND NOTARIZED				
TEST TEMP. (°F)	STRESS PSI	HOURS	% ELONG IN 2"	ANNEALED HARDNESS	AGED HARDNESS	GRAIN SIZE	I. G. A. DEPTH							
1														
2														
3														
CERTIFIED BY					DATE									
J. H. Brown					July 6, 1967									
NOTARIZED					NOTARIZED									

TEST REPORT

☐ 917 PENNSYLVANIA AVE.
PITTSBURGH, PA. 15223

☐ 6101 GRAND AVE
CLEVELAND, OHIO 44128

☐ 7440 REINHOLD DR.
CINCINNATI, OHIO 45237

WILLIAMS AND COMPANY, INC.

"The House of Metals"

☐ 900 WILLIAMS AVE.
COLUMBUS, OHIO 43218

☐ 946 KANE ST.
TOLEDO, OHIO 43622

☐ 1109 S. PRESTON ST.
LOUISVILLE, KY. 40203

SOLD TO:

BATTELLE MEMORIAL INSTITUTE
505 KEEB AVENUE
COLUMBUS, OHIO 43201

Date:

Customer's Order No:

Williams and Company's Order No:

8-11-67

V-3150

B-010411-10

Item	Heat No.	Description	Specification
1	54669	TYPE 304 STAINLESS PLATE 7/16" x 24" x 48"	Mfg. Jessop Steel Company
2	3330888	TYPE 304 STAINLESS SHEET 2B FINISH .140" x 48" x 48"	Mfg. Republic Steel Corporation

CHEMICAL COMPOSITION

Item	Heat No.	C	Mn	P	S	Si	Cr	Ni	Fe	Cu	Al	Mg	Mo	Co
1	54669	.052	1.50	.022	.018	.47	18.32	9.53		.24			.22	.082
2	3330888	.059	1.72	.027	.010	.56	18.25	9.03		.14			.24	.10

PHYSICAL COMPOSITION

Item	Heat No.	Ten. Str. Psi	Yield Psi	Elong. % - 2"	Red. Area %	Hrdns.	Grain Size	HEAD TEST	INT. CHAR.
1	54669	81,365	37,402	61%	70%	76-77	#3	OK	SATISFACTORY
2	3330888	84,400	45,870	60%		B 83	#6	OK	SATISFACTORY

Sworn to and subscribed before me

this 11 th day of AUGUST 19 67

We hereby certify that the above data is a true copy of the data furnished us by the producing mill or supplier or of the data resulting from tests performed in approved laboratories and meets the requirements of the specification noted.

WILLIAMS AND COMPANY, INC.

By

APPENDIX B

DENSIFICATION AND BONDING OF PROTECTIVE OXIDE COATINGS ONTO HASTELLOY X AND TD NICKEL

APPENDIX B

DENSIFICATION AND BONDING OF PROTECTIVE OXIDE
COATINGS ONTO HASTELLOY X AND TD NICKEL

by

A. N. Ashurst, J. N. Fleck, and M. J. Ryan

Summary

Protective oxide coatings on Hastelloy X and chromallized TD nickel substrates were applied by plasma spraying along with a preferential parting layer, densified and bonded by gas-pressure bonding, and evaluated by metallographic analyses primarily but also by scratch tests, bend tests, and thermal-shock tests. Ungraded zirconia coatings and coatings graded with Ni-20Cr alloy powder were prepared and compared, and six different parting layers were examined. Two larger (4 by 8 inch) Hastelloy X plates were coated with the ungraded oxide, and an alumina parting layer was used on these samples.

Metallographic examinations showed that the coatings were sound, dense, and of uniform thickness, and they appeared to be well bonded to the substrates.

None of the coatings spalled or peeled during bend testing but remained bonded to the substrate despite severe cracking in the oxide at the bend.

Graded coatings generally survived thermal-shock tests better than ungraded coatings. The notable exceptions were the ungraded coatings on chromallized TN nickel substrates. These latter coatings survived thermal-shock tests much better than any of the other ungraded coating systems and as well as any of the graded coating systems.

The use of a parting layer that separates preferentially aids in the transference of the coating from a mandrel to the surface that requires protection. This "transfer concept" simplifies the coating of internal surfaces and makes the process attractive for protecting thrust-chamber liners, internal engine parts, nozzle surfaces, afterburner walls, and piping subjected to hot corrosive fluids and gases.

Introduction

Components exposed to environments in nuclear reactors, energy converters, and aerospace systems require higher strengths at higher operating temperatures, resistance to various modes of corrosion, thermal-shock resistance, and resistance to radiation conditions. Increased serviceability under these conditions is possible with ceramic-metal composites by improving the bonds of ceramic-to-metal joints.

Conventional uses do not normally require these properties, and the joints produced are of low strength. To fabricate joints of high strength for long-time service in

severe environments, a combination of advanced techniques is applied. Several such methods are chemical and physical vapor coating, slurry coating, and plasma spraying, followed by hot pressing, gas-pressure bonding, explosive bonding, and various adaptations of diffusion-press bonding. Intermediate layers are sometimes used, either as an infiltrant or as a solid-phase-bonding aid as when ceramic coatings are applied via graded cermets.

The object, generally, is to apply a dense impermeable coating onto a substrate with a strong enough bond to survive the bonding process and subsequent environmental stresses. These bonds are established either mechanically or metallurgically (by chemical diffusion) or by a combination of the two. Ceramic-to-metal diffusion bonds attempted at low temperatures permit only limited diffusion between the metal and ceramic, and the bonds are not well established. Limited solubility between the metal and ceramic yields a limited diffusion zone, and such bonds give low strength characterized by fracture at the interface. In such cases, an increase in bond strength can be achieved either by increasing the bonding temperature and time or by mechanically interlocking the ceramic particles into the metal matrix. This "micromechanical joint" is accomplished with the cermet intermediate layer, but is also achieved by localized chemical attack, by intentional surface roughening, or by forcing the hard ceramic particles into the metal surface. Increasing the bonding temperature increases the diffusional processes but may also result in gross reactions at the interface, in metal deterioration (by recrystallization, incipient melting in grain boundaries, and loss of dimensional control), and in fracture or spallation of the coating due to differences in thermal-expansion coefficients.

Presented herein are the results of recent attempts to put oxidation-resistant coatings on high-performance rocket-engine liners and provide protection to the walls of the engine from conditions of high heat flux and burn temperatures (4000 F) and severe oxidation. Gas-pressure bonding was selected as one technique to develop a dense, strongly bonded oxide ceramic coating on Hastelloy X and TD nickel liner shells. In conjunction with gas-pressure bonding, the coatings were applied by plasma spraying. Plasma-sprayed coatings are reasonably dense (better than 80 percent of theoretical), are sufficiently adherent for subsequent handling and assembly steps, and even though manually operated, are uniformly applied to the extent that variations in thickness are usually less than 2 mils.

In gas-pressure bonding ceramic coatings onto the metal substrates, the bonding achieved was primarily micromechanical; however, significant contributions to the bond strength from chemical bonding between the ceramic and metal were evident.

Two types of coatings were studied: (1) pure oxide, specifically, CaO-stabilized ZrO_2 , and (2) graded oxide (or cermet) containing stabilized ZrO_2 . The cermet coatings were prepared by mixing the oxide powder with various amounts of Ni-20Cr alloy powder and bonding the cermet to the metal substrates in stepped gradations. Since the protective coating was required on the inside (inner diameter) surface of the rocket engine, a coating-transfer technique was developed that allowed the plasma spraying to be done on the OD of a mandrel and subsequent transfer of the coating to the ID of the liner surface. Since preferential release of the coating from the mandrel was required to promote the transfer, separator layers were introduced between the mandrel and coating interface. The separator layer was designed to be the weaker interface and crack preferentially, leaving the coating bonded to the liner surface. Six different

separator layers were examined: beryllium, Al_2O_3 , MgO , Nb-1Zr, a W/ ZrO_2 coupled layer, and a Mo/ ZrO_2 coupled layer. These layers were also put down by plasma spraying.

The samples described in this report were flat rather than curved, so that the best type of coating (graded or ungraded) and the most suitable separator layer could be determined before proceeding to cylindrical or shell samples which would permit the transfer of the coating to inner (ID) surfaces. The gas-pressure-bonded coatings were evaluated primarily by metallographic analyses, but some qualitative testing was performed, consisting of bend tests, scratch tests, and thermal-shock tests. Since all the coatings studied in this program survived the cooling cycle in the pressure-bonding autoclave (from 2300 F to RT) in which the coatings undergo high compressive and shear stresses owing to thermal-expansion mismatch, the coating-to-metal liner bond strengths must have been especially good from the start. The metallographic and qualitative test results reported herein support this conclusion and give additional information pertaining to the behavior, physical characteristics, and potential of these gas-pressure bonded ceramic-to-metal joints.

Materials

The oxide powder used for all coatings was a fused, stabilized, plasma-spraying grade of ZrO_2 . The Ni-20Cr (Nichrome) alloy powder filler used in making intermediate cermet layers was Plasmalloy 207-M screened to -200 +325 mesh. The plasma-sprayed separator layers were all Plasmalloy products except for the ZrO_2 in metal/oxide coupled layers, which was a product of Atlantic Equipment Engineers. One separator layer consisted of a Nb-1Zr alloy which was placed on the mandrels as a 30-mil sheet rather than sprayed powder. The mandrel material onto which the coating was plasma sprayed was done was 0.100-inch-thick Tinamel (titanium-killed low-carbon steel) which had been vacuum outgassed at 2200 F. The gas-pressure bonding containers were prepared from Armco iron and from low-carbon steel. The substrate liners onto which the coatings were transferred were Hastelloy X and TD nickel. Vendors reports of chemical analysis for these substrate materials are summarized in Table B-1.

The TD nickel substrates were diffusion coated with a minimum of 20 weight percent chromium to a depth of 0.005 inch. This was done for several reasons. First, program goals did not permit the use of a TD Nichrome alloy as a substrate material. Second, the gas-pressure-bonding approach involved the use of carbon-steel containers to encapsulate the samples. As will be discussed later, it was necessary to remove the containers by leaching with nitric acid. Since TD nickel is readily attacked by the leaching solution, it was necessary to protect it. Third, chrome plating of the TD nickel did not completely protect it, although this was tried early in the program. Localized defects in the plating caused the TD nickel substrate to be severely attacked. It was known that a nickel-base alloy with about 20 weight percent chromium is resistant to nitric acid attack. Therefore, the TD nickel substrates were chromium pack diffused (chromallized). Electron-microprobe analysis of a section of the treated material revealed that the chromium content at a depth of .005 inch was 23.5 weight percent. Subsequent tests of chromallized TD nickel samples in hot nitric acid showed that the samples were resistant to acid attack. To prevent intergranular corrosion of the Hastelloy X during leaching (which would occur since the slow cooling cycle after gas-pressure bonding destabilizes the alloy), the specimens with Hastelloy X substrates

were heat treated and then air cooled under a fan. This stabilization heat treatment was completed after the gas-pressure-bonding cycle but before any sectioning of specimens was started.

TABLE B-1. CHEMISTRY OF SUBSTRATE MATERIALS

Element	Hastelloy X (.020-Inch Thick)	TD Nickel (.032-Inch Thick) ^(a)
Cr	22.19	0.03
W	0.47	--
Fe	18.09	0.01
C	0.08	0.001
Si	0.39	--
Co	1.85	0.08
Mn	0.27	--
Mo	8.76	--
P	0.016	--
S	0.005	0.0012
Cu	--	0.001
Ti	--	0.001
ThO ₂	--	2.16
Ni	Bal.	Bal.

(a) After chromallizing, the TD nickel substrates were .037 inch thick because of the chromium addition.

Preparation of Samples

Two sizes of substrate samples were prepared. The smaller size, on which most of the tests and data were generated, was 2 by 2 by nominally .03 inch. The larger size plates were 4 by 8 by about .03 inch. Coating thicknesses on ungraded coatings were .002 to .006 inch thick as plasma sprayed; on graded coatings, the total coating thicknesses as plasma sprayed were .008 to .019 inch, depending somewhat on the thickness of individual graded layers on the sprayed surface. Cermet mixtures were prepared by weighing appropriate amounts of ZrO₂ and the Nichrome powder into a plastic jar and mixing these dry on mill rollers. The powder was fed into a Plasmadyne Roto-feed 1000 powder hopper and sprayed with a hand-held Plasmadyne Model SG-1B powder spray gun using argon as the carrier gas. The mandrels and substrate materials were cleaned by degreasing in methyl ethyl ketone, washing in water and methyl alcohol, then rinsing thoroughly in 200-proof ethyl alcohol.

Plasma-Spraying Procedures

The first step in the sequence of plasma spraying was to lay down the parting agent (or separator layer) on the Tinamel mandrel surface. The sprayed thickness of the parting agent was .002 inch except when Mo/ZrO₂ or W/ZrO₂ coupled parting agents were deposited. The coupled layers were deposited by spraying a .002 inch thick layer of

ZrO₂ on the mandrel followed by a .005 inch thick layer of the refractory metal. After depositing the parting agent, the ZrO₂ protective coating was sprayed on to a thickness of about .005 inch.

On six samples, the plasma spraying of the .005 inch thick ZrO₂ completed the coating process. These six samples, Specimens C-7 through C-12, constituted the "ungraded" coating specimens. Six other samples were given additional sprayed layers consisting of separate gradations of cermets. These additional layers were deposited as follows: first, a layer consisting of a mixture of 25 weight percent Nichrome-75 weight percent ZrO₂ was deposited to a thickness of about .006 inch; next, the 50-50 mixture was deposited; then, finally, the 75 weight percent Nichrome-25 weight percent ZrO₂ was deposited. These six samples made up the "graded" coating specimens. The sketches in Figures B-1 and B-2 illustrate the coating sequence for the twelve 2 inch by 2 inch specimens. The as-sprayed thicknesses of these additional layers could not be determined but were known to have varied considerably from sample to sample. Estimates of the as-sprayed coating thicknesses on these graded coating systems were made only after metallography had been performed on gas-pressure bonded specimens. As will be shown, not only did the thicknesses of the graded layers vary considerably, but the proportion of metal-to-oxide mixing in each layer was also quite a bit different than planned. The source of this problem was probably in the plasma spraying powder feeder, but the cause could not be determined.

Two large (4 by 8 inch) plate specimens with Hastelloy X substrates were similarly prepared. Armco iron materials, each 4 by 8 by about 1/4 inch, were degreased, cleaned, and degassed in vacuum at 2200 F. After degassing, the plates were vapor blasted, again cleaned by scrub washes than ultrasonically cleaned. These mandrel plates were then plasma sprayed with .004 inch of Al₂O₃ as a parting agent followed by .010 inch of the ZrO₂ protective coating layer (ungraded in both specimens). The coating system for the large plates was selected after completing evaluations on the smaller 2 by 2 inch specimens. Several systems appeared to have high potential as far as bond strength, parting layer effectiveness and compatibility, but the Al₂O₃ parting agent was chosen for the large plate specimens for its availability, ease of handling, and good spraying qualities, as well as for its usefulness as a parting layer. The ungraded coating type was selected because of greater interest and acceptability of this type for the program goals.

Assembly for Gas-Pressure Bonding

Containers for gas-pressure bonding were cut from 1/16 inch thick low carbon steel plate, degreased in MEK, rinsed in alcohol and vapor blasted. The pieces were assembled and TIG welded except for the top lid on each container. A molybdenum diffusion barrier foil, .003 inch thick, was placed between the substrate and container lid to prevent interdiffusion between the substrate metal (either Hastelloy X or chromallized TD nickel) and the low carbon steel containers. Diffusion into the low carbon steel, particularly of chromium, makes the steel resistant to the leaching solution and results in "scales" of the steel remaining on the substrate back face. Also, the loss of chromium and other elements from the substrate metal reduces its elevated temperature strength properties. Molybdenum was selected as the barrier layer since it can be removed in the leaching solution along with steel.

0.006	75 NiCr - 25 ZrO ₂
0.006	50 NiCr - 50 ZrO ₂
0.006	25 NiCr - 75 ZrO ₂
	0.005 ZrO ₂
	0.002 Be
	0.100 Ti Name1

C-1

0.006	75 NiCr - 25 ZrO ₂
0.006	50 NiCr - 50 ZrO ₂
0.006	25 NiCr - 75 ZrO ₂
	0.005 ZrO ₂
	0.002 Al ₂ O ₃
	0.100 Ti Name1

C-2

0.006	75 NiCr - 25 ZrO ₂
0.006	50 NiCr - 50 ZrO ₂
0.006	25 NiCr - 75 ZrO ₂
	0.005 ZrO ₂
	0.002 MgO
	0.100 Ti Name1

C-3

0.006	75 NiCr - 25 ZrO ₂
0.006	50 NiCr - 50 ZrO ₂
0.006	25 NiCr - 75 ZrO ₂
	0.005 ZrO ₂
	0.002 Mo
	0.002 ZrO ₂
	0.100 Ti Name1

C-4

0.006	75 NiCr - 25 ZrO ₂
0.006	50 NiCr - 50 ZrO ₂
0.006	25 NiCr - 75 ZrO ₂
	0.005 ZrO ₂
	0.002 W
	0.002 ZrO ₂
	0.100 Ti Name1

C-5

0.006	75 NiCr - 25 ZrO ₂
0.006	50 NiCr - 50 ZrO ₂
0.006	25 NiCr - 75 ZrO ₂
	0.005 ZrO ₂
	0.030 Nb - 1 Zr

C-6

FIGURE B-1. PLASMA-SPRAYED COATING SEQUENCE FOR GRADED COATINGS

0.006 ZrO ₂
0.002 Be
0.100 Ti Name1

C-7

0.006 ZrO ₂
0.002 Al ₂ O ₃
0.100 Ti Name1

C-8

0.006 ZrO ₂
0.002 MgO
0.100 Ti Name1

C-9

0.006 ZrO ₂
0.002 Mo
0.002 ZrO ₂
0.100 Ti Name1

C-10

0.006 ZrO ₂
0.002 W
0.002 ZrO ₂
0.100 Ti Name1

C-11

0.006 ZrO ₂
0.030 Nb - 1 Zr

C-12

FIGURE B-2. PLASMA-SPRAYED COATING SEQUENCE FOR UPGRADED COATINGS

The plasma-sprayed mandrels were inserted into the containers with the coated face up, followed by the substrate (either Hastelloy X or TD nickel), the diffusion barrier, and the container lid. A schematic of the assembly procedure is shown in Figure B-3. The container lids were clamped on, placed in an inert gas chamber which was evacuated to 10^{-3} torr then back filled with argon, and the lids welded in place. The containers were immediately transferred to an electron beam welding chamber and sealed off at 10^{-4} torr. Each container was checked for leaks by pressuring externally with 200 psi of helium for 5 min then submerging the containers in an alcohol bath to inspect for leaks. No leaks were detected in any of the containers.

Gas-Pressure-Bonding Procedures

The twelve smaller 2 by 2-inch specimens were gas-pressure bonded at 2200 F and 15,000 psi for 3 hours. The two larger 4 by 8-inch specimens were gas-pressure bonded at 2150 F and 15,000 psi for 6 hours. The sealed specimens were located within a wound resistance heater in a cold wall autoclave. The temperature was raised to 1800 F while maintaining a low helium pressure (less than 300 psi), then temperature and pressure were raised simultaneously to maximum conditions and held at these conditions for the indicated time. Temperatures in the autoclave were measured with ten Pt-Rh thermocouples positioned along the side of the specimens, 180 degrees apart. Temperatures varied by ± 25 F during the hold period. After completing the bonding cycle, the specimens were cooled under pressure (about 12,000 psi minimum) until the specimens temperature was about 300 to 400 F. The specimens were leak checked after the cycle. No leaks were detected in any of the specimens.

Evaluation of Small 4 by 8-Inch Coating Samples

The coatings on the 2 by 2-inch samples were tested or examined at four stages. First, the gas-pressure bonding container was sectioned with a cut-off wheel through the coating, and each sample was metallographically inspected. Next, the low carbon steel containers, molybdenum diffusion barriers, and the tinamel mandrels were completely removed by leaching in a solution of 50 percent HNO_3 -50 percent H_2O heated to 150 F. The coated substrate was then sectioned with a cut-off wheel and examined metallographically. The microstructures of canned samples were compared with those of the decanned samples. The third stage consisted of scratch tests and bend tests. The scratch test was done by dragging a knife edge across the oxide surface, particularly at the edges and corners, to spot weakly bonded areas and to check coating density. Two separate bend tests were made. The first bend tests consisted of grasping the ends of sections of the coated substrates with pliers and bending the substrates back and forth several times over an angle of about 45 degrees. The radius of bending was approximately 1/4 inch. This test indicated most of the coatings were well bonded to the substrates since none of the coatings peeled off or broke away in large chunks except in two cases. The second bend tests were conducted over a 1/4-inch diameter mandrel. Each sample was bent once around the mandrel over an angle ranging from 15 degrees to 90 degrees. These substrates were then mounted and examined metallographically. The remaining sections of the coated substrates were about 1 by 3/4 inch and these were thermal-shock tested to complete the fourth stage tests. Thermal-shock tests consisted simply of heating the samples in air to temperatures of 1200 F to 2000 F, removing the samples from the oven and cooling rapidly in air with a fan, and determining the amount

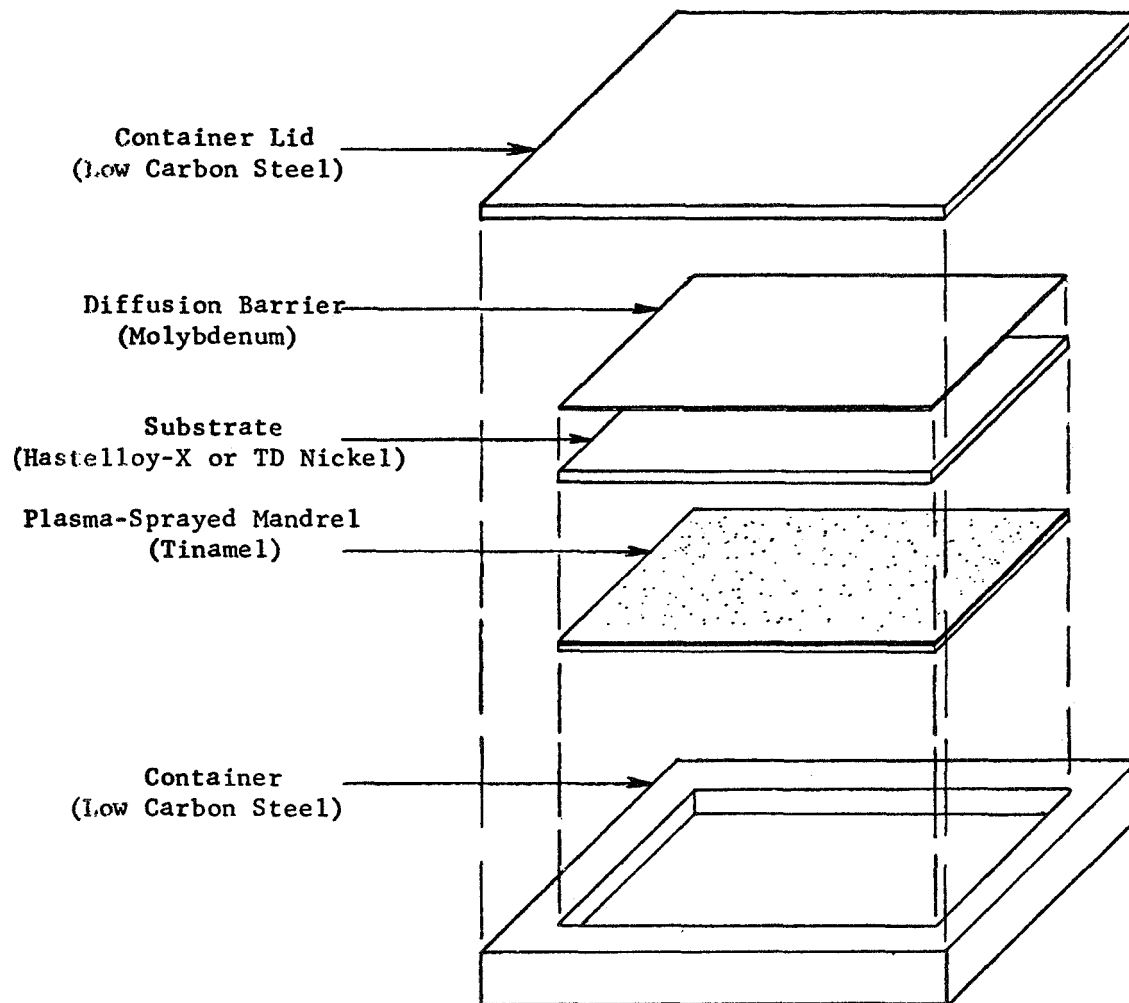


FIGURE B-3. ASSEMBLY SKETCH FOR OXIDE-COATING SPECIMENS

and type of deterioration (blistering, scaling, peeling) that occurs to the oxide coating. Each sample was thermal shocked through five cycles. Comparisons were made between graded and ungraded coatings.

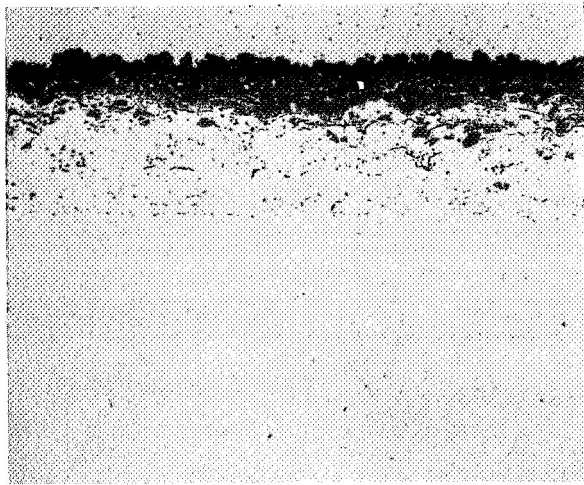
Inspection of Coatings in Gas-Pressure Bonding Containers

All but three coating systems examined metallographically in their containers were cracked. In cutting through the containers with the cutoff wheel, the heat and stress generated by scrapping the container edges in the cross-sectioned surface was apparently sufficient to crack most of the coatings in this region of the cut. Fortunately, the cracking was localized and did not extend through the coating across the whole sample. This was discovered when the container on a sample was leached off with nitric acid, sectioned away from the damaged region, and then mounted for metallographic examination. The coating was intact, sound, and even had some of the parting agent still bonded to the coating surface.

The coatings in three systems did not break up completely after cutting through the container but either separated neatly at the coating layer/parting agent interface, or else cracked very near this interface leaving most of the coating intact. These three systems were C-1 (graded oxide with Be parting agent), C-7 (pure oxide with Be), and C-12 (pure oxide with Nb-1Zr), and are shown, as-sectioned, in Figure B-4. Specimen C-6 is of the same system as Specimen C-12 except that the coating was graded. The Nb-1Zr agent generated a crack at the coating/parting layer interface, but because of a gross reaction between components, shown in Figure B-5, which severely embrittled the Hastelloy X substrate, evaluation of this system was difficult.

Typical of the remaining cracked coatings observed in samples sectioned in the containers was that of Specimen C-5 shown in Figure B-6a. The same specimen is shown in Figure B-6b after leaching off the container and then sectioning. By leaching the container off first before sectioning this specimen, the coating was preserved from cracks, and even some of the parting agent (in this case, a coupled parting agent of W/ZrO₂) was retained. Machining or cutting off the containers from the rest of the samples would have cracked the coatings across the whole substrate surface; therefore, the containers were removed by leaching in a 50 percent HNO₃-50 percent H₂O solution heated to 150 F.

Although it could not be proven that the parting agents produced the expected preferential cracking away from the coatings (except in the three samples noted already), there was evidence that separation did occur at the coating/parting layer interface. After leaching off the containers, it was expected that the Be, Al₂O₃, and W/ZrO₂ layers, which are resistant to nitric acid attack, would be retained and bonded to the coating surface. In fact, the W/ZrO₂ parting layer was the only one retained and only part of this was found on the graded coating; no other specimen retained any of the parting layer on the coating surface. This could only mean that the other parting layers dissolved (as, e. g., the Mo in the Mo/ZrO₂ layer) or else broke away physically (as it did with the Nb-1Zr layer). Thus, the Be, Al₂O₃, and a portion of W/ZrO₂ parting layers had to bond strongly to the Tinamel mandrel and separate at the parting layer/ZrO₂ coating interface, thereafter being washed away with the leaching solution.

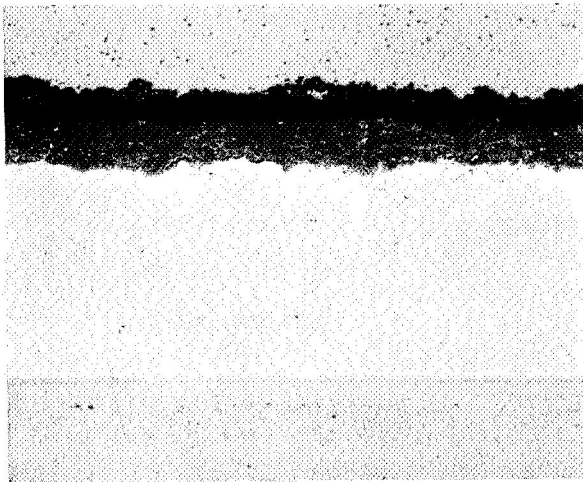


50X Specimen C-1 2E051

Tinamel
Be Parting Agent
Crack

Graded ZrO_2

TD Ni



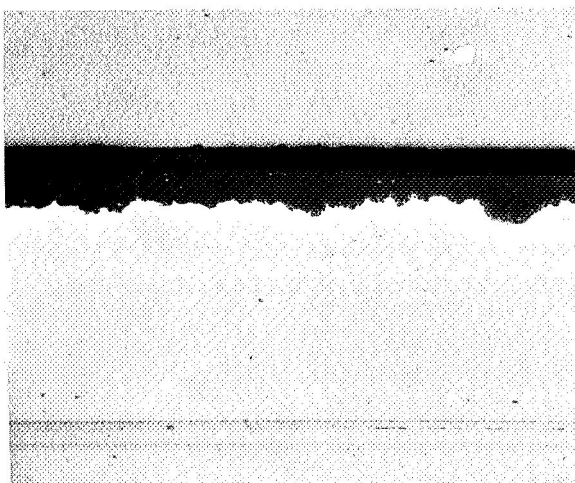
50X Specimen C-7 2E064

Tinamel
Be Parting Agent
Crack
Pure ZrO_2

Hastelloy X

Mo Barrier

Low Carbon Steel



50X Specimen C-12 2E074

Nb-1Zr Parting Agent

Crack
Pure ZrO_2

Hastelloy X

Mo Barrier
Low Carbon Steel

FIGURE B-4. THREE SPECIMENS SECTIONED THROUGH CONTAINER AFTER GAS-PRESSURE BONDING

These coatings remained sound and the cracks occurred at or near parting agent.

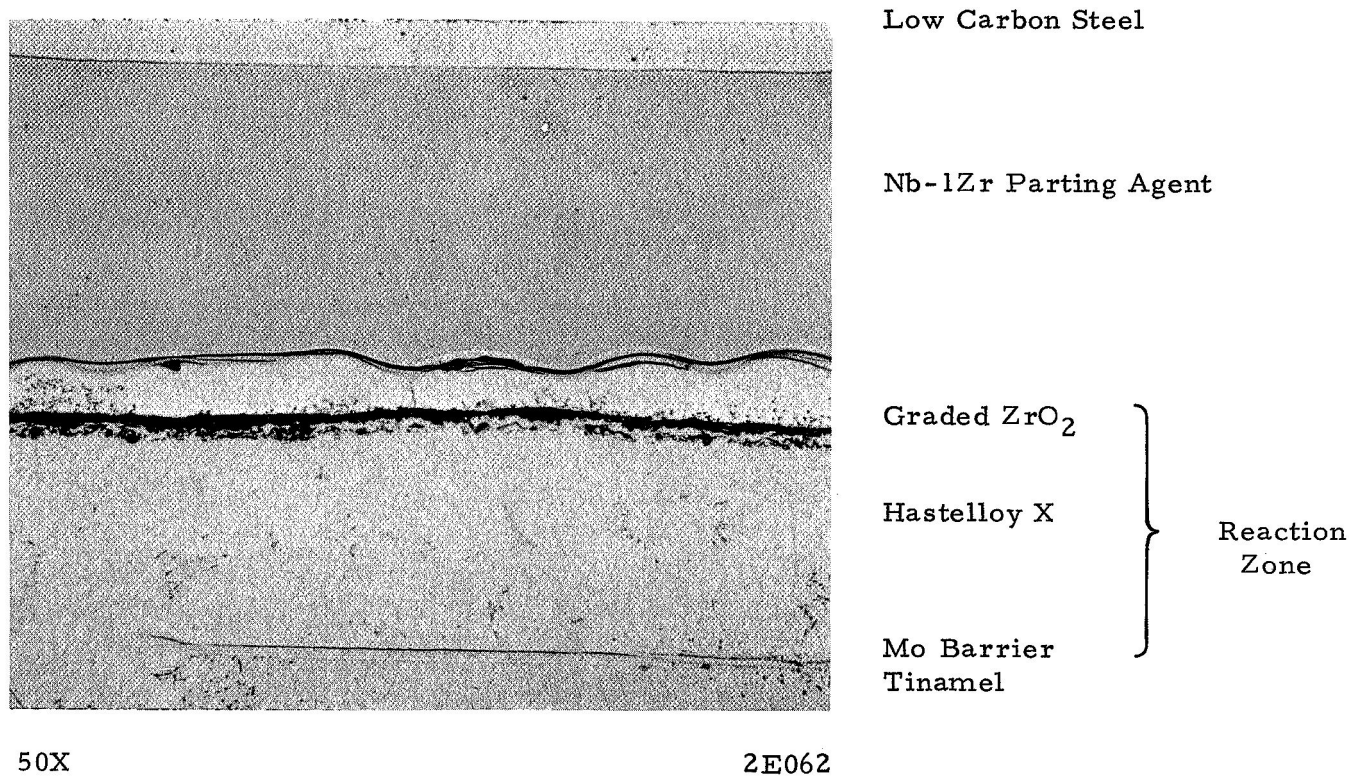
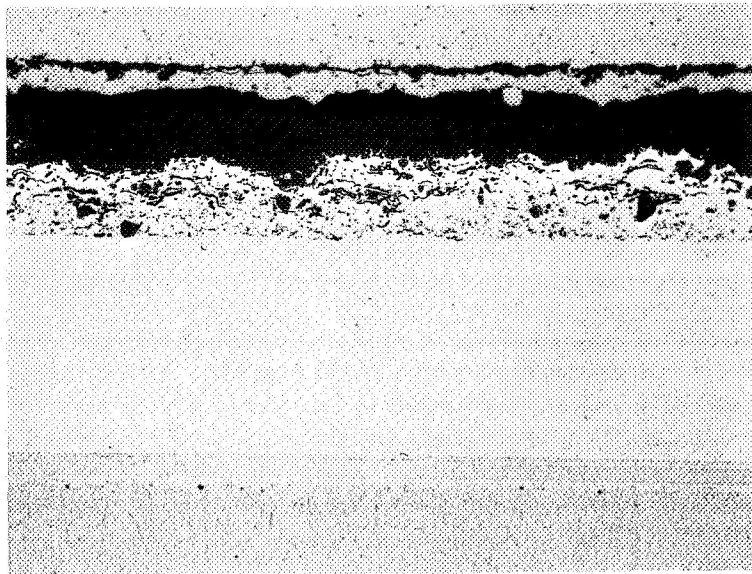


FIGURE B-5. SPECIMEN C-6, SECTIONED IN CONTAINER, SHOWING PREFERENTIAL CRACK AT Nb-1Zr/ ZrO_2 COATING SURFACE

Gross reaction between components and embrittlement of Nb-1Zr parting agent obscured useful results in this specimen.

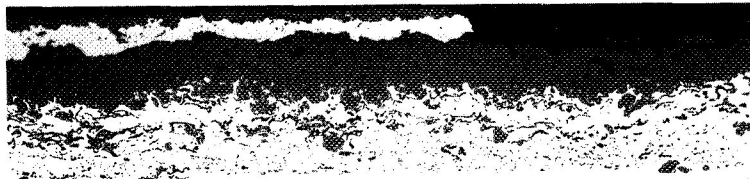


50X

2E059

a. With Container on Specimen

Specimen was sectioned with gas-pressure-bonding container intact. Cracks were produced in the ZrO_2 coating but not in the parting agent. The parting layer stuck to the container surface.



50X

2E179

b. After Container was Leached off Specimen

Container was leached off in nitric acid; then the specimen was sectioned away from damaged region shown above in a. The ZrO_2 coating was sound, and some of the parting agent was retained on the coating surface.

FIGURE B-6. COMPARISON OF SECTIONING EFFECTS
IN SPECIMEN C-5

Inspection of Samples After Removing Containers

Zirconia-coated metal substrates are shown in Figures B-7 through B-12. Each illustration shows a graded coating system and an ungraded coating system that used the same parting layer. Figure B-7, for example, shows Specimens C-1 (graded coating) and C-7 (ungraded coating) both of which had beryllium as the parting agent.

Effects of Parting Layers. The only two parting agents that had any noticeable chemical or diffusional effects on the microstructure were MgO and Be. Specimens C-3 and C-9 in Figure B-9 both have relatively higher porosity within the coating than other systems, and a reaction zone due to interaction with MgO parting layer through the coating and about .002 inch into the substrate metal is evident. Specimen C-1, shown in Figure B-7, also has a detectable reaction zone in the graded coating layer, and some penetration into the substrate is evident in both Specimens C-1 and C-7. The interaction of the parting layer with the coating and substrates of Specimens C-1 and C-3 are somewhat obliterated by the confusion in the graded coatings. Note, instead, the reaction zone at the coating/substrate metal interface in Specimen C-7 and Specimen C-9. The reaction zone is small but quite obvious when compared with other ungraded coated specimens. The effect of the Mo/ZrO₂ coupled parting layer was different in that it seemed to produce more cracking in the coating layer than occurred in other systems. Note also the ZrO₂ coating layer thickness in these specimens (C-4 and C-10) shown in Figure B-10. While some variation in coating thickness may be due to plasma spraying anomalies, the very small coating thickness in Specimen C-10 is obviously due to cracking and loss of the coating.

Porosity and Density. The coatings in all specimens, excepting Specimens C-3 and C-9, appeared to have little porosity. Where voids do occur, they are due partly to unclosed pores and partly to particle pull-out during metallographic polishing. Thus, gas-pressure bonding of pure ZrO₂ and ZrO₂ graded with various percentages of Ni-20Cr alloy powder at 2200 F and 15,000 psi for 3 hours produces densities very near theoretical densities in both the alloy powder and in ZrO₂.

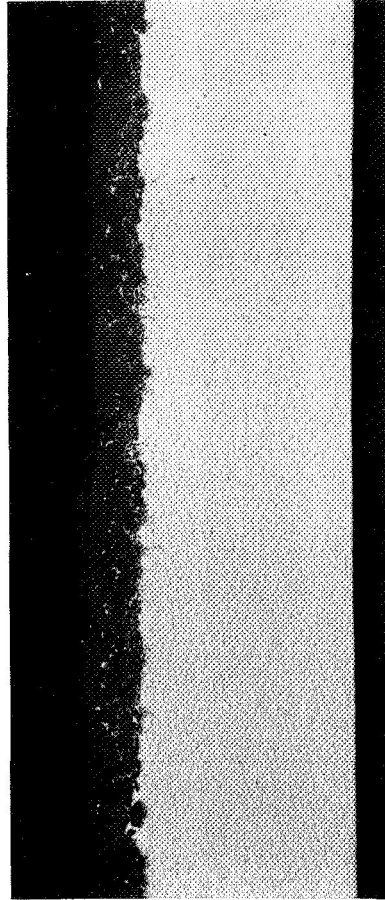
Bond Quality. The bonds between metallic particles in graded layer mixtures, and between these particles and the metal substrate, appeared to be strong, well-established diffusion bonds. The bonds produced between the ceramic and metal matrices, on the other hand, were primarily mechanical in general, depending more on interlocking than on diffusion. In graded coatings, interlocking between ceramic and metallic particles was established initially during plasma spraying. Gas-pressure bonding consolidated the network to a higher density and bond strength. In the pure (ungraded) coating layers, mechanical bonds were produced during gas-pressure bonding by the penetration of the hard ceramic particles into the softer surface of the metal substrate. The depth of penetration in Hastelloy X was about the same as in the TD nickel substrate. Exceptions to the general observations just made on bond quality and type are Specimens C-7 and C-9. Chemical or diffusional interactions inhibited ceramic particle penetration into the metal substrates of these two specimens.



55X

a. Graded Coating (Specimen C-1)

2E175



55X

b. Ungraded Coating (Specimen C-7)

2E182T

FIGURE B-7. OXIDE-COATING TEST SPECIMENS C-1 AND C-7

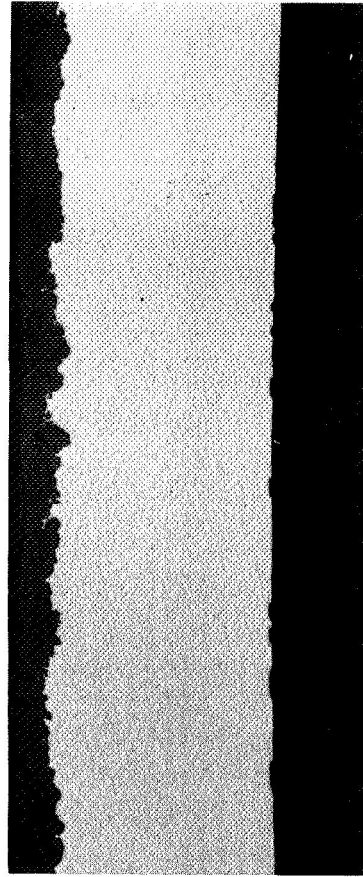
Parting layer was beryllium.



55X

a. Graded Coating (Specimen C-2)

2E176



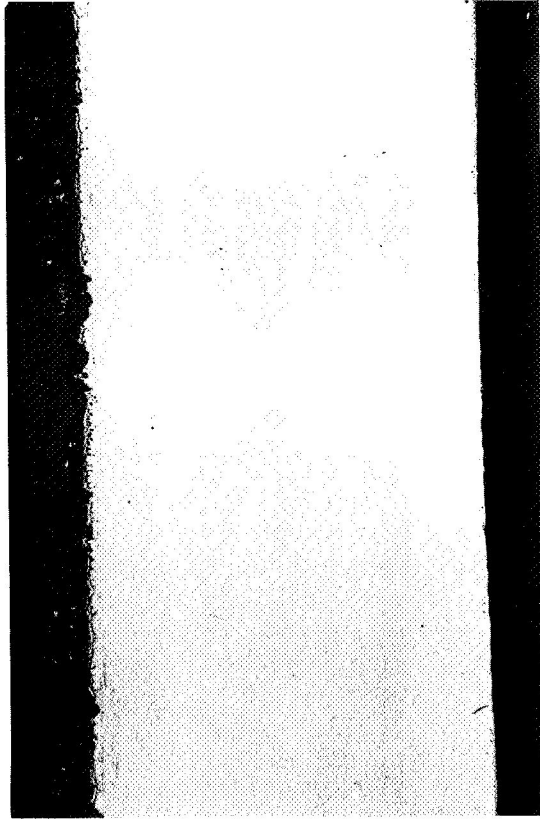
55X

b. Ungraded Coating (Specimen C-8)

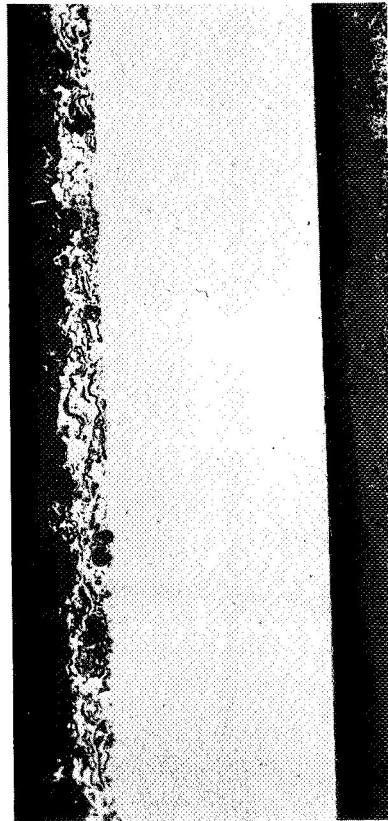
2E182B

FIGURE B-8. OXIDE-COATING TEST SPECIMENS C-2 AND C-8

Parting layer was alumina.



55X 2E183
b. Ungraded Coating (Specimen C-9)



55X 2E177
a. Graded Coating (Specimen C-3)

FIGURE B-9. OXIDE-COATING TEST SPECIMENS C-3 AND C-9

Parting layer was magnesia.

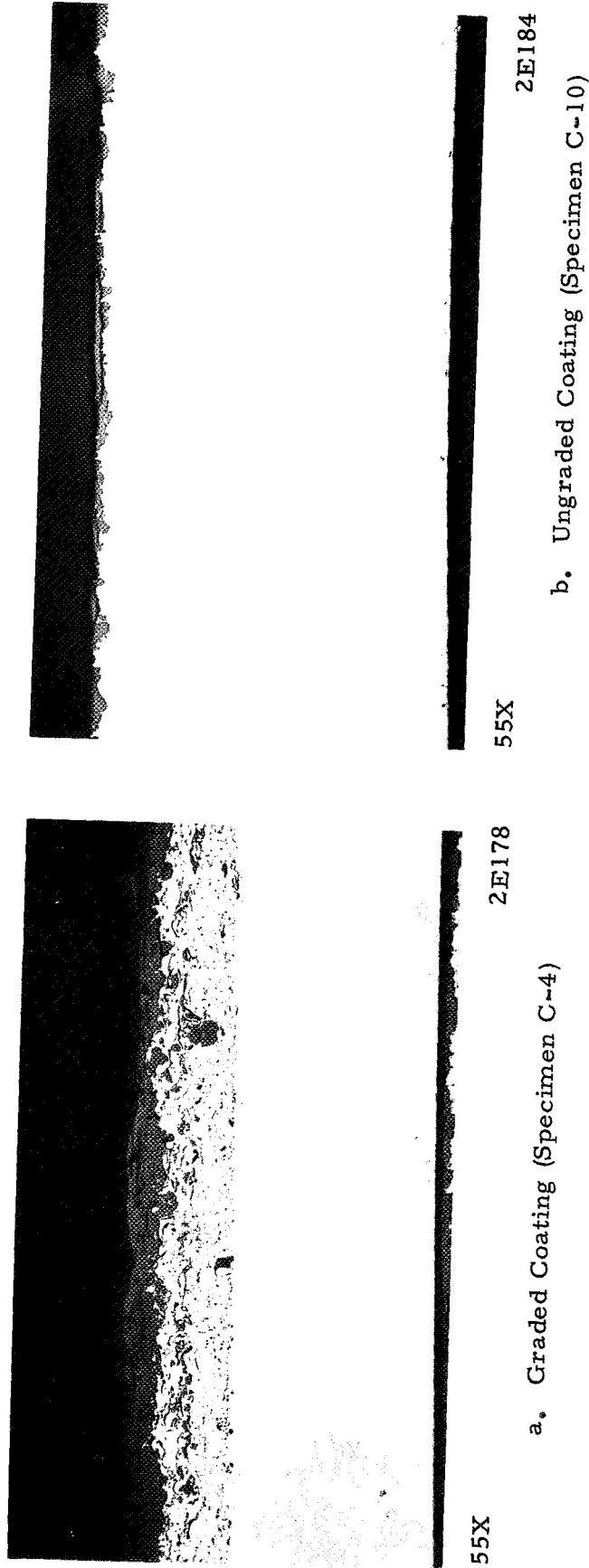
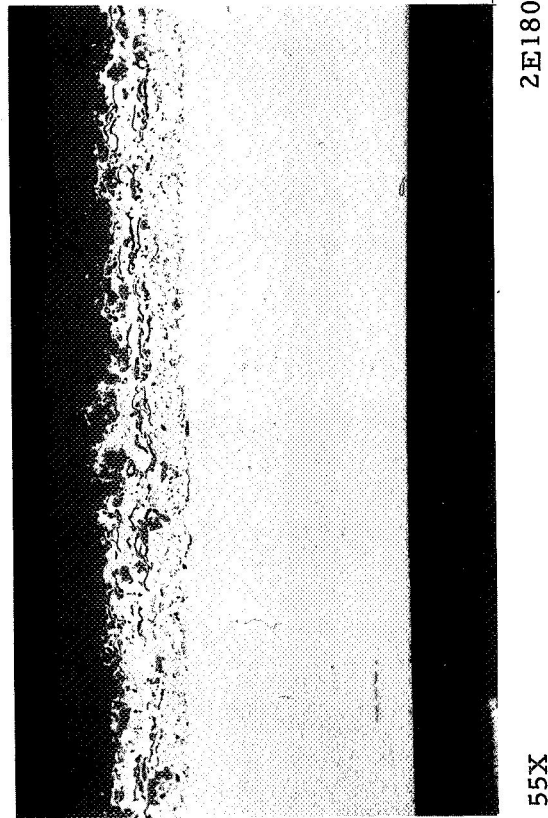
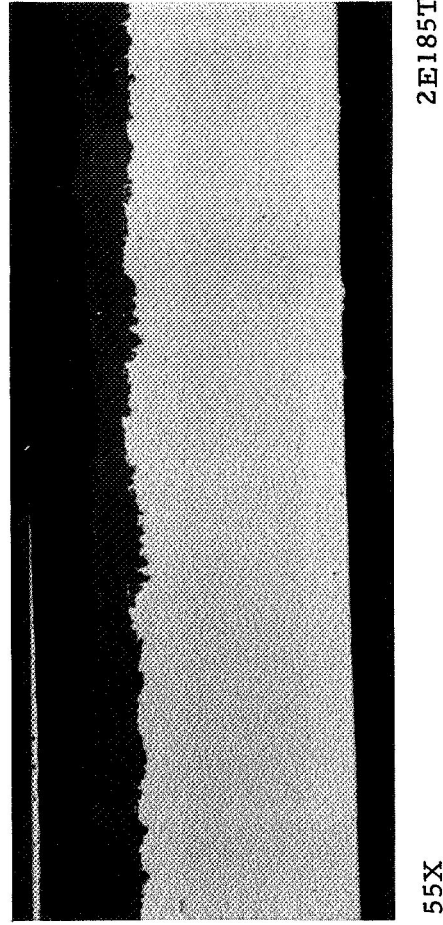


FIGURE B-10. OXIDE-COATING TEST SPECIMENS C-4 AND C-10

Parting layer was a coupled layer consisting of zirconia and tungsten (see Figure B-6).



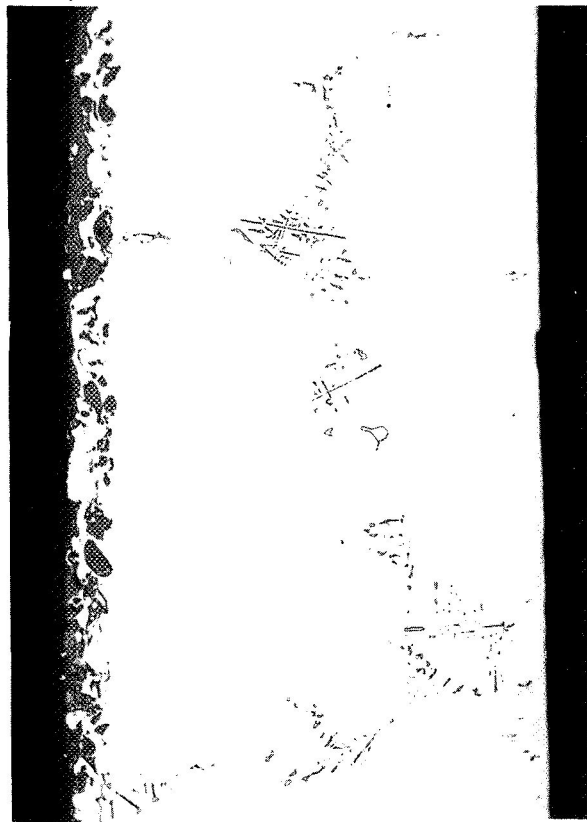
a. Graded Coating (Specimen C-5)



b. Ungraded Coating (Specimen C-11)

FIGURE B-11. OXIDE-COATING TEST SPECIMENS C-5 AND C-11

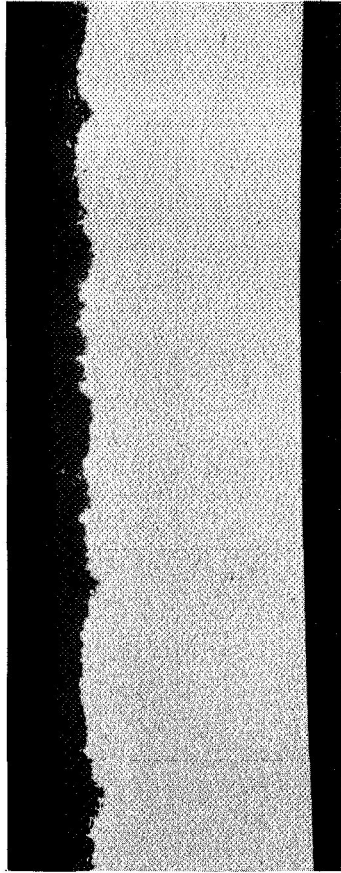
Parting layer was a coupled layer consisting of zirconia and molybdenum.



55X

a. Graded Coating (Specimen C-6)

5E699



55X

b. Ungraded Coating (Specimen C-12)

2E185B

Figure B-12. OXIDE COATING TEST SPECIMENS C-6 AND C-12

Parting layer was Nb-1Zr alloy sheet.
(See Figure B-4.)

Graded Coatings. Examination of the graded coating microstructures in Figures B-7 through B-12 revealed that most coating systems had one graded layer and sometimes two graded layers missing. After reviewing the plasma spraying procedures in detail, it was found that difficulties had been encountered during the application of the metal-rich graded layers, and that certain of these layers were either not sprayed or else were sprayed to very small thicknesses. The source of the problem appeared to be in the powder feeding mechanism in the plasma sprayer and could possibly have been a powder flow problem caused by moisture contamination, but the cause could not be definitely proven. Specimen C-1 contained all the layers specified. Specimens C-2 through C-5 did not have the 75NiCr-25ZrO₂ layers, and Specimen C-3 also did not have the 50-50 percent layer. The 50-50 layer on Specimen C-2 was thinner (about .003 inch as sprayed) than specified and the 25NiCr-75ZrO₂ layers on Specimens C-3 and C-6 were less than .002 inch as sprayed.

Thickness of Coatings. Thickness measurements of the coatings were made on each specimen and these are tabulated in Table B-2. In taking thickness measurements, the ZrO₂ layer in cracked coatings was measured only from the surface that was still soundly attached to the next layer, either a graded layer or the metal substrate. Coating thickness measurements were all smaller for the ZrO₂ layer in the container compared to measurements taken after the containers had been leached off. This is additional evidence that sectioning through the containers caused severe localized coating damage, and that delaying the sectioning of the samples until after the containers had been leached off eliminated this localized damage to the coating.

With the exception of Specimens C-6 (which underwent a gross chemical reaction that obscured thickness measurements) and C-10, the ZrO₂ coating layer on these specimens had a final thickness of at least 2 mils and less than 5-1/2 mils. The average of representative ZrO₂ coating thicknesses was 3.7 mils \pm 1.5 mils. On the other hand, the thickness of graded layers below the ZrO₂ coating layer varied far and wide, being as large as 10 mils in one case (Specimen C-1) and as small as 2.5 mils (estimated in the case of Specimen C-6).

Scratch Tests and Bend Tests

When flakes of the oxide peeled or broke off under pressure of a knife edge scrapped across the oxide surface, the metal liner was not exposed but only the graded layers beneath the oxide surface. The only specimens which flaked during the scratch test were C-3, C-5, and C-6. All three specimens had graded oxide layers beneath the ZrO₂ coating layer. The flaking in Specimen C-5 was attributed not to the oxide coating but only to the removal of the parting layer (ZrO₂/W coupled parting agent which was retained after leaching off the containers, see Figure B-6). The flaking in Specimen C-3 can be traced to the weak bond and porous ZrO₂ layer resulting from interaction with the MgO parting layer. The gross reaction observed between components in Specimen C-6 is the source for the weak bond in this specimen. None of the ungraded coating systems showed any weakness of bonding during the scratch tests.

When the initial bend tests were conducted, considerable crackling in the oxide coatings occurred, and small particles flew off during the second and third bends back which put the ceramic coating in compression. The oxide coatings on Specimens C-3 and C-6 were observed to fly off in relatively large flakes, and this behavior can be

TABLE B-2. THICKNESS MEASUREMENTS ON GAS-PRESSURE-BONDED COATINGS(a)

Specimen	Layer	Thickness as Measured in Container, inch	Thickness as Measured After Containers Removed, inch
C-1	ZrO ₂	.0027	.0033
	Graded Layers	.0109	.0098
	TD nickel	.0364	--
C-2	ZrO ₂	.0018(c)	.0022
	Graded Layers	.0036	.0036
	Hastelloy X	.0200	.0200
C-3	ZrO ₂	.0013(c)	.0036
	Graded Layers	.0036	.0055
	Hastelloy X	.0200	--
C-4	ZrO ₂	.0022(c)	.0033
	Graded Layers	.0082	.0073
	Hastelloy X	.0200	.0200
C-5	ZrO ₂	.0040	.0045
	Graded Layers	.0073	.0082
	Hastelloy X	.0200	.0200
C-6(b)	ZrO ₂	.0005	.0015
	Graded Layers	.0007	.0025
	TD nickel	.0200	--
C-7	ZrO ₂	.0033(c)	.0047
	Hastelloy X	.0200	--
C-8	ZrO ₂	.0013(c)	.0031
	Hastelloy X	.0200	.0200
C-9	ZrO ₂	.0022(c)	.0051
	TD nickel	.0364	--
C-10	ZrO ₂	.0006(c)	.0005(c)
	TD nickel	.0364	--
C-11	ZrO ₂	.0015(c)	.0044
	Hastelloy X	.0200	--
C-12	ZrO ₂	.0022	.0025
	Hastelloy X	.0200	.0200

(a) Averages were determined by sweeping across layers with a graduated scale at 50X.

(b) Measurements on Specimen C-6 were obscured by gross reaction zone.

(c) Layer thickness measurement of cracked coatings was taken from the cracked surface to the layer interface.

attributed to the same causes listed above which resulted in the weakly bonded coating layers of these specimens. Flakes of material also flew off the surface of Specimen C-5 during the initial bend tests, but this was attributed to the separation of the parting layer rather than to a weakly bonded oxide coating layer.

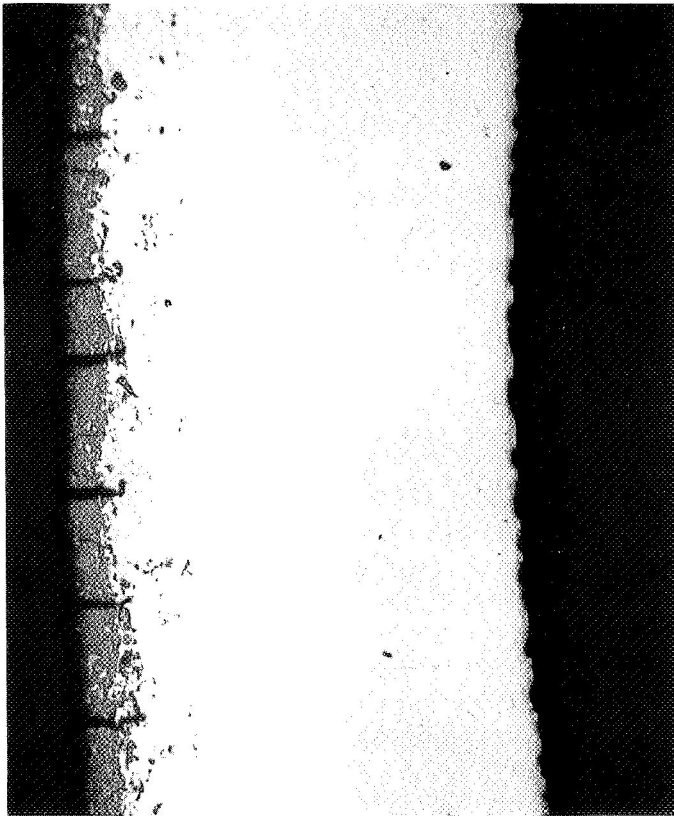
The second series of bend tests were conducted to determine the degree and type of cracking accompanying fracture of the oxide coating. The small radius of curvature (1/8-inch radius) assured coating failure; the angle of bending promoted fracture over progressively larger surface areas so that the fracture mode, crack paths, and resultant exposure to the underlying metal substrate could be visualized and examined. Fracture was initiated almost immediately upon applying bending stress. These first stage cracks are observed in Figure B-13 showing Specimens C-1 (graded coating) and C-7 (ungraded coating) after bending over an angle of 15 degrees. As the angle of bending becomes greater, the first stage cracks open up, then (in the case of graded coatings), proceed through the various graded layers toward the substrate, and finally stop at the substrate surface. These stages are depicted in Figures B-14 through B-16. The graded layers inhibit crack growth to the substrate significantly, whereas in the ungraded coating the cracks penetrate immediately to the substrate. The cracked oxide coatings do not spall off immediately, but remain bonded to the underlying layers in segments. Only when the angle of bending around the sharp radius becomes greater than 45 degrees does significant spalling and exposure of the underlying layers and the substrate occur. Under large angle bending, the graded coatings tend to survive spalling damage better than ungraded coatings.

Thermal-Shock Tests

All but four specimens survived thermal shocking during the first three cycles from 1200 F (first cycle), 1400 F (second cycle), and 1600 F (third cycle). The spalling that was observed among the four specimens (C-6, C-7, C-11, and C-12) was very slight. After the fifth and last thermal-shock cycle from 2000 F, six of the twelve specimens showed very little spalling or no spalling at all of the oxide coating. These were Specimens C-1, C-2, C-4, C-5, C-9, and C-10. Better than a third of the oxide coating on other specimens had peeled off after the thermal-shock tests. In Specimen C-6, although only 10 percent spallation was recorded, it was also noted that the substrate had oxidized completely and could not be distinguished from the oxide. Specimen C-6 was not representative of other samples. After completing the thermal shock tests, three representative samples were mounted for metallographic inspection. A tabulation of thermal shock test results is given in Table B-3.

As would be expected, the graded oxide coatings tended to survive the thermal shocks better than the ungraded oxide coatings. The two exceptions to this were Specimens C-9 and C-10 which survived the thermal-shock tests with the ungraded coating intact. But, it is also notable that these same two specimens had chromallized TD nickel substrates, whereas all other specimens except C-1 had Hastelloy X substrates. From these data, it appears that TD nickel with a chromallized surface promotes a better bond to ZrO_2 than does Hastelloy X.

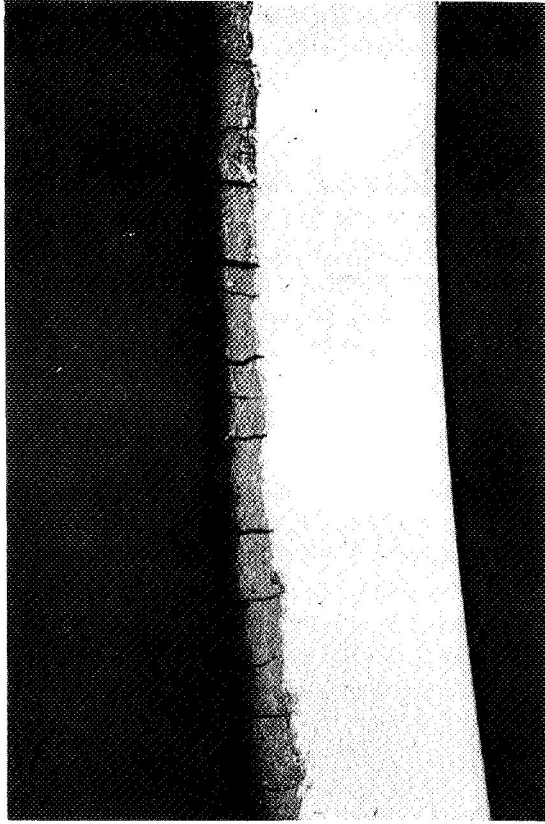
The parting layer used on each coating surface also had an observable effect during thermal shock tests. Color changes on pairs of specimens that had the same parting layer were generally the same, and these color changes occurred approximately during the same thermal cycle for this pair. Specimens C-1 and C-7 both had a beryllium



46X

6E089

a. Graded Coating (Specimen C-1)



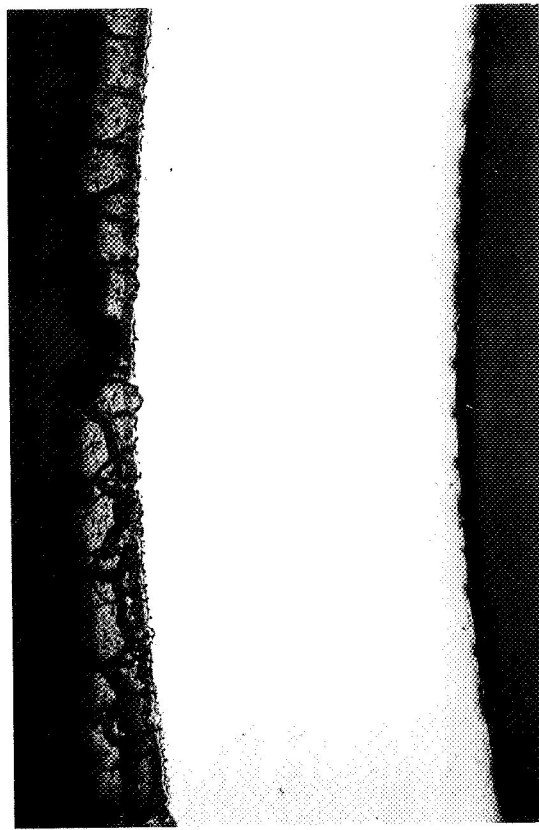
46X

6E095

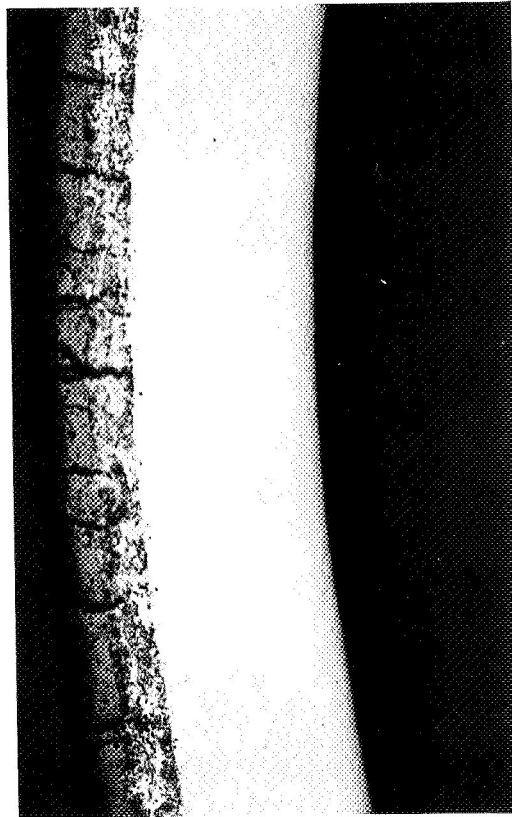
b. Ungraded Coating (Specimen C-7)

FIGURE B-13. INSPECTION OF OXIDE COATING AFTER 15-DEGREE BEND

The cracks in C-1 opened more than those in C-7 because of greater strain in outer layer of C-1 due to larger thickness of TD nickel substrate (0.037 in.) in C-1 compared with Hastelloy X (0.020 in.) in C-7. Cracks in C-7 penetrate to substrate, but in C-1, crack growth to substrate is inhibited by graded layers.



46X 6E091 b. Ungraded Coating (Specimen C-9) 6E097



46X 6E091 a. Graded Coating (Specimen C-3) 6E097

FIGURE B-14. INSPECTION OF OXIDE COATING AFTER 30-DEGREE BEND

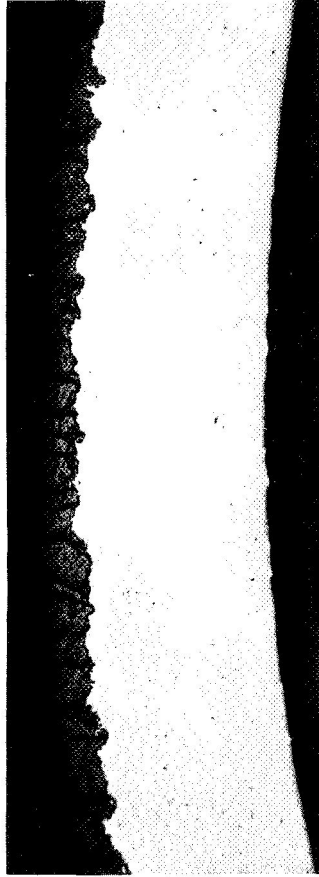
Damage to coating in C-9 is greater than in C-3 partly because of differences in thickness of the substrates. Oxide layer remains well bonded to underlying layers in C-3 despite extensive crack damage.



46X

6E090

a. Graded Layer (Specimen C-2)



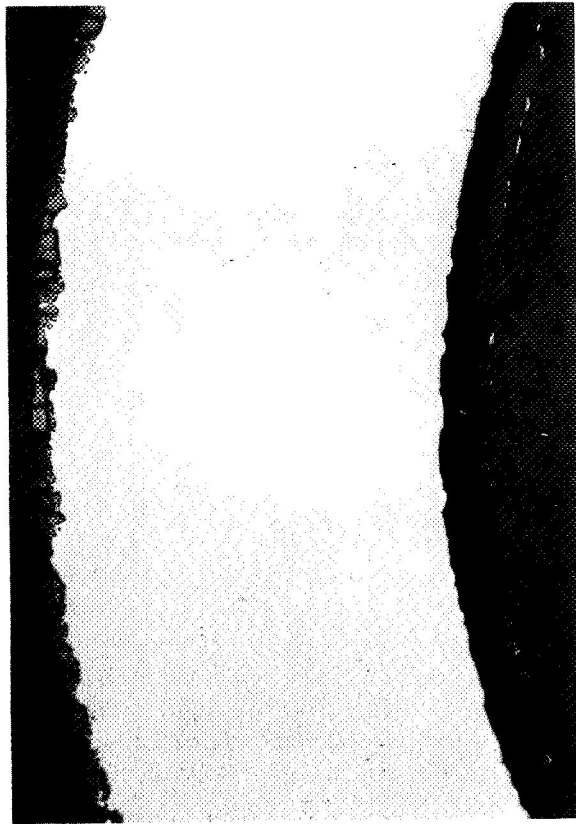
46X

6E096

b. Ungraded Layer (Specimen C-8)

FIGURE B-15. INSPECTION OF OXIDE COATING AFTER 45-DEGREE BEND

Cracks extended up to or very near to the substrate in C-2, and some spalling and exposure of underlying layers was observed. Crack damage was not so great in C-8 as in C-9 (Figure B-14) which was bent over a smaller angle but was strained more because of thickness factor.



5E701

b. Ungraded Coating (Specimen C-10)

46X



6E092

a. Graded Coating (Specimen C-4)

46X

FIGURE B-16. INSPECTION OF OXIDE COATING AFTER 90-DEGREE BEND

Crack damage to coatings is extensive; flakes of the coatings broke away leaving the underlying metal layers exposed.

TABLE B-3. THERMAL-SHOCK-TEST RESULTS

Specimen	Type Coating	Substrate	Barrier Layer	Accumulative Percent Spall After Thermal Shocking				
				1st Cycle 1200 F	2nd Cycle 1400 F	3rd Cycle 1600 F	4th Cycle 1800 F	5th Cycle 2000 F
C-1	Graded	TD nickel	Be	0	0	0	0	5
C-2	Graded	Hastelloy X	Al ₂ O ₃	0	0	0	0	0
C-3	Graded	Hastelloy X	MgO	0	0	0	10	35
C-4	Graded	Hastelloy X	Mo/ZrO ₂	0	0	0	0	0
C-5	Graded	Hastelloy X	W/ZrO ₂	0(a)	0	0	0	0
C-6	Graded	Hastelloy X	Nb/1Zr	-(b)	-(b)	5	10	10(c)
C-7	Ungraded	Hastelloy X	Be	0	5	15	35	40
C-8	Ungraded	Hastelloy X	Al ₂ O ₃	0	0	0	60	95
C-9	Ungraded	TD nickel	MgO	0	0	0	0	0
C-10	Ungraded	TD nickel	Mo/ZrO ₂	0	0	0	0	0
C-11	Ungraded	Hastelloy X	W/ZrO ₂	0	5	5	50	70
C-12	Ungraded	Hastelloy X	Nb/1Zr	-(b)	-(b)	5	85	95

(a) On Specimen C-5, a thin layer of bright yellow oxide, presumably the W/ZrO₂ parting layer, started peeling off after thermal shocking from 1200 F and was completely peeled off after thermal shocking from 1600 F. The underlying layer of ZrO₂ remained intact.

(b) Specimens C-6 and C-12 started thermal-shock tests from 1600 F rather than 1200 F.

(c) After thermal shocking from 2000 F, Specimen C-6 was completely oxidized through; the substrate could not be distinguished from the oxide.

parting layer, for example, and showed no color changes through three cycles, but after the fourth cycle (from 1800 F) both specimens had pink spotted surfaces, and after the fifth cycle (from 2000 F), both had turned greenish gray while retaining the pink spots. Specimens C-2 and C-8 changed color and became a greenish pink immediately after the very first cycle (from 1200 F). Both progressed identically through gray at 1400 F to beige at 1600 F, 1800 F, and 2000 F. The beige colored oxide on Specimen C-8 spalled off almost completely while the same color oxide on Specimen C-2 remained intact throughout the tests. The oxide on Specimens C-3 and C-9 had the same color changes per cycle, becoming 60 percent greenish black and 40 percent brown at the end of the fifth cycle. The brown colored surfaces on Specimen C-3 spalled, whereas those on Specimen C-9 remained intact. The greenish-black oxide on both was also retained. Specimens C-4 and C-10 started out with greenish-pink oxide through the first two cycles, then C-4 became silver colored with pink spots from the third to fifth cycle, while C-10 became silver colored with a greenish-pink tint. The biggest difference in color changes per cycle of pairs of specimens having the same parting layer were observed in Specimens C-5 and C-11 (with W/ZrO₂ parting layer). About 80 percent of the surface on C-5 became yellow brown after the second cycle and spalled off completely after the third cycle. However, the underlying layer exposed after the second cycle was pink colored but changed to beige during the fourth and fifth cycles. It was apparent that the first layer which came off quickly was simply the W/ZrO₂ coupled parting layer retained on Specimen C-5. The underlying layer behaved much like the oxide coatings in Specimens C-2 and C-3 but did not spall at all. About 30 percent of the oxide on Specimen C-11 changed to a dull white after the very first thermal cycle; this oxide was unchanged thereafter and did not spall off the surface. The remaining oxide surface on Specimen C-11 turned beige after the third and fourth cycles and spalled off completely after the fifth cycle.

Specimens C-6 and C-12 had similar color changes even though the massive reaction within C-6 during gas-pressure bonding made evaluations and comparisons difficult. Both C-6 and C-12 showed bright yellow edges on the oxide surface after thermal shocking from 1600 F. Both turned yellowish white after thermal cycling from 2000 F; however, the oxide on C-12 spalled completely after the 2000 F cycle. It is probable that had the substrate on C-6 not oxidized completely during thermal cycling, the oxide coating would have behaved similarly to that on C-12. Any effects of the parting layer on thermal-shock resistance are not readily apparent except for the systems using Nb-1Zr (in Specimens C-6 and C-12).

From these tests, it was shown that the graded oxides on Hastelloy X survive thermal shocking better than ungraded oxides on Hastelloy X but that ungraded oxides on chromallized TD nickel survive as well as any system. The only parting layer that definitely affected the thermal-shock behavior adversely was Nb-1Zr. Other parting layers simply generated different color changes within the oxide coatings without having any apparent effects on thermal-shock properties. Although the W/ZrO₂ parting layer on Specimens C-5 and C-11 tended to obscure thermal shock test data by the premature spalling of the tungsten oxide, no detrimental effect to the underlying oxide coating was apparent from retaining the parting layer on the oxide coating surface.

Metallographic examination of the coating systems after thermal-shock tests revealed that the oxides generally had cracks running parallel to the coated surfaces except in coatings that were very thin as in Specimen C-10 (Figure B-19). Some of these cracks already existed in the coatings before thermal-shock tests, as was evident in Figures B-8 and B-10, so that the additional extent of cracks due to thermal shocking

in coatings that survived these tests is rather small. Little other change in microstructure is observed after thermal-shock tests in Specimens C-2 and C-4 when these are compared with the microstructures before testing - compare Figure B-17 with Figure B-8a, and Figure B-18 with Figure B-10a. A change in microstructure was observed in Specimen C-10 (Figure B-19) after thermal-shock tests, not to the oxide coating itself, but to the substrate, owing to chromium depletion and oxidation at the surface of the chromallized TD nickel. This phenomenon did not appear to adversely affect the bond quality of the oxide to the substrate; in fact, the coating on C-10 had the most "inert"-looking appearance of any of the coating systems after thermal-shock testing. The same behavior and appearance would be expected of Specimen C-9, which was also an ungraded coating on chromallized TD nickel, and (except for color differences in the oxide) this was indeed the case. In spite of the diffusional effects from the MgO parting layer in Specimen C-9, this specimen showed exceptionally high thermal shock resistance. A closer examination of the microstructure of these specimens as bonded in Figures B-9b and B-10b shows that just below the oxide layer in the chromallized TD nickel substrates, there is an apparent interdiffusion zone only about .001 inch thick. Whereas other coatings on Hastelloy X substrates show no such apparent reaction zone (thus making the bond one that is primarily mechanical), the oxide coatings on chromallized TD nickel substrates did react with the substrates thus setting up strong diffusional bonds as well as mechanical bonds. The chromium apparently diffuses from the liner to the interface, interacts with the oxide, and thereby promotes this strong thermal-shock resistant bond. The system warrents further study, whatever the mechanism.

Evaluation of Large 4 by 8-Inch Coating Samples

The larger samples were evaluated by visual and metallographic examinations, and by scratch tests. After the samples were decanned in 50HNO_3 - $50\text{H}_2\text{O}$, one specimen had a white oxide surface while the other had a beige oxide surface. The white oxide surface was about .003 inch thick and came off easily by scrapping with a fingernail. This was the alumina parting layer which had adhered more on one specimen to the zirconia surface than on the other sample. The oxide beneath the alumina was beige colored and it strongly adhered to the Hastelloy X substrate. The zirconia coatings on these larger samples were lighter colored as-bonded than were the comparable zirconia coatings on the smaller samples (C-8 in particular which was darker colored). The lighter color may be due to the larger coating thickness (.006 inch instead of .003) and the mixing of zirconia with some alumina or other impurity.

Micrometer measurements indicated the zirconia coating thickness was 0.0065 ± 0.0015 inch thick on both coating samples. Figure B-20 is a photograph of the larger coating samples after the containers had been removed.

Sections were cut off 1/4 inch from one end of each sample with an abrasive cut-off wheel for metallographic examinations. Figures B-21 and B-22 show the microstructure of the sections. As measured on the microphotos, the average coating thickness on these sections was .0062 inch. Oxide penetration into the Hastelloy X substrate was significant and comparable to that in the smaller samples. The oxide layer appears to have two phases in it; this more than likely is some alumina that mixed in with the zirconia during plasma spraying. Some of the alumina parting layer was retained on the zirconia oxide surface and under bright light illumination it was slightly darker in color than the zirconia. Under polarized light there was no detectable distinction between the two

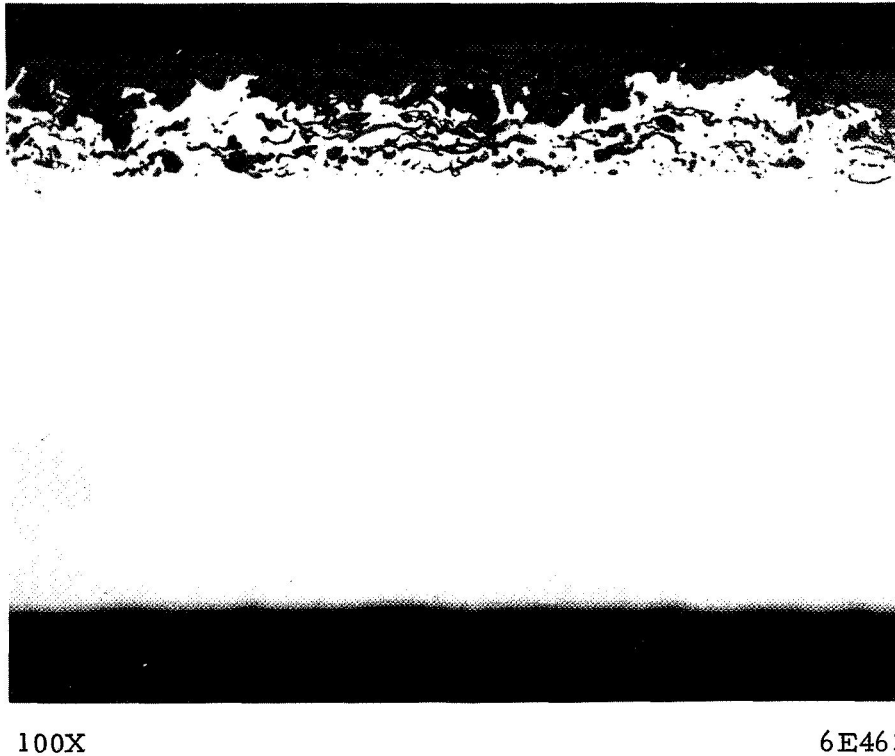
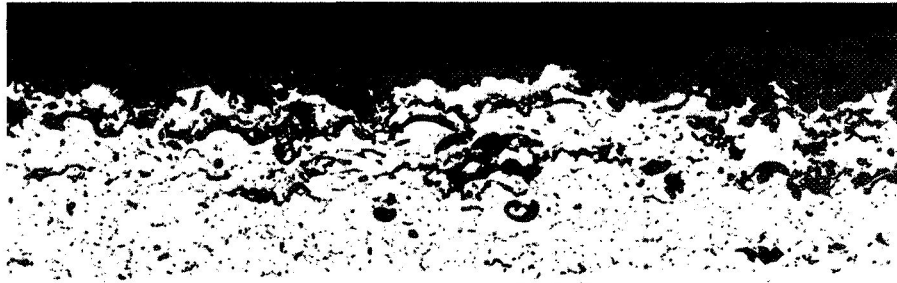


FIGURE B-17. GRADED OXIDE COATING ON HASTELLOY X AFTER THERMAL-SHOCK TESTING (SPECIMEN C-2)

Most of the coating remained bonded to the Hastelloy X substrate. Some lamellar-type cracks developed because of thermal shock, but these were not severe.



100X

6E464

FIGURE B-18. GRADED OXIDE COATING ON HASTELLOY X AFTER THERMAL-SHOCK TESTING (SPECIMEN C-4)

This specimen was examined to compare what effect different parting layers might have on the final micro-structure after thermal-shock testing. Specimen C-2 in Figure B-17 had Al_2O_3 ; Specimen C-4, above, had a Mo/ZrO_2 parting layer. No differences can be directly attributed to effects on the parting layer.

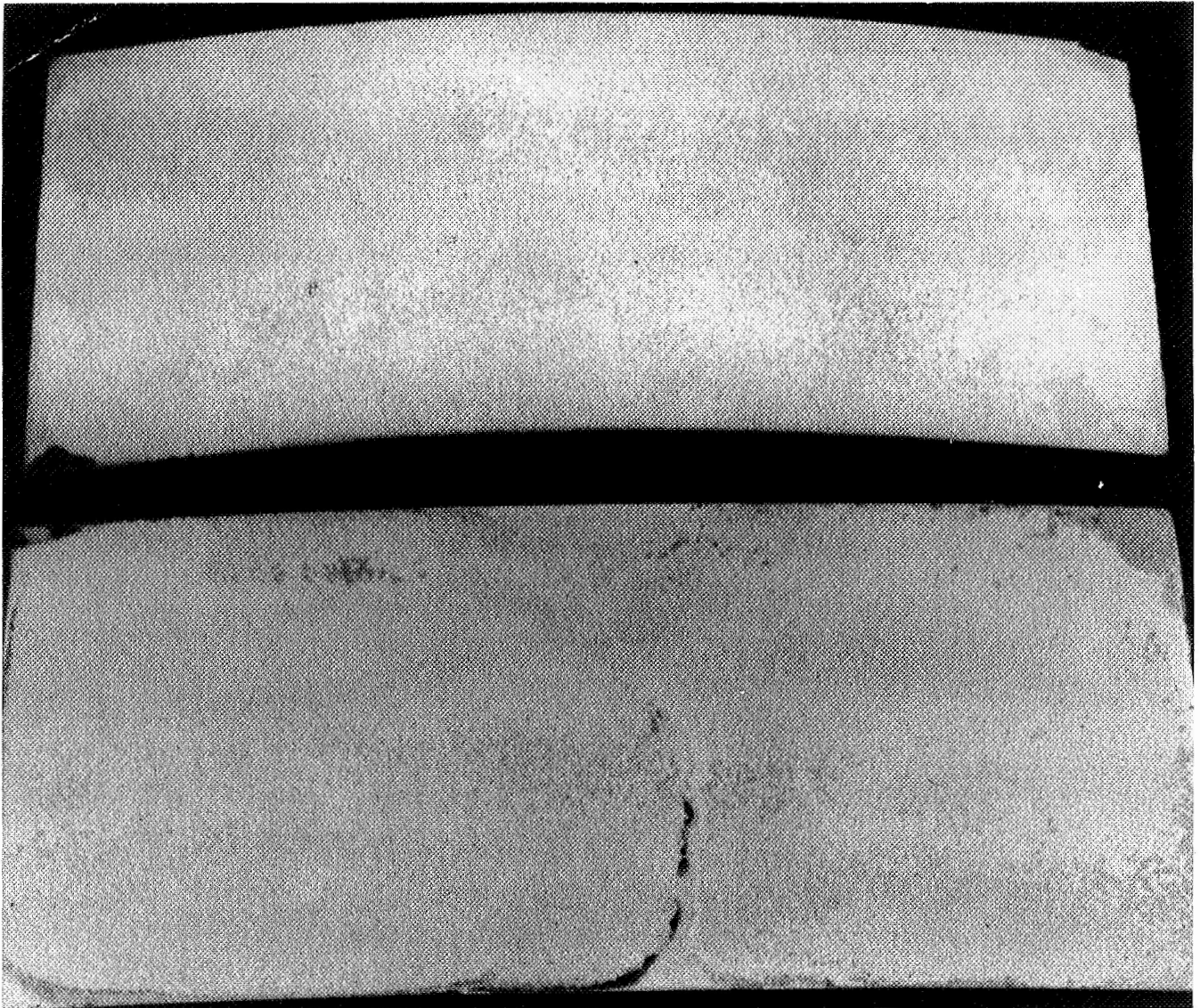


100X

6E466

FIGURE B-19. UNGRADED OXIDE COATING ON CHROMALLIZED TD NICKEL AFTER THERMAL-SHOCK TESTING (SPECIMEN C-10)

This specimen is different in two respects from C-2 and C-4: first, the oxide is ungraded; second, the substrate is chromallized TD nickel rather than Hastelloy X. Ungraded oxides generally did not survive thermal-shock testing except when the oxide was bonded to chromallized TD nickel, as above. Ungraded oxides bonded to this substrate survived testing as well as or better than any specimen.



Specimen A (Top)
Specimen H (Bottom)

48390

FIGURE B-20. UNGRADED OXIDE COATING ON LARGER (4 BY 8-INCH)
HASTELLOY X PLATES

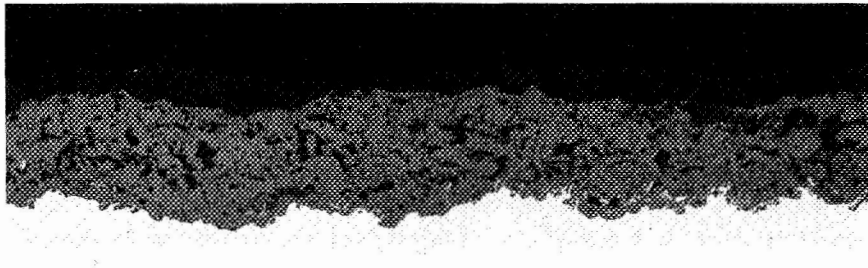
Both plates had a residue of the alumina parting layer on top of the zirconia coating and gave a lighter color shade to the surfaces. The alumina flaked off easily, leaving the strongly adherent, beige-colored zirconia. The dark corners are residue iron which was not completely leached off but which could be peeled off from the oxide surface. The shading figure at the midregion of the bottom plate appeared to be a plasma-spraying artifact.



100X

6E767

FIGURE B-21. MICROSTRUCTURE OF OXIDE-COATING LAYER
ON LARGER SAMPLE (SPECIMEN A)



100X

6E766

FIGURE B-22. MICROSTRUCTURE OF OXIDE COATING LAYER
ON LARGER SAMPLE (SPECIMEN H)

phases. The oxide appeared to be quite dense on both samples and little if any porosity was evident in the coating layer. The edges of the coating layer adjacent to the cut section did not chip or break off and indicated the bond strength was quite high. Scratch tests with a knife edge also failed to chip or flake the oxide coating.

Summary of Results

Protective oxide coatings on Hastelloy X and chromallized TD nickel substrates were applied by plasma spraying along with a preferential parting layer, densified and bonded by gas-pressure bonding, and evaluated by metallographic analyses primarily but also by scratch tests, bend tests, and thermal shock tests. Ungraded zirconia coatings and coatings graded with Ni-20Cr alloy powder were prepared and compared, and six different parting layers were examined. Two larger (4 by 8 inch) Hastelloy X plates were coated with the ungraded oxide, and an alumina parting layer was used on these samples.

All of the small (2 by 2 inch) samples were gas-pressure bonded at 2200 F and 15,000 psi for 3 hours. The larger plate samples were gas-pressure bonded at 2150 F and 15,000 psi for 6 hours.

Metallographic examinations showed that the coatings were sound, dense, of uniform thickness, and appeared to be well bonded to the substrates. In cases where the coating sample was cut through before leaching off the bonding container, the protective oxide coating was severely cracked locally and the parting layers tended to stick to the container instead of cracking preferentially. When the coating samples were first decanned by leaching and then sectioned, the protective coatings did not crack but were retained intact on the substrate, and the parting layers were either removed or in some cases even retained on top of the protective oxide coating.

The MgO and Be parting layers were the only parting layers that had an effect on the microstructure, and these were minor. The Mo/ZrO₂ parting layer was associated with tendencies to produce more cracking in the protective oxide coatings, but this could not be definitely affirmed. The Nb/1Zr parting layer may have contributed to a gross reaction in one specimen, and this reaction tended to obscure useful results on this specimen.

The ceramic-to-metal bonds were fairly strong mechanical bonds in general for ungraded coatings. The notable exceptions to this were the ceramic-to-metal bonds on chromallized TD nickel substrates. These bonds were chemical diffusion bonds which produced exceptionally tight bonds at the ceramic metal interfaces. Graded coatings all produced satisfactory bonding between the Ni-20Cr alloy powder filler and the metal substrate.

All coating systems survived scratch tests with the exception of a graded coating having a MgO parting layer. The MgO interaction with the protective oxide layer may have reduced the scratch resistance of the oxide layer.

Graded coatings generally survived thermal shock tests from 2000 F better than ungraded coatings. The notable exceptions were, again, the ungraded coatings on

chromallized TD nickel substrates. These latter coatings survived thermal shock tests much better than any of the other ungraded coating systems and as well as any of the graded coating systems.

The coatings on the larger plate samples were lighter in color than on the smaller samples, and this was due partly to the larger oxide coating thickness on the larger samples and partly to the mixing of a small amount of alumina with the zirconia during plasma spraying. The protective oxide layer survived scratch testing, while the alumina parting layer on top of the oxide layer tended to flake off easily.

Metallographic examination of the oxide coating on the larger samples showed that the oxide had relatively uniform thickness over the surface, was thicker (.0065 inch) than the oxide layers on the smaller samples (which was .003 inch), was dense, well bonded, and had achieved significant penetration into the metal substrate surface.

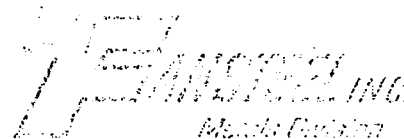
Conclusions

- (1) Dense and protective zirconium oxide coatings are strongly bonded to metal surfaces by a combination of plasma spraying and gas-pressure bonding.
- (2) The resultant coatings are scratch resistant, remain bonded to the metal despite severe deformation of the metal substrate, and show high thermal shock resistance.
- (3) The use of a parting layer that separates preferentially aids in the transference of the coating from a mandrel to the surface that requires protection. This "transfer concept" simplifies the coating of internal surfaces and makes the process attractive for protecting thrust chamber liners, internal engine parts, nozzle surfaces, afterburner walls, and piping subjected to hot corrosive fluids and gases.

APPENDIX C

CERTIFICATION SHEETS FOR MATERIALS
USED IN TASK II

FAHSTEEL CERTIFICATION



5101 TANTALUM PLACE
BALTIMORE, MARYLAND 21226
Phone: 301/355-0600 TWX: 710/234-2496

Battelle Memorial Institute
505 King Avenue

Customer Columbus, Ohio 43201

PURCHASE ORDER NO. Y6257 PRODUCTION NO. 078246 QUANTITY See Below

ALLOY Nickel-2% Thoria H. T. CONDITION Stress Relieved FORM Sheet

[illegible]

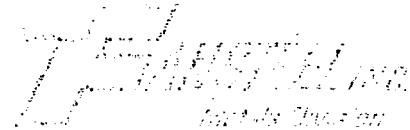
PERCENT CHEMICAL ANALYSES

[illegible]

We certify this material meets your Purchase Order and Specification No. DPH(P)201B except Ultimate
tensile strength. Approval to ship given by cognizant representative of your Company and
DATE January 23, 1969 J. Clark of Fansteel Inc. [Signature]
QUALITY CONTROL REPRESENTATIVE

FAR

ACTION



5101 TANTALUM PLACE
BALTIMORE, MARYLAND 21226

Phone: 301/355-0600 TWX: 710/234-2496

Battelle Memorial Institute
505 King Avenue

CUSTOMER Columbus, Ohio 43201

PURCHASE ORDER NO. Y6257 PRODUCTION NO. 078246 QUANTITY


ALLOY Nickel-2% Thoria H.T. CONDITION Stress Relieved FORM Sheet

MECHANICAL PROPERTIES

ITEM	TEST TEMP.	U. T. S. ksi	Y. S. ksi	ELONG. % IN (1")	R. A. %	2000° F STRESS RUPTURE			105° Bend
						STRESS, ksi	HOURS	ELONG. % IN (1")	
	Room 2000° F	57.9 14.0	45.3 13.8	16.1 3.2		5.5	Exceeds 20	4.0	1 T
	Room 2000° F								
	Room 2000° F								
	Room 2000° F								
	Room 2000° F								
	Room 2000° F								
	Room 2000° F								
	Room 2000° F								
	Room 2000° F								
	Room 2000° F								
	Room 2000° F								
	Room 2000° F								
	Room 2000° F								
	Room 2000° F								
	Room 2000° F								

We certify this material meets your Purchase Order and Specification No. DPN(P)261B

DATE January 21, 1959


QUALITY CONTROL REPRESENTATIVE

CERTIFIED REPORT OF CHEMICAL ANALYSIS AND MECHANICAL TESTS

ANALYST'S NO.	61015	DATE RECEIVED	
SOLD TO	BUYER		

BATTELLE MEMORIAL INSTITUTE
ATTN INV AUDIT
505 KING ST
COLUMBUS, OHIO 43201



UNION CARBIDE CORPORATION
MATERIALS ENGINEERING DIVISION
200 WEST PARK AVENUE, SPRINGFIELD, OHIO 45504

This material annealed and cooled in dry hydrogen.

BATTELLE MEMORIAL INSTITUTE
505 KING ST
COLUMBUS, OHIO 43201

REC'D JAN 27 1969

Y 6258	QUANTITY ORDERED	QUANTITY SHIPPED	REMARKS:
2 pcs	2 pcs		<input checked="" type="checkbox"/> 1. THIS MATERIAL HAS PASSED THE BEND TEST AND IS CAPABLE OF MEETING THE STRESS RUPTURE REQUIREMENTS PER SPECIFICATION. <input type="checkbox"/> 2. THIS MATERIAL IS CAPABLE OF MEETING THE STRESS RUPTURE REQUIREMENTS PER SPECIFICATION. <input type="checkbox"/> 3. THIS MATERIAL IS CERTIFIED TO THE CHEMISTRY ONLY. THE ABOVE PROPERTIES ARE REPORTED FOR INFORMATION. <input type="checkbox"/> 4. TEST SPECIMEN OBTAINED FROM A FORGED TEST INGOT THAT IS PROPERLY HEAT TREATED.
.031 x 36 x 36 LG CRS ANL& AND PICKLE HASTELLOY ALLOY X AMS-5536F			

HEAT NO.	PIECES	Cr	W	Fe	C	Si	Co	Ni	Mn	Cb+Ta	V	Mo	P	S
2600-8-4672	72	22.19	.54	18.73	.07	.41	2.18	Ba1	.62			8.72	.014	.004
1														
2														
3														
4														
5														
6														

Al	Ti	B	Cu	Zr	Ta	Mg	O ₂	H ₂	N ₂
		.002							
1									
2									
3									
4									
5									
6									

TENSILE TEST AT ROOM TEMPERATURE					TENSILE TEST AT °F				
ULTIMATE PSI	.2% YIELD PSI	.02% YIELD PSI	% ELONG IN 2"	% R. A.	ULTIMATE PSI	.2% YIELD PSI	.02% YIELD PSI	% ELONG IN 2"	% R. A.
104,400	46,450		55.5						
-1					-1				
-2					-2				
-3					-3				

STRESS RUPTURE								THIS IS TO CERTIFY THAT THE ORIGINAL OF THIS REPORT HAS BEEN PROPERLY SIGNED AND NOTARIZED	
	TEST TEMP. (°F)	STRESS PSI	HOURS	% ELONG IN 2"	ANNEALED HARDNESS	AGED HARDNESS	GRAIN SIZE		I. G. A. DEPTH
1							4		
2									
3									

CERTIFIED BY	DATE
<i>W. E. Conell</i>	January 22, 1969

SUBSCRIBED AND SWORN TO BEFORE ME
John J. Jansky
 NOTARY
 My Commission Expires 16 Sept. 1973

BUFFALO, N. Y.
CHICAGO, ILL.
CLEVELAND, OHIO

255 BENT STREET
CAMBRIDGE, MASSACHUSETTS 02141

MONTCLAIR, N. J.
SOUTHINGTON, CONN.

CERTIFICATE OF TEST

Battelle Memorial Institute
505 King Avenue
Columbus, Ohio 43201

7111 Wall Street
Cleveland, Ohio 44125

YOUR ORDER NO. Y5696				OUR INVOICE NO. E-44299				DATE SHIPPED 2-3-69					
ITEM	TYPE	MATERIAL - SPEC.										SHIPPED	HEAT NUMBER
1.	347	16 ga 2D finish										30#	58054
2.	347	18 ga 2D finish										24#	68051
ITEM	C	MN	P	S	SI	CR	NI	MO	CU	CB	TI	CO	OTHER ELEMENTS
1.	.062	1.45	.019	.016	.67	18.15	11.30	.16	.11			.17	TA .76
2.	.060	1.50	.023	.014	.70	18.67	10.75	.33	.16			.16	TA .70
ITEM	TENSILE	.2% YIELD	% ELONG.	% R.A.	SHIPPED HARDNESS	HARDEN- ABILITY	REMARKS: 1, 2, 3, 4, 5, 6, ETC.						
1.	91,500	42,800	45		RB81		No. 3						
2.	93,600	44,500	43		30T67		No. 3						

INDUSTRIAL STAINLESS STEELS, INC. CERTIFIES THAT
THIS IS A TRUE COPY OF ORIGINAL TEST REPORT NOW
ON FILE AND THAT THE MATERIAL SHIPPED MEETS
THE REQUIREMENTS OF THE ORDER.

BY

Carl Eisenwinter

ASSISTANT METALLURGIST

1. Macro test OK.
2. Solution heat treated and free from continuous carbide network
3. Bend test OK.
4. Intergranular corrosion OK to ASTM A-393....
5. Hydrostatic test OK.
6. Embrittlement Test OK.

APPENDIX D

PROCEDURAL STEPS INVOLVED IN THE MODIFIED PREPARATION AND ASSEMBLY PROCESSES FOR CYLINDRICAL-SPOOL-PIECE COMPONENTS

APPENDIX D

PROCEDURAL STEPS INVOLVED IN THE MODIFIED PREPARATION
AND ASSEMBLY PROCESSES FOR CYLINDRICAL SPOOL PIECE COMPONENTS

1a. Specimen 2

The Tinamel sleeve and mandrel were vapor degreased. Care was taken to avoid flaking off any loose edges of molybdenum foil on either part. After thorough drying, the Tinamel sleeve was assembled on mandrel, aligned accurately with cut grooves, and aero clamped 1/2 inch from each end and at 2-inch intervals.

1b. Specimen 1

The gap and separation between Tinamel and molybdenum foil was flushed with 200-proof alcohol, degreased, and allowed to dry thoroughly and an aero clamp was installed 1 inch from each end of the Tinamel and at 2 inch intervals.

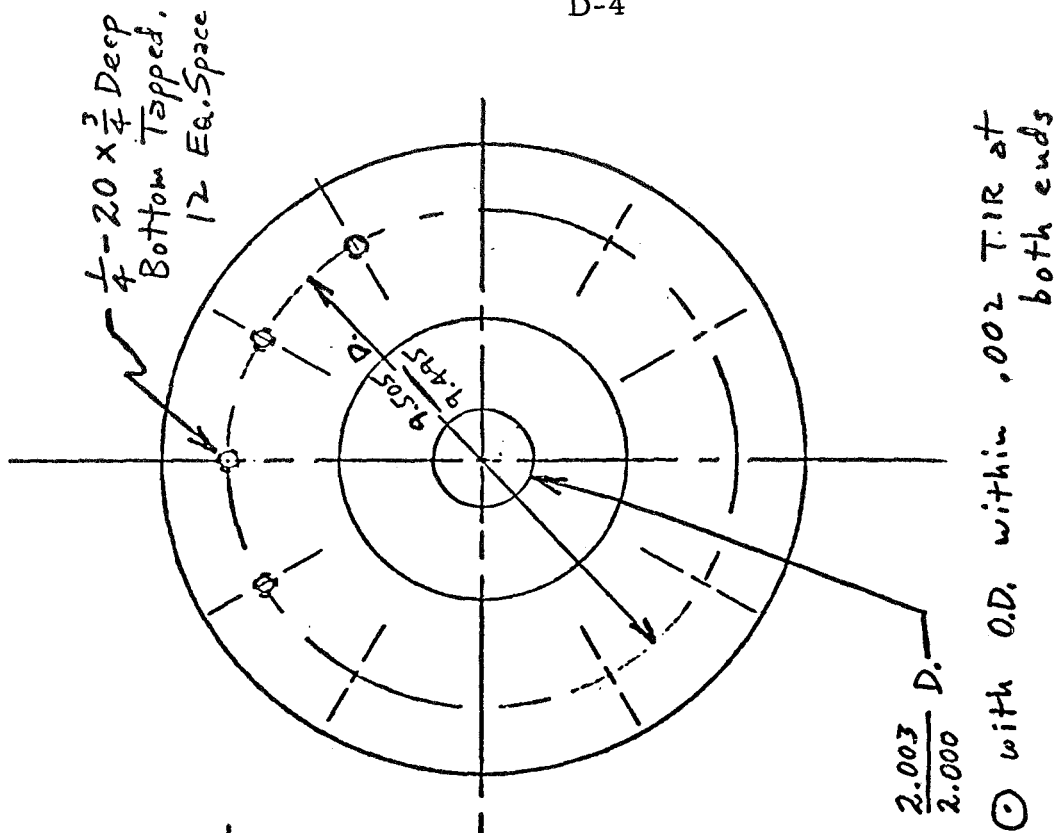
2. Center holes were drilled and bored and bolt holes machined per Drawing SK8635-A.
3. End clamps were made per SK8635-B and degreased, and then installed on the mandrel.
4. Degreased aero clamps were installed on one-half the mandrel length.
5. Half of the mandrel length was slotted dry per SK8635-C. Degreased aero clamps were installed on slotted half of mandrel and the other half was then slotted.
6. The mandrel assembly was degreased, cleaned, and dried.
7. Stainless steel ribs were cut to proper length and configuration according to Drawing SK8635-D.
8. The ribs were degreased, cleaned, and kept under alcohol until assembled.
9. The end rib spacer (SK8635-E) was installed on both ends of the mandrel assembly.
10. The mandrel was placed in vertical position; all aero clamps were removed except the center one, and this one was loosened and supported to stay at center of the mandrel.
11. The ribs were installed in slots against the end rib spacer.

12. By using rubber strips under the aero clamps, the different heights of Tinamel tooling and ribs were compensated for.
13. A series of diametral measurements were taken of ribs and recorded for each assembly.
14. Filler blocks were press fitted into the spool pieces with the outer ends flush with ID of large end groove.
15. A light cut was taken on the ID of the large end groove. The diameters were measured per SK8635-F, and part locations were marked for drilling after bonding per SK8635-G.
16. Large rings were fabricated to fit grooves per SK8635-F.
17. The large end rings were installed.
18. Grooves for the small end rings were then machined. The OD was measured per SK8635-F.
19. Small end rings were fabricated to fit the grooves per SK8635-F.
20. The small end rings were installed.
21. The ID of the spool assembly was bored to make a .002 to .006.inch diametral clearance with the mandrel assembly.
22. An assembly fixture was prepared per SK8635-H and degreased.
23. The end clamp and rib spacer were removed from one end of the mandrel assembly. All tapped holes used for clamping were plugged and cut flush or slightly below the surface.
24. The mandrel assembly was lowered on the fixture, and the aero clamps removed as lowering progressed. The end clamp was taken off to complete the lowering and then the rib spacer was removed.
25. All tapped holes were plugged as in Step 23.
26. The shaft extension was removed.
27. End closures were fabricated per SK8635-1.
28. The closure without stems was welded to the spool and mandrel.

29. The assembly was inverted and the bottom plate removed.
30. The shaft was welded around.
31. The stemmed closure was then welded to mandrel and spool.
32. The guide rails were attached to the spool per SK8635-J to accommodate the thermocouples.
33. The evacuation stem was connected to sniffer and the specimen evacuated. Helium lance was applied around all joints and welds to check for leaks.
34. After finding the welds gastight, the spool pieces were outgassed and sealed by hot forge welding.

Machine Mod. 10

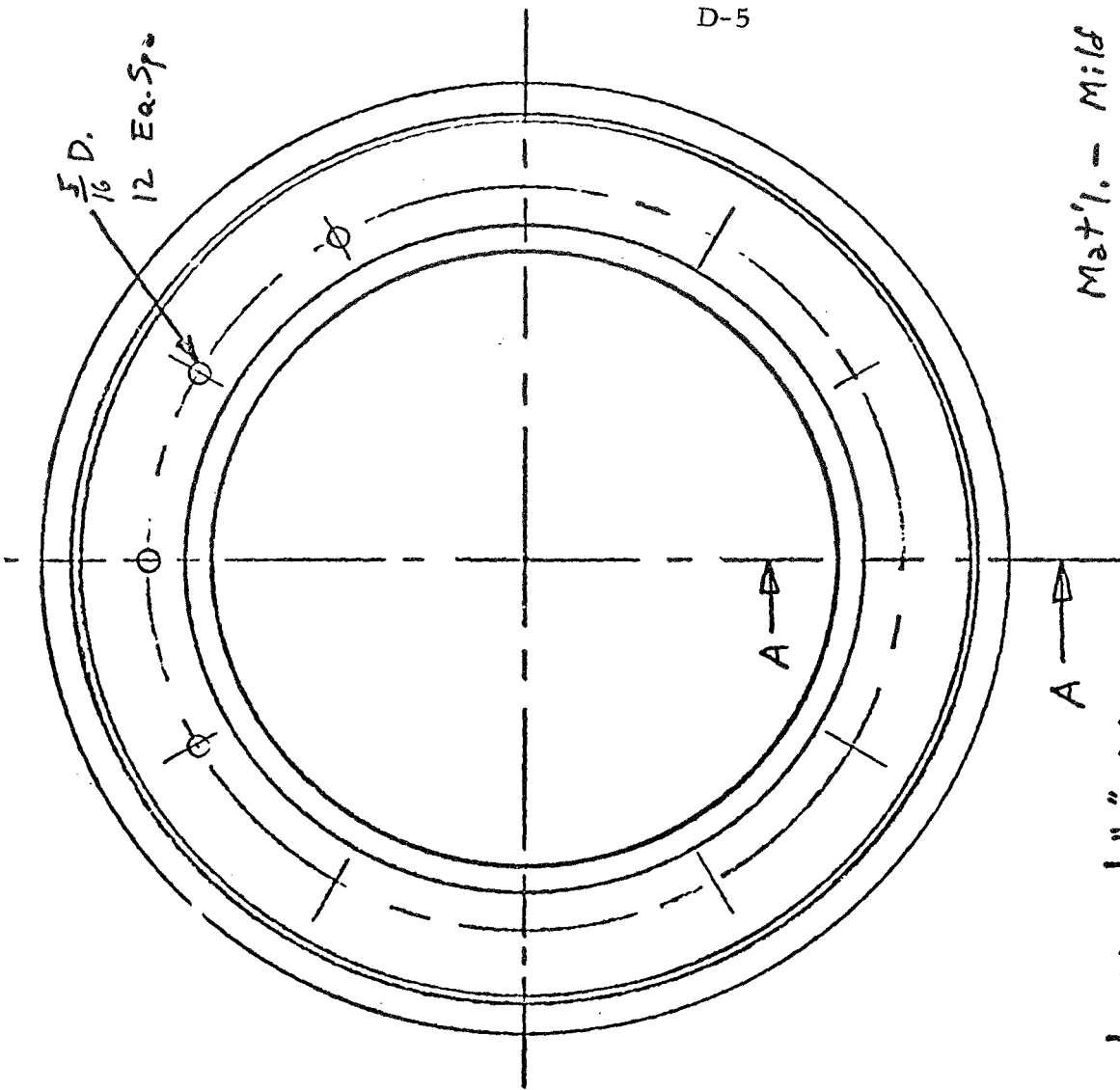
D-4



SK 8635-A

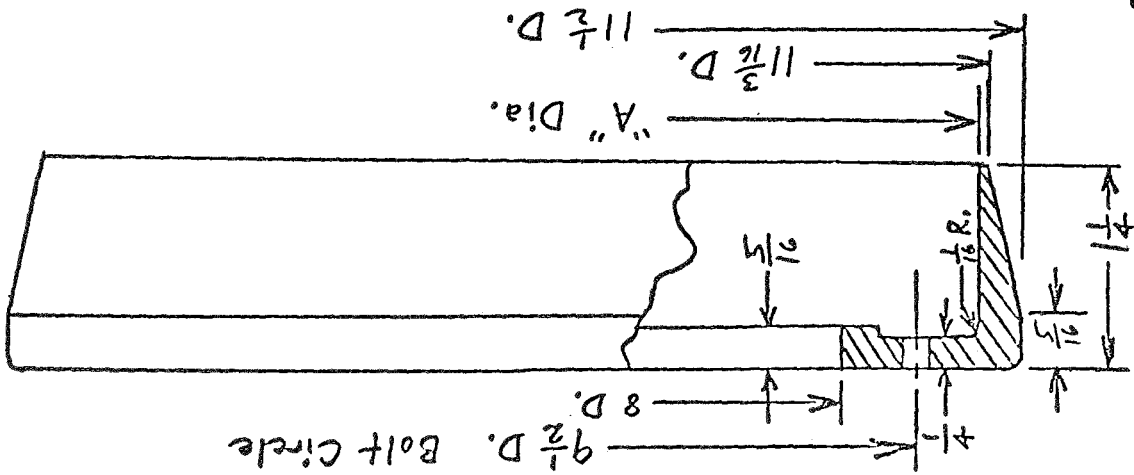
Important Note: Machine dry.
Clean all contacting parts
of machine. Keep part
completely free of oil,
grease, dirt, etc. If
necessary to use cutting
fluid, use 200 proof
alcohol.

D-5

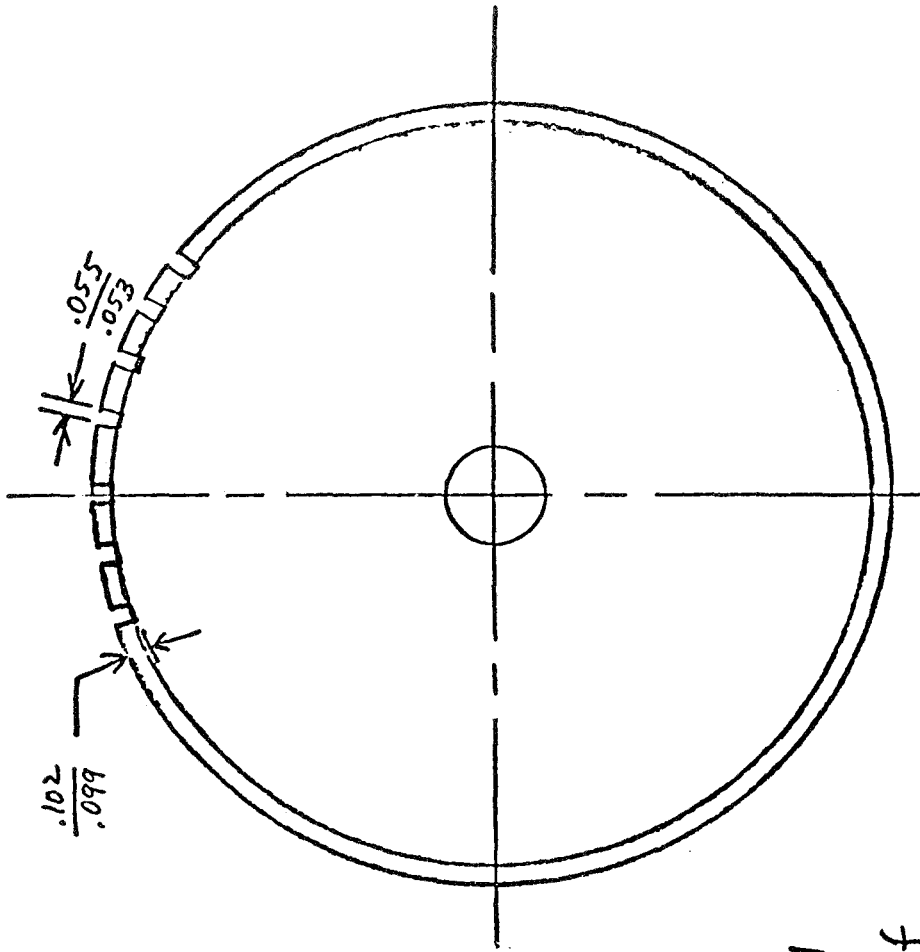


Mat'l. - Mild

SK 8635-B



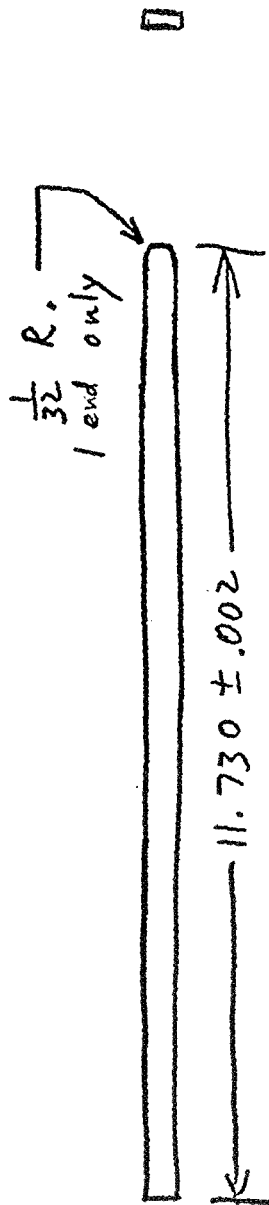
P.T. No.	Qty.	"A" Dia.
1	2	$11.014 \pm .002$
2	2	$11.020 \pm .002$



120 Slots,
Eq. Spaced

Important Note: Clean all contacting parts of machine. Machine dry, or use 200 proof alcohol as cutting fluid. Keep part completely free of oil, grease, dirt, etc.

SK 8635-C

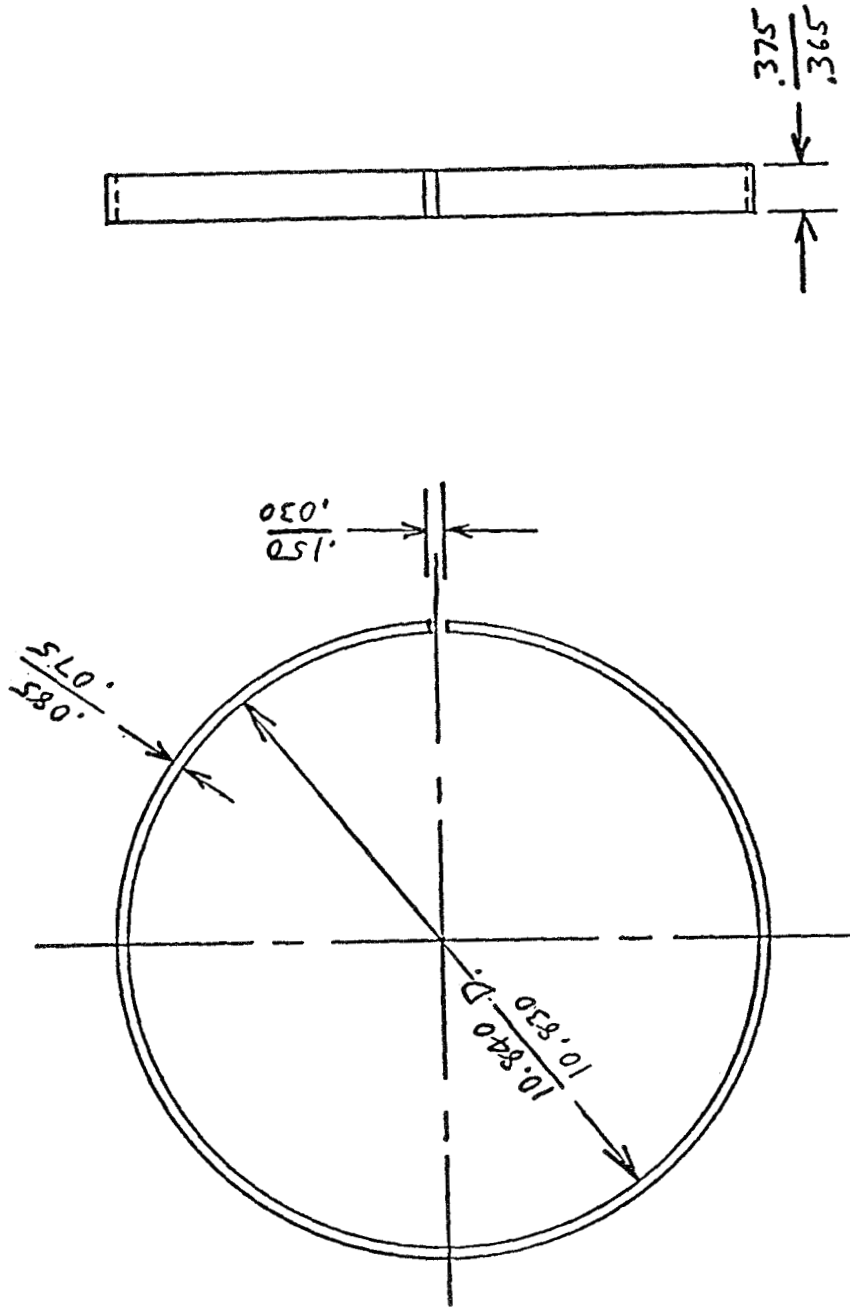


Cut ribs to above length from
existing 12" long ribs
240 req'd.

SK 8635- D

✓

1110 spec



Mat'l. - Steel

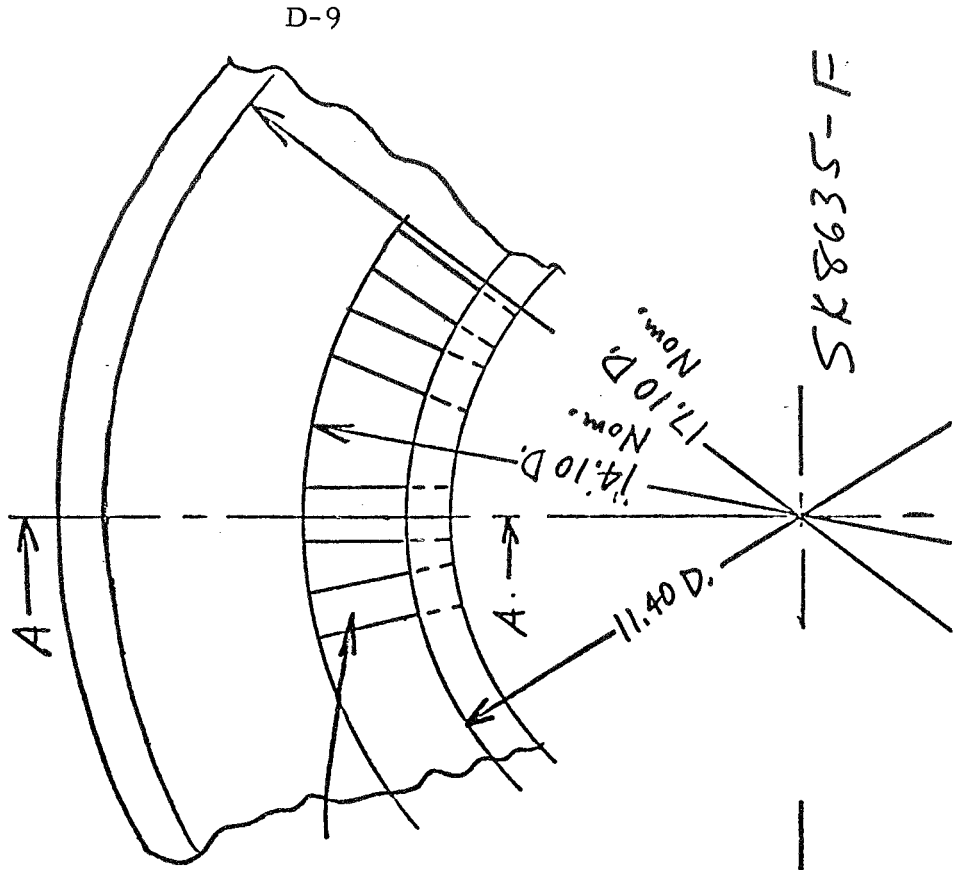
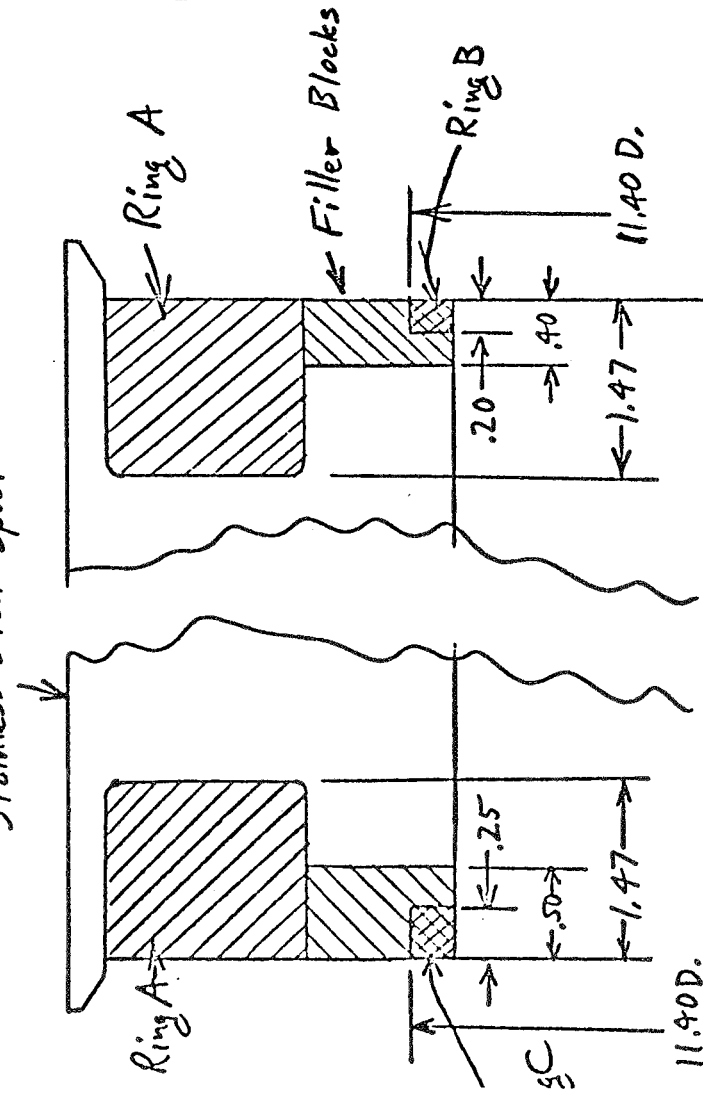
4 req'd.

SK 8635-E

Steel Tooling Inserts

Section A-A

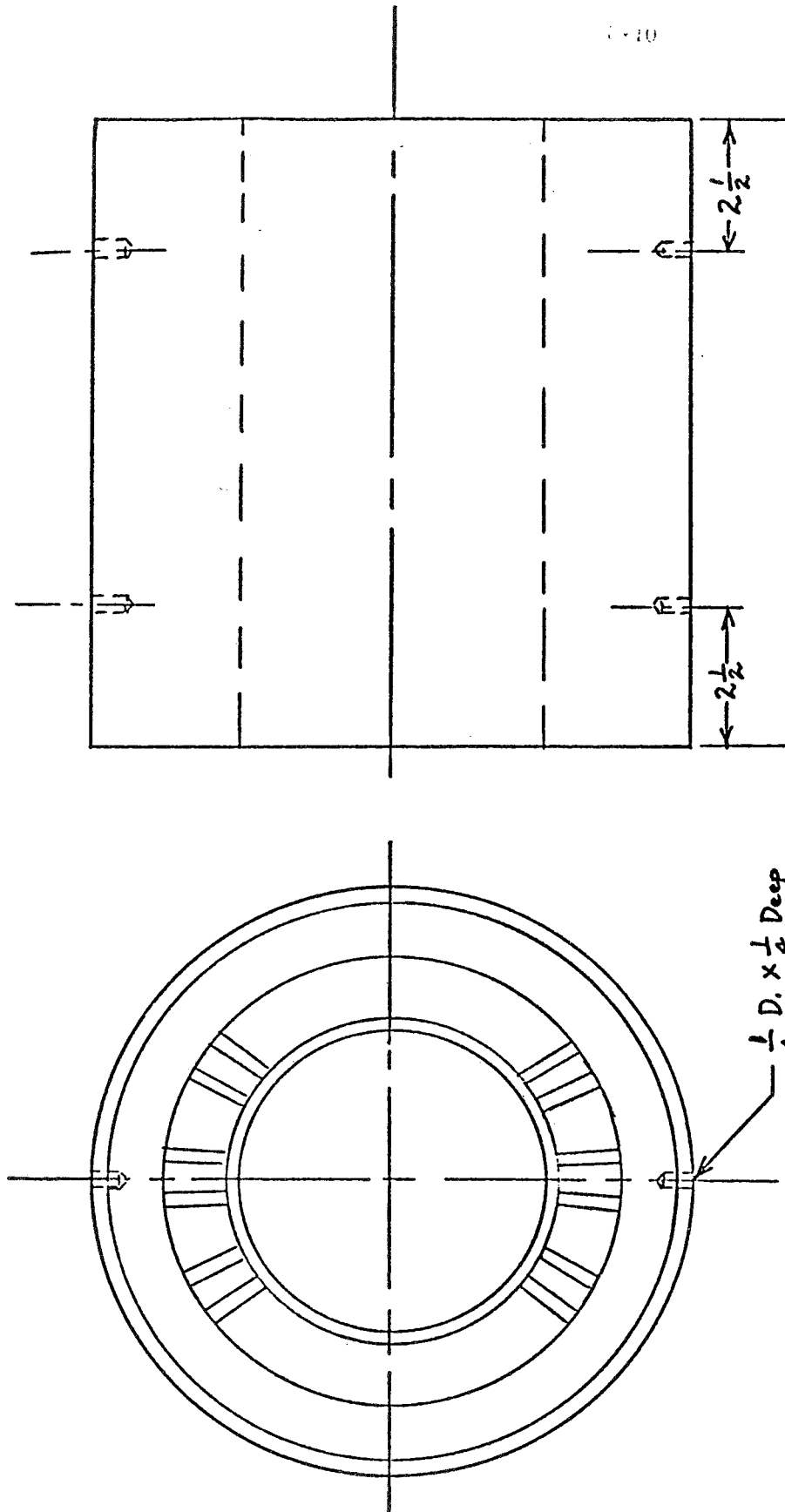
Stainless Steel Spool



D-9

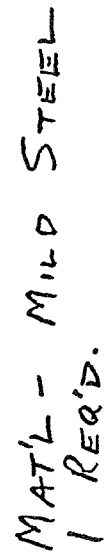
SK8635-F

Location Holes



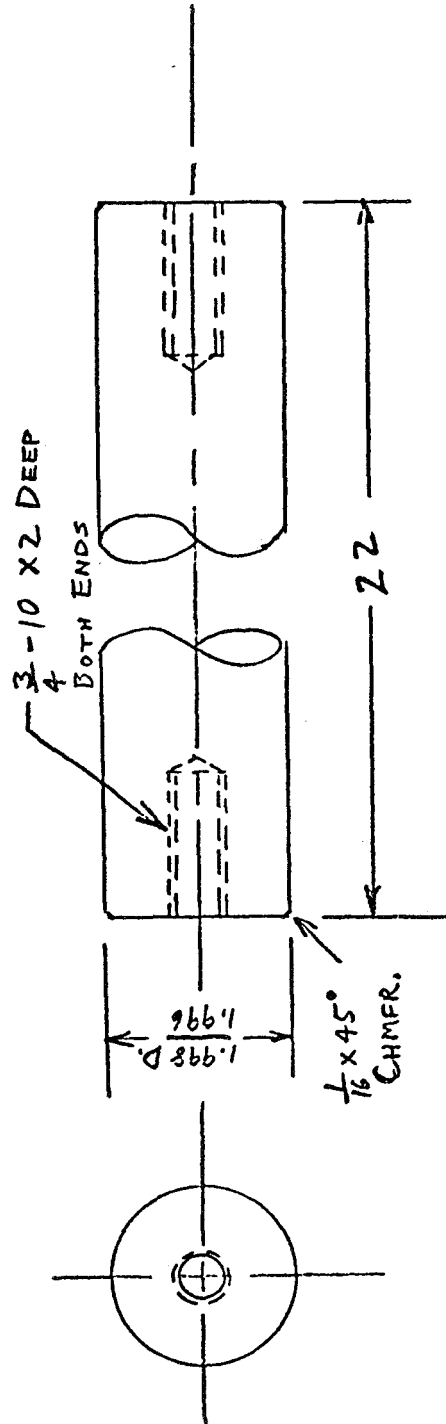
SK 8635 - G

Drill holes as shown
in 2 parts



SK-8635-H1

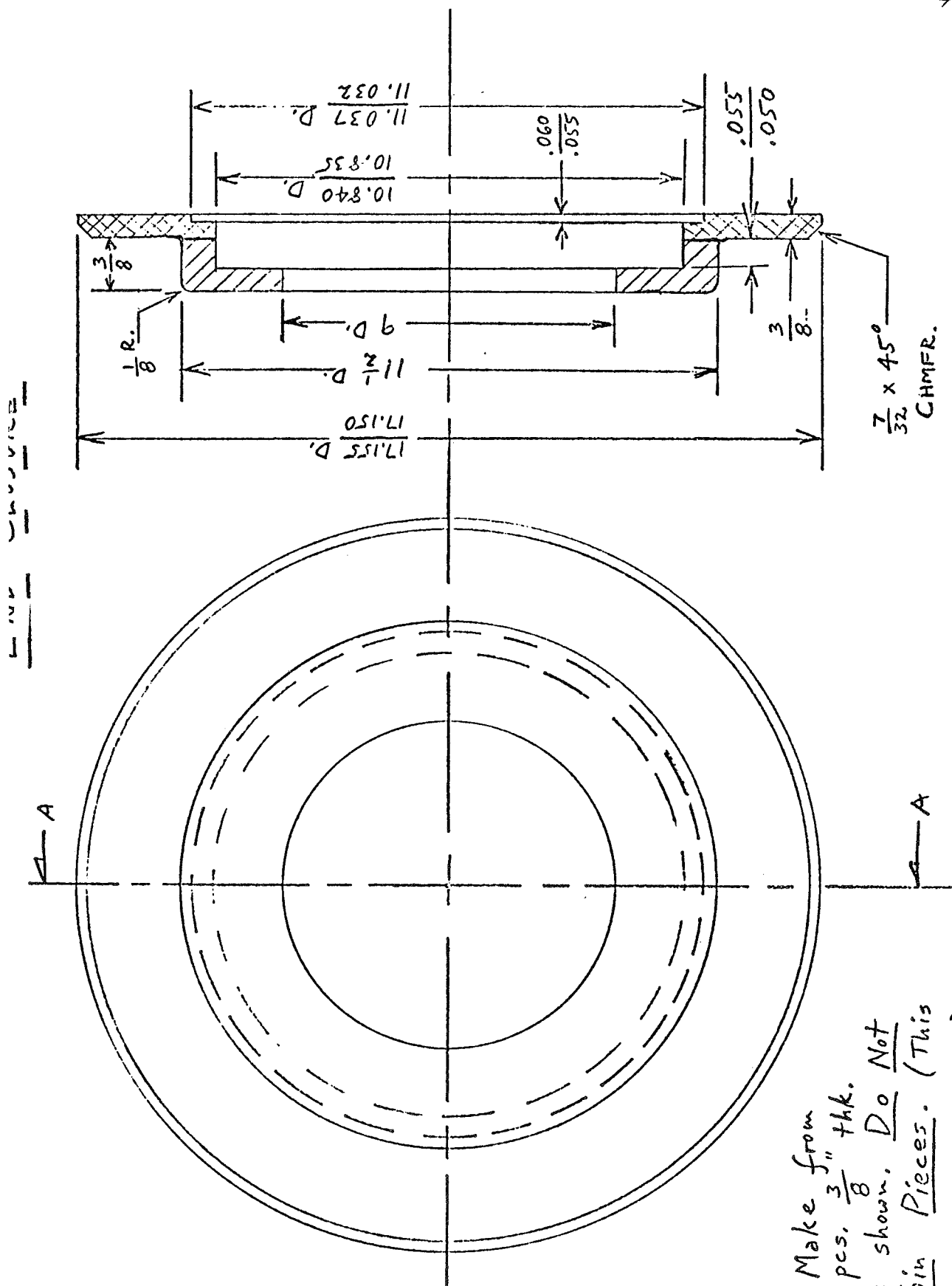
SHAFT



MAT'L - STEEL

1 REQ'D.

SK-8635-H2



Make from
2 pcs. $\frac{3}{8}$ " thk.
as shown. Do Not
Join Pieces. (This
will be done later).

MAT'L — 347 Stainless STL.
4 REQ'D.

SK-8635-I

447, D-4

DISTRIBUTION LIST FOR FINAL REPORT ON CONTRACT NAS3-10305

	<u>Copies</u>		<u>Copies</u>
National Aeronautics and Space Administration Lewis Research Center 21000 Brookpark Road Cleveland, Ohio 44135		National Aeronautics and Space Administration Manned Spacecraft Center Houston, Texas 77001	
Attn: Contracting Officer, MS 500-313	1	Attn: Library	1
Large Engine Technology Branch, MS 500-203	2	National Aeronautics and Space Administration	
Technical Report Control Office, MS 5-5	1	George C. Marshall Space Flight Center	
Technology Utilization Office, MS 3-16	1	Huntsville, Alabama 35812	
AFSC Liaison Office, MS 4-1	2	Attn: Library	1
Library, MS 60-3	2	Jet Propulsion Laboratory	
Howard W. Douglass, MS 500-203	1	4800 Oak Grove Drive	
John M. Kazaroff, MS 500-203	25	Pasadena, California 91103	
National Aeronautics and Space Administration		Attn: Library	1
Washington, D. C. 20546		Defense Documentation Center	
Attn: Code RPX	1	Cameron Station	
Code RPL	1	Alexandria, Virginia 22314	1
Scientific and Technical Information Facility		Air Force Rocket Propulsion Laboratory (RPR)	
P. O. Box 33		Edwards, California 93523	1
College Park, Maryland 20740		Director (Code 6180)	
Attn: NASA Representative	6	U. S. Naval Research Laboratory	
Code CRT		Washington, D. C. 20390	
National Aeronautics and Space Administration		Attn: H. W. Carhart	1
Ames Research Center		Air Force Aero Propulsion Laboratory	
Moffett Field, California 94035		Research & Technology Division	
Attn: Library	1	Air Force Systems Command	
National Aeronautics and Space Administration		United States Air Force	
Flight Research Center		Wright-Patterson AFB, Ohio 45433	
P. O. Box 273		Attn: APRP (C. M. Donaldson)	1
Edwards, California 93523		Mr. W. E. Russell, MS 14-1	
Attn: Library	1	National Aeronautics and Space Administration	
National Aeronautics and Space Administration		Lewis Research Center	
Goddard Space Flight Center		21000 Brookpark Road	
Greenbelt, Maryland 20771		Cleveland, Ohio 44135	1
Attn: Library	1	Mr. Eugene W. Broache	
National Aeronautics and Space Administration		Defense Division	
John F. Kennedy Space Center		Westinghouse Electric Corporation	
Cocoa Beach, Florida 32931		Baltimore, Maryland	1
Attn: Library	1	National Aeronautics and Space Administration	
National Aeronautics and Space Administration		Langley Research Center	
Langley Research Center		Langley Station	
Langley Station		Hampton, Virginia 23365	
Hampton, Virginia 23365		Attn: Mr. Neal Kelly	1
Attn: Library	1		